Three qubits interacting with an environment

Master-Thesis

by

Stefanie Nicole Garni

Supervisor: Prof. Dr. Christoph Bruder

Co-Supervisor: Dr. Maximilian Rinck

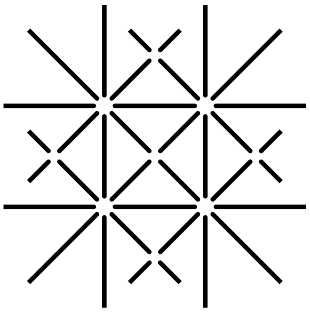

UNI
BASEL

Department of Physics

University of Basel

Switzerland

Basel, May 16, 2011

Contents

Chapter 1

Introduction

Quantum entanglement is one of the most interesting quantum mechanical phenomena, especially in relation to quantum information theory. Since the transmission of information is based on the distribution of special types of correlation, the quantum entanglement, any description of a faultless transmission begins with a discussion of how it is possible to prevent the information from degrading.

Thus the subject of this thesis is the entanglement dynamics of a quantum system which consists of an arbitrary number of qubits coupled linearly to a thermal bath. This coupling shows environmental influences in the context of decoherence effects and leads to a fundamental description of the entanglement dynamics within time. But the entanglement dynamics primarily requires a full understanding of the system dynamics. Therefore, we assume that the system-bath couplings are weak so that the reduced system dynamics can be described by the Markovian master equations. We first consider a system of two qubits embedded in a thermal bath. For such a bipartite system the entanglement is fully understood and gives us an intuitive comprehension of the entanglement dynamics. Especially we are interested in environment-induced entanglement which shows that such a coupling of a quantum system cannot only destroy the entanglement but also create it, transiently or permanently. To obtain a complete description we shall investigate how different entangled states appear by variation of the coupling constants. This requires a substantial study of the coherent physics, the Lamb-shift and entanglement-sudden-death which is a typical effect induced by the dissipative dynamics. Additionally to the entanglement behaviors we are also interested in finding a solution to prevent the information from decohering. This is possible whenever an initial state of the dissipative dynamics has a component remaining constant which is only the case for certain subspaces, known as decoherence-free subspaces.

In the second part of this thesis our theory of entanglement dynamics will be extended from a two qubit system to a three qubit system. This extension is a qualitative one as there is no formulation of the entanglement dynamics of mixed tripartite states. Another difficulty of a tripartite system is that the dynamics given by the reduced density matrix is huge in comparison to the bipartite system. As a consequence of this we have to find a method to generate the master equation algorithmically from the abstract differential equation given in the semi-group definition and implement this equation numerically. This allows quantitative statements on the basis of the numerical implementation of the dynamics. In the end we shall obtain a fundamental description of the dynamics of three qubits embedded in a thermal bath which can be compared with the dynamics of the bipartite system. Based on this dynamics the steady state between the qubit system and the environment shall be discussed in the context of the thermal occupation, so that a fundamental description of the time-dependent distribution of an initial occupation under the influence of the dissipative dynamics is given. Finally the entanglement dynamics of this tripartite system will be discussed. In particular, the focus is going to be on similar effects like in the bipartite case: environment-induced entanglement, decoherence-free subspaces, entanglement sudden death, coherent physics induced by the bath, and the influence of different couplings.

Outline

The outline of this thesis is the following. In chapter 2 we introduce the mathematical description of entanglement in the context of bipartite and multipartite systems. In addition to these definitions we introduce some separability criteria which determine if a given state is separable or entangled. The main part of this chapter will be the introduction of an entanglement measure based on the properties of entanglement, the non-local correlations. In section 2.3 we will discuss such an entanglement measure for a bipartite system, the concurrence. In the last part we consider the concurrence of a tripartite system which is limited to pure states.

In chapter 3 we begin with a discussion of the Jaynes-Cummings model to obtain a description of the interaction of the qubits with a bosonic field. Then the unitary dynamics of closed quantum systems is discussed and from this, we derive the dynamics of open quantum systems under the Markovian assumptions. In section 3.2 we derive the master equation in Lindblad form for our qubit system under the restriction that the system-bath coupling is weak. At the end of this chapter we discuss how it is possible to prevent the information from decohering in the context of the theory of decoherence-free subspaces.

In chapter 4 we consider a bipartite qubit system embedded in a thermal environment described by the Markovian master equation. Primarily we discuss the dynamics of this system, the steady state between the qubits and the thermal bath in the context of the occupation of the states. Then we introduce the entanglement theory based on the stationary solution of the master equation, particularly the theory of environment-induced entanglement and decoherence-free subspaces. In sections 4.2 and 4.3 we then discuss the numerical results with this theoretical background. In the next section we rewrite the Lamb-shift contribution of the master equation in the pseudo-spin representation to obtain an intuitive understanding of the coherent physics. In the last part of this chapter we discuss the corresponding numerical result of the time-dependent concurrence of this representation.

In chapter 5 we extend the bipartite system to a tripartite system. We first discuss the dynamics of this tripartite system in the context of the stationary solution which describes the occupation in time. To obtain a fundamental description of the coherent physics we only consider the pseudo-spin representation of the Lamb-shift contribution. Then we consider the entanglement dynamics for a symmetric coupling for several initial states. At the end of this section we compare these numerical results of the time-dependent concurrence with the numerical results of the bipartite system. In the last part of this chapter we change the symmetric coupling of the qubits to a chain representation. This leads to a comparison of the concurrence and occupation behavior defined by different couplings.

Chapter 2

Quantum entanglement

2.1 Quantum state space of qubits

The quantum bit, or qubit for short, is the basic unit of quantum information theory [1]. Many different physical systems are suitable for the realization of qubits, for example a spin $\frac{1}{2}$-particle, a two-level atom or the polarization of a single photon. The state of a qubit is a vector $|\psi\rangle$ in a two dimensional complex Hilbert space $\mathbb{C}^2$. The vectors of the computational basis states form an orthonormal basis of that space and are represented in matrix form as

$$|0\rangle = \begin{pmatrix} 1 \\ 0 \end{pmatrix}, \quad |1\rangle = \begin{pmatrix} 0 \\ 1 \end{pmatrix}.$$

In contrast to classical information which is either 0 or 1, any superposition of these two states is possible

$$|\psi\rangle = a\,|0\rangle + b\,|1\rangle\,,$$

where a and b are complex numbers with $|a|^2 + |b|^2 = 1$. The scalar coefficients a and b are referred as quantum probability amplitudes, because their squared magnitudes $|a|^2$ and $|b|^2$ are the probabilities for the measurement results.
The Bloch sphere representation is a way to describe a qubit mathematically. Any quantum state $|\psi\rangle$ of a qubit can be represented by the Bloch vector

$$|\psi\rangle = e^{i\gamma}\left(\cos\left(\frac{\theta}{2}\right)|0\rangle + e^{i\varphi}\sin\left(\frac{\theta}{2}\right)|1\rangle\right),$$

where the spherical coordinate angles θ and φ define a point on the three-dimensional unit sphere. The global phase $e^{i\gamma}$ is irrelevant in quantum mechanics. This quantum state space is constructed via a special class of linear operators acting in it, the statistical operator ρ which allows a statistical description of every available state of the (2×2) qubit system. These operators are complex Hermitian trace-one matrices $[\rho_{ij}] \in \mathrm{Mat}(\mathbb{C}, 2)$, also known as density matrices. A fundamental description of this density matrices is given in terms of the Pauli operators

$$\sigma_1 = |0\rangle\langle 1| + |1\rangle\langle 0| = \begin{pmatrix} 0 & 1 \\ 1 & 0 \end{pmatrix},$$
$$-i\sigma_2 = |0\rangle\langle 1| - |1\rangle\langle 0| = \begin{pmatrix} 0 & -1 \\ 1 & 0 \end{pmatrix},$$
$$\sigma_3 = |0\rangle\langle 0| - |1\rangle\langle 1| = \begin{pmatrix} 1 & 0 \\ 0 & -1 \end{pmatrix}, \tag{2.1.0.1}$$

with $\mathbb{1}_2 = \sigma_1^2 = \sigma_2^2 = \sigma_3^2$ and the identity matrix $\mathbb{1}_2$

$$\rho = \begin{pmatrix} \rho_{11} & \rho_{12} \\ \rho_{21} & \rho_{22} \end{pmatrix} = \frac{1}{2}\begin{pmatrix} 1+s_3 & s_1+is_2 \\ s_1-is_2 & 1-s_3 \end{pmatrix} = \frac{1}{2}(\mathbb{1}_2 + \vec{s}\cdot\sigma).$$

The vector $\vec{s} = \{s_1, s_2, s_3\}$ is known as the Bloch vector. In the case of pure qubit states, the statistical operators are projectors onto one-dimensional subspaces and can be associated with points on the Bloch sphere, the vector has unit length $|\vec{s}| = 1$. By contrast, mixed states, that can be formed from pure states, lie in the interior of the Bloch sphere and the Bloch vector is therefore $|\vec{s}| \leq 1$.

Quantum information theory is based on the behavior of qubits. The information of an n qubit system constitutes a Hilbert space with the corresponding dimension $2^{\otimes n}$ represented by a tensor product of multiple copies of the two-dimensional complex Hilbert space. Such systems are traditionally associated with the spin subspaces of elementary particles which represent the fundamental properties of quantum information theory like entanglement and decoherence.

2.2 Entangled states

Entanglement of quantum systems is produced by the interaction of two or more systems. It refers to the situation where only the state of the whole composite system is defined, but not the states of the single system. Erwin Schrödinger describes an entangled state by "the best possible knowledge of the whole does not include the best possible knowledge of its parts" [2].

We first consider a system composed of two single qubits [3][4]. The four-dimensional Hilbert space is a tensor product $\mathcal{H} = \mathcal{H}_A \otimes \mathcal{H}_B$ of the predefined two-dimensional Hilbert spaces associated with each of the two single qubits. For each state one distinguishes between separable and entangled. A pure state $|\psi\rangle$ is called separable or a product state, if it can be written as the direct product of subsystem states

$$|\psi\rangle = |\psi_A\rangle \otimes |\psi_B\rangle = |\psi_A\rangle|\psi_B\rangle \quad |\psi_A\rangle \in \mathcal{H}_A, |\psi_B\rangle \in \mathcal{H}_B.$$

For example the product state $|\psi\rangle = |0\rangle \otimes |1\rangle = |0\rangle|1\rangle$ contains the information of the composite system and of the single qubit states, one qubit is in the state $|0\rangle$ while the other is in the state $|1\rangle$. Thus such states contain the information of the full system and of the single systems.
The remaining states are entangled states which cannot be written as the direct product of the subsystem states

$$|\psi\rangle \neq |\psi_A\rangle \otimes |\psi_B\rangle = |\psi_A\rangle|\psi_B\rangle \quad \forall\, |\psi_A\rangle \in \mathcal{H}_A, |\psi_B\rangle \in \mathcal{H}_B.$$

We consider for instance the entangled Bell states $|\psi_\pm\rangle = \frac{|00\rangle \pm |11\rangle}{\sqrt{2}}, |\phi_\pm\rangle = \frac{|01\rangle \pm |10\rangle}{\sqrt{2}}$. The entanglement of these states can be illustrated by imagining that the two qubits of the state are sent to different locations l_1 and l_2. If we measure the qubit at location l_1 the result will determine the measurement outcome of the second qubit at

location l_2. Thus a measurement of one qubit will determine the measurement outcome of the second qubit as a result of correlation [5]. Thus a typical quantum mechanical property of entangled states is that they can be defined by nonlocal correlations. [1]

The use of density operators allows a statistical description of a composite quantum system and gives additional information if the considered system is in a pure or mixed quantum state. For pure states the quantum state is described by the state vectors. In contrast to mixed states which cannot be described by state vectors. The representation of the density operator in the convex decomposition, the sum over an ensemble in the sense of statistical mechanics, allows to distinguish between pure and mixed states

$$\rho = \sum_i p_i \left(|\psi_i\rangle \otimes \langle\psi_i| \right),$$

where p_i is the probability of the system being in the ith state of the ensemble $|\psi_i\rangle$, where $|\langle\psi_i|\psi_i\rangle| = 1$. If there exists only one probability $p_i = 1$ the state is a pure state

$$\rho = |\psi_i\rangle \langle\psi_i| .$$

This density operator is just the projection operator onto the state $|\psi_i\rangle$. The square of the density operator of pure states is $\rho^2 = |\psi_i\rangle \langle\psi_i|\psi_i\rangle \langle\psi_i| = |\psi_i\rangle \langle\psi_i| = \rho$ and thus it follows

$$Tr(\rho)^2 = Tr(\rho) = 1.$$

A pure state is separable if it can be written as a direct product of the density operators $\rho_{AB} = \rho_A \otimes \rho_B = |\psi_A\rangle \langle\psi_A| \otimes |\psi_B\rangle \langle\psi_B|$, where ρ_A and ρ_B describe the states of the subsystems A and B. Otherwise it is entangled.

The remaining states are mixed states where the probability of the convex decomposition is $\sum_i p_i^2 \leq 1$. This defines a sum of the projection operators over the ensemble weighted with the probabilities of each member of the ensemble. For a fundamental criterion for mixed states we take the trace of the statistical mixture

$$\begin{aligned} Tr(\rho^2) &= \sum_n \sum_{i,j} p_i p_j \langle\varphi_n|\psi_i\rangle \langle\psi_i|\psi_j\rangle \langle\psi_j|\varphi_n\rangle \\ &= \sum_n \sum_{i,j} p_i p_j \langle\psi_i|\psi_j\rangle \langle\psi_j| \underbrace{\varphi_n \langle\varphi_n\rangle}_{=\mathbb{1}} |\psi_i\rangle \\ &= \sum_{i,j} p_i p_j \underbrace{\langle\psi_i|\psi_j\rangle \langle\psi_j|\psi_i\rangle}_{\leq |\psi_i|^2 |\psi_j|^2} \\ &\leq \sum_{i,j} p_i p_j . \end{aligned}$$

The last term of the equation is only one if $|\langle\psi_i|\psi_j\rangle|^2 = 1$ which is only possible for pure states when all states. The square of the density matrix for mixed states holds the relation

$$Tr(\rho)^2 < 1.$$

Mixed states are separable when they can be written in a convex decomposition

[1] That two entangled states have nonlocal correlations was found by the EPR-effect of Einstein, Podolski and Rosen [6]. They have introduced a fundamental thought experiment which should prove that the quantum-mechanical description of reality is uncomplete. In this experiment they have found that quantum mechanics behaves not like the classical theory as a consequence of this correlations.

$$\rho = \sum_i p_i \left(\rho_A^i \otimes \rho_B^i \right), \tag{2.2.0.2}$$

where the density matrices $\rho_{A,B}$ give a statistical description of the corresponding systems A, B, and p_i is the probability being in the ith state of the ensemble with $\sum_i p_i = 1$. All other states are entangled mixed states. This decomposition into separable mixed states is not straightforward. For special separable mixed states, we give an example (see appendix) to decompose this states into separable states like in equation (2.2.0.2)

Entanglement of multi-partite systems

The definition of entangled states can be generalized to multi-partite systems, i.e. systems that decompose into more than two subsystems. An n-partite system is described by a Hilbert space $\mathscr{H}$ which is a tensor product of all subsystems $\mathscr{H}_1 \otimes \mathscr{H}_2 \otimes ... \otimes \mathscr{H}_n$. A pure state is separable if it can be written as a direct product of n states, otherwise the pure state is entangled. A mixed state is separable if it can be written as a convex sum of product states. Any mixed state that cannot be represented as a convex sum of separable states is entangled.

2.2.1 Schmidt decomposition

The Schmidt decomposition refers to a particular way of expressing a vector in a tensor product of two different subsystems. The Schmidt decomposition allows to classify pure bipartite states $|\psi\rangle$ of a composite systems A, B [1]. The Hilbert spaces of the components are defined by $\mathscr{H}_A$ and $\mathscr{H}_B$ with dimensions d_A and d_B. Then there exists orthonormal states $|m\rangle \in |\psi_A\rangle$ and $|v\rangle \in |\psi_B\rangle$ such that

$$|\psi\rangle = \sum_{m=1}^{d_A} \sum_{v=1}^{d_B} \lambda_{mv} |m\rangle |v\rangle \tag{2.2.1.1}$$

where λ_{mcv} are non-negative real numbers satisfying $\sum_{mv} \lambda_{mv}^2 = 1$, known as Schmidt coefficients.
This representation is provided for all pure states, which is shown easily. A state of the composite system is defined as a product of any fixed orthonormal basis $|n\rangle, |\mu\rangle$ for the subsystems A, B

$$|\psi\rangle = \sum_{n,\mu} c_{n\mu} |n\rangle |\mu\rangle$$

for some matrix C of complex numbers $c_{n\mu}$. This state is rewritten by the singular value decomposition $c = udv$, where d is a diagonal matrix with non-negative elements and u and v are unitary matrices, as

$$|\psi\rangle = \sum_{mvn\mu} u_{nm} d_{mv} v_{v\mu} |n\rangle |\mu\rangle .$$

This expression gives the Schmidt decomposition (2.2.1.1), defining $|m\rangle = \sum_{mn} u_{mn} |n\rangle, |v\rangle = \sum_{v\mu} v_{v\mu} |\mu\rangle$, and $\lambda_{mv} = d_{mv}$. The basis $|m\rangle$ forms an orthonormal set from the unitary of u and the orthonormality of $|n\rangle$ and similarly for $|v\rangle$.
The Schmidt coefficients allows to distinguish separable from entangled states. For a separable state the Schmidt decomposition of the single state is $\rho_A = \sum_m \lambda_m^2 |m\rangle \langle m|$ and $\rho_B = \sum_v \lambda_v^2 |v\rangle \langle v|$, the eigenvalues of ρ_A and ρ_B are identical, namely λ_{mv}^2 for both density operators. The Schmidt vector which is created by the Schmidt coefficients has only one non-vanishing entry $\vec{\lambda} = [1, 0, ..., 0]$, namely the product state composed of the two pure states that determine the reduced state. In contrast to fully entangled states where the Schmidt vector has n components $\vec{\lambda} = [1/d, ..., 1/d]$. Therefore it is important to have all the Schmidt coefficients for the characterization of all the correlations of the pure state. An n-dimensional system has $(n-1)$ independent Schmidt coefficients, because of the normalization $\langle \psi | \psi \rangle = 1$.

The Schmidt decomposition for maximally entangled states exhibits maximally mixed reduced states. The form of the maximally entangled states are

$$|\psi_{max}\rangle = \frac{1}{\sqrt{d}} \sum_{i=1}^{d} |e_i\rangle \otimes |f_i\rangle .$$

Thus different maximally entangled states only differ in their Schmidt basis, but not in their Schmidt coefficients.

2.2.2 Separability criteria

For mixed states the Schmidt decomposition is not a sufficient criterion for the separability [4]. In general, the characterization of a set of separable mixed states appears to be extremely complex, because the given density operator has infinitely many ensemble decompositions. Thus we introduce operational and non-operational criteria which are known to describe partially a set of quantum states.

Operational separability criteria

We distinguish between three different operational separability criteria, namely the Peres-Horodecki criterion (positive partial transpose), reduction criterion and the majorization criterion [7]. The positive partial transpose criterion, or for short the PPT criterion, provides for all mixed states a necessary criterion of entanglement, because it is based on the fact that any transposition operation of a separable state leads always to another separable state.
We consider a bipartite mixed system represented by a separable density matrix ρ_{AB} which can be described in an arbitrary product basis as

$$\rho_{m,\mu,n\nu} = \langle m,\mu|\rho|n,\nu\rangle ,$$

where Latin indices are referring to the subsystem A and Greek ones to the subsystem B. The partial transpose of this composite density matrix is given by the transpose of only one subsystem. For example, the partial transpose of the subsystem B is given by the new density matrix $\rho_{AB}^{\mathrm{T}_B}$ with matrix elements in the fixed product basis as

$$\langle m|\langle\mu|\rho_{AB}^{\mathrm{T}_B}|n\rangle|\nu\rangle = \langle m|\langle\nu|\rho_{AB}|n\rangle|\mu\rangle .$$

Thus the operation T_B, the partial transpose, corresponds to transposition of indices of subsystem B. To obtain an intuitive representation of the partial transpose of any separable state we use the decomposition according to (2.2.0.2). With this definition any separable state can be written as

$$\rho_{sep}^{\mathrm{T}_B} = \sum_i p_i \left(\rho_A^i \otimes (\rho_B^i)^T\right) = \sum_i p_i \left(|m_i\rangle\langle m_i| \otimes (|\nu_i\rangle\langle\nu_i|)^T\right),$$

since the transposed density matrix $\left(\rho_B^i\right)^T = (|\nu_i\rangle\langle\nu_i|)^T$ is again a valid density matrix for B. The density matrix ρ_{AB} is an operator matrix in an orthogonal basis which has a non-negative spectrum. Thus the corresponding transposed matrix $(\rho_{AB})^T$ is also a quantum state and positive and we obtain the following relation

$$\rho_{AB,sep} \geq 0 \Rightarrow \left(\rho_{AB,sep}\right)^{T_B} \geq 0.$$

The relation $\rho^{AB} \geq 0$ is synonymous with the fact that all eigenvalues of this matrix are positive or zero. The spectrum of the matrix and the transposed matrix is equal which can easily be shown by the relation $\det(\rho^{AB} - \lambda\mathbb{1}) = \det((\rho^{AB})^T - \lambda\mathbb{1})$ and thus the eigenvalues of the transposed separable matrix are also positive or zero.

If the partial transposition operation is performed on a separable mixed state the result is always another positive density matrix with non-negative eigenvalues. Then the partial transpose criterion says that if $\rho^{T_{AB}} \leq 0$ then ρ is entangled.

A. Peres [8] shows that the partial transpose criterion is only perfectly adequate , i.e. necessary and sufficient for the characterization of separability and entanglement for low-dimensional systems, $2 \otimes 2$ or $2 \otimes 3$ dimensional systems. For higher dimensional systems only the existence of entangled PPT states can be shown and thus the partial transpose criterion is not a sufficient criterion for such systems.

Non-operational separability criteria

In the following, we want to discuss a non-operational separability criterion, namely positive maps. The criteria of positive maps is an extension of the partial transpose criterium through a general analysis of the problem of separable states in terms of linear positive maps. A map is called a positive map, if it takes positive operators to positive operators

$$\Lambda(\rho) \geq 0, \quad \rho \geq 0,$$

where the operator ρ is positive semi-definite according to its definition. The crucial property of this criterion is that if $\Lambda \geq 0$ not every map is necessarily positive. We consider for example a positive map on the second subsystem B and define $\mathbb{1} \otimes \Lambda$ with Λ acting only on the second subsystem B and $\mathbb{1}$ is the identity map on the first subsystem A. If the considered state is separable, its convex decomposition into product states is given by

$$(\mathbb{1} \otimes \Lambda)\rho = \sum_i p_i \left(\rho_i^A \otimes \Lambda \rho_1^B\right).$$

Thus we obtain the following relation for separable states

$$(\mathbb{1} \otimes \Lambda)\rho \geq 0.$$

In contrast to states which are not separable the extended map is not positive, there are some states ν such that $(\mathbb{1} \otimes \Lambda)\,\nu \ngeq 0$. Such states ρ are necessarily entangled.

A state is also separable if the extended map is positive and can be written in its convex decomposition and all expectation values of this quantity are non negative, otherwise it is entangled. To show that a state is entangled it is sufficient to find only one positive map Λ with $(\mathbb{1} \otimes \Lambda)(\rho) < 0$. Since the positive maps criterion is based on the theory of the PPT-criterion it is also limited for low-dimensional systems, $(2 \otimes 2)$ and $(2 \otimes 3)$. In higher dimensional system there are entangled states which cannot be detected by this criterion [7]

2.3 Entanglement measures and monotones

The entanglement properties must be fully understood for the introduction of a theoretically correct formulation of entanglement measure. A fundamental description of entanglement is given in the context of operations, particularly local operations and classical communication(LOCC) [9]. These operations allow to create controllable quantum correlations and thus we are able to coherently prepare, manipulate, and measure individual quantum systems. We will discuss the entanglement measure by concentrating on the finite dimensional bipartite case.

2.3.1 Properties of entanglement measures

For the introduction of entanglement measures we start with an operational point of view in the context of quantum communication experiments. Plenio describes the quantum communication by "Perfect quantum

communication is essentially equivalent to perfect entanglement distribution" [10]. This means that it must be possible to share the information of a particle by two distantly separated laboratories without decoherence. If we consider for example a qubit the information of it is perfectly transmitted when it is possible to distribute the entanglement from one laboratory to the other. Such a perfectly distribution of the information of the states can be achieved by local operations and classical communication [10].

In the following, we give the mathematical description of the different operations for two finite dimensional systems as it has been proposed in Ref.[9].

Local operations

An operation is local, if both subsystems evolve independently of each other under the action of this operation. In terms of the operator sum the local operation can be represented by the operators of the subsystem in the following way

$$\varepsilon_{loc}(\rho) = \sum_{ij} A_i \otimes B_j \rho B_j^\dagger \otimes A_i^\dagger \quad \text{with} \quad \sum_{ij} A_i^\dagger A_i \otimes B_j^\dagger B_j = \mathbb{1}_{\mathscr{H}_1 \otimes \mathscr{H}_2},$$

where the operators $A_i, A_i^\dagger$ and $B_j, B_j^\dagger$ correspond to the first subsystem, respectively to the second subsystem. Possible entanglement between these two subsystems defined by preexisting correlations remains unaffected when both system evolve unaffected by each other. Thus the entanglement can neither increase nor decrease. As a consequence of the remaining correlation under all local operations, the product state of both subsystems remains a product state and can be written in terms of the operators

$$\varepsilon_{loc}(\rho_1 \otimes \rho_2) = \left(\sum_i A_i \rho_i A_i^\dagger \right) \otimes \left(B_i \rho_2 B_i^\dagger \right)$$

as well any separable state will remain separable under local transformations

$$\varepsilon_{loc} \left(\sum_i p_i \rho_1^i \otimes \rho_2^i \right) = \sum_i p_i \left(\sum_i A_i \rho_1^i A_i^\dagger \right) \otimes \left(\sum_i B_i \rho_2^i B_i^\dagger \right)$$

Any separable state can thus be created by local operations alone.

Global operations

In contrast to the local operation, a global operation should take into account that the two involved subsystems evolve dependently of each other, thus an interaction between these both subsystems exists. If we assume that the two subsystems are uncorrelated at the beginning then the initial state is a separable state and become an entangled state only by the interaction of the two subsystems. Thus an entangled state can be created from any initial separable state and vice versa, because the interaction between the subsystems leads to an entanglement decrease or increase. In other words, global transformations due to the interaction of the subsystems allow to create entangled states.

Local operations and classical communication(LOCC)

Local operators and classical communication(LOCC) provide a method to perform local operations on a part of a system and transmit this information by classical communication to another part of the system. This allows an exchange of the created information between the involved subsystems. In the following we introduce the mathematical description of LOCC.
The LOCC transformation in terms of the operator sum is expressed as

$$\varepsilon_{LOCC}(\rho) = \sum_i A_i \otimes B_i \rho B_i^\dagger \otimes A_i^\dagger \quad \text{with} \sum_i A_i^\dagger A_i \otimes B_i^\dagger B_i = \mathbb{1}_{\mathscr{H}_1 \otimes \mathscr{H}_2}.$$

In contrast to the definition of a local transformation this operator sum is defined by only one sum. This results in the theory that separable states can be created on different parts of the system. If the first operator A_i is applied to the first subsystem the other operator B_i is applied to the second subsystem. Thus the LOCC operations create then a classical correlation between these two subsystems. But a product state will not remain a product state under this transformation as a result of the exchange between both subsystems

$$\varepsilon_{LOCC}(\rho_1 \otimes \rho_2) = \sum_i \left(A_i \rho_1 A_i^\dagger\right) \otimes \left(B_i \rho_2 B_i^\dagger\right) = \sum_i p_i \rho_1^i \otimes \rho_2^i,$$

with

$$\rho_1^i = \frac{A_i \rho_1 A_i^\dagger}{Tr(A_i \rho_1 A_i^\dagger)} \quad \rho_2^i = \frac{B_i \rho_1 B_i^\dagger}{Tr(B_i \rho_1 B_i^\dagger)}, \quad \text{and} \quad p_i = Tr(A_i \rho A_i^\dagger) Tr(B_i \rho B_i^\dagger)$$

Thus any separable state will remain separable under the LOCC transformation, but entangled states can not be created by LOCC operations.

2.3.2 Entanglement monotones

In addition to the conventional requirements that a measure of entanglement should be nonnegative and normalized, we introduce a fundamental pair of monotonicity conditions to obtain a good measure of entanglement. The most important postulate in the context of operationally defined measures was introduced by Bennett, DiVincenzo et al. [11]. The entanglement measure can be interpreted as functionals $E(\rho)$ that characterize the strength of quantum correlations, the existing entanglement between both subsystems. The definition of such a functional $E(\rho)$ is based on the theory of LOCC transformations which guarantees that the entanglement measurement have no influence on the correlations. The basic axiom or fundamental postulate is the monotonicity under LOCC; entanglement cannot increase under local operations and classical communication

$$E(\Lambda(\rho)) < E(\rho),$$

where $\Lambda(\rho)$ is any local operation that can be written as $\Lambda(\rho) = \sum_{ij} A_i \otimes B_j(\rho) A_i^\dagger \otimes B_j^\dagger$ with the operations A_i of the first subsystem and B_j to the second (but not vice versa). The known entanglement measures usually satisfies a stronger condition, namely that the average for each local operation is monotonic

$$\sum_i p_i E(\rho_i) \leq E(\rho),$$

where p_i are the probabilities of the states ρ_i. This condition may also be written in the form of a convex function which is monotonic under mixing

$$E\left(\sum_i p_i \rho_i\right) \leq \sum_i p_i E(\rho_i).$$

The function E that serves as an entanglement quantifier needs to fulfill several requirements which has been proposed in Ref.[10]:

- Discrimination of separable and entanglement states:

$$E(\rho) = 0 \text{ for separable } \rho, \text{ and}$$
$$E(\rho) > 0 \text{ for entangled } \rho,$$

- Invariance under local unitary transformations:

$$E(U_A \otimes U_B \rho U_A^\dagger \otimes U_B^\dagger) = E(\rho),$$

- Convexity, entanglement should not increase under mixing:

$$E\left(\sum_i p_i \rho_i\right) < \sum_i p_i E(\rho_i),$$

- Monotonicity on average under local maps and under LOCC-operations which means that $\Lambda(\rho) \otimes \mathbb{1}$ yields the state $\sum_i p_i \rho_i$ with an ensemble of states ρ_i and probability p_i, it holds

$$\sum_i p_i E(\rho_i) \leq E(\rho).$$

  Also entanglement of the total state cannot increase because of convexity:

$$E\left(\Lambda(\rho) \otimes \mathbb{1}\right) \leq E(\rho).$$

If a function E satisfies the monotonicity postulate, it turns out that for separable states it is constant. This follows from the fact that every separable state can be transformed to any other separable state by LOCC. In contrast to separable states where the function E vanishes. These two conditions imply that the function E is a non negative function. All other conditions are necessary for a fundamental description of entanglement by systems with collective, global properties.
To obtain an intuitive description of an entanglement measure the partial additivity and the continuity condition are used

- The entanglement of n copies of a state ρ is defined by n times the entanglement of one copy

$$E(\rho^{\otimes n}) = nE(\rho),$$

- If $\langle \psi^{\otimes n} | \rho_n | \psi^{\otimes n} \rangle \to 1$ for $n \to \infty$, then

$$\frac{1}{n} |E(P(|\psi\rangle)^{\otimes n}) - E(\rho^n)| \to 0,$$

  the index n defines the number of pairs of qubits ρ^n.

This additive criterion is not a necessary condition and is therefore not one of the basics axioms. This results in the fact that for any given measure E where the additivity is not fulfilled, it is possible to define a regularized, or asymptotic version of this condition

$$E^\infty(\rho) := \lim_{n\to\infty} \frac{E(\rho^{\otimes n})}{n}.$$

This definition of the measure satisfies automatically the additivity. The full additivity, for any pair of states ρ and σ holding the relation $E(\rho \otimes \sigma) = E(\rho) \otimes E(\sigma)$, is in most cases a too strong condition and is therefore not fulfilled. A good entanglement measure is given by the four basic properties. In the next section we introduce the concurrence, a special measure of entanglement which gives a correct entanglement description.

2.4 Concurrence and entanglement of formation

2.4.1 Concurrence of bipartite systems

Wootters [12] has introduced an applicable formula for the entanglement of formation for a bipartite system by the concurrence C. The entanglement measure $E(\psi)$ of a pure state living in a product Hilbert space $\mathscr{H} = \mathscr{H}_A \otimes \mathscr{H}_B$ with the general density matrix $\rho = \sum_i |\psi_i\rangle \langle \psi_i|$ is described by the von Neumann entropy $S(\rho)$

$$E(\psi) = S(\rho) = -\operatorname{Tr}_B(\rho_A \log \rho_A) = -\operatorname{Tr}_A(\rho_B \log \rho_B)$$

where $\operatorname{Tr}_{A,B}$ are the partial traces over the subsystems. This knowledge cannot simply be applied to mixed states in terms of an average over the mixture of pure state entanglement. The problem is that two decompositions of the same density matrix usually lead to a different average entanglement and there is no clear definition which is the correct one. Thus the entanglement measure by the entanglement of formation E_f represents the minimal possible entanglement over all pure state decomposition of ρ, where $E(|\psi\rangle\langle\psi|) = S(Tr\{|\psi\rangle\langle\psi|\})$ is taken and the measure, is then defined by

$$E_f(\rho) = \inf \sum_i p_i E(\psi_i),$$

where the infimum is taken over all possible probability distributions. This equation is the so called convex roof of the entanglement of formation for pure states and a decomposition leading to this convex roof value is called an optimal decomposition.
The concurrence provides an analytic formula for the entanglement. The concurrence C of a pure state $|\psi\rangle$ is defined to be $C(\psi) = |\langle\tilde{\psi}|\psi\rangle|$, where the tilde denotes the spin-flip transformation. This transformation is a function applicable to states of an arbitrary number of qubits

$$|\tilde{\psi}\rangle = \sigma_y |\psi^*\rangle,$$

where $|\psi^*\rangle$ defines the complex conjugated of $|\psi\rangle$ and σ_y is the matrix $\begin{pmatrix} 0 & -i \\ i & 0 \end{pmatrix}$ represented in the basis $\{|\uparrow\rangle, |\downarrow\rangle$.
For n qubits such a spin-flip can be obtained by applying the above transformation on each qubit. If we consider two qubits with the general density matrix given in the basis $\{|\uparrow\uparrow\rangle, |\uparrow\downarrow\rangle, |\downarrow\uparrow\rangle, |\downarrow\downarrow\rangle\}$ the spin-flip state is the scalar product of ρ with the elementwise conjugated

$$\tilde{\rho} = (\sigma_y \otimes \sigma_y)\rho^*(\sigma_y \otimes \sigma_y).$$

For example, this spin-flip transformation leaves the singlet state $|\psi\rangle = \frac{1}{\sqrt{2}}(|\uparrow\downarrow\rangle - |\downarrow\uparrow\rangle)$ unchanged and thus its concurrence $|\langle\psi|\tilde{\psi}\rangle|$ takes the maximum value. In contrast to an unentangled pure state such as $|\uparrow\downarrow\rangle$ which is not unchanged by the flip transformation because it is mapped to an orthogonal state and therefore the concurrence is zero. The von Neumann entropy is expressed as the function of the Concurrence C

$$\begin{aligned} E(\psi) &= \epsilon(C(\psi)) \\ &= h\left(\frac{1}{2}\left(1 + \sqrt{1 + C(\psi)^2}\right)\right), \end{aligned} \tag{2.4.1.1}$$

where $h(x) =: -x\log_2 x - (1-x)\log_2(1-x)$ is the binary entropy. The function $\epsilon(C)$ increases monotonically for $0 \le C \le 1$, thus the concurrence is regarded as a measure of entanglement.
For mixed states ρ the von Neumann entropy as a function of the concurrence is defined similarly. The function $\epsilon(C)$, in addition to be increasing monotonically is also convex for mixed states

$$\varepsilon(C(\rho)) = \inf \varepsilon\left(\sum_j p_j C(\psi_j)\right) \le \inf \sum_j p_j \varepsilon\left(C(\psi_j)\right) = E_f(\rho),$$

where $\varepsilon(C(\rho))$ is also a lower bound on $E_f(\rho)$. The explicit formula for the concurrence C is

$$C(\rho) = \max\{0, \lambda_1 - \lambda_2 - \lambda_3 - \lambda_4\}, \tag{2.4.1.2}$$

where the $\lambda_i' s$ are the square roots of the eigenvalues of $\rho\tilde{\rho}$ in descending order. Therefore the formula for entanglement of a pair of qubits in any mixed state ρ is given by

$$E_f(\rho) = \varepsilon\left(C(\rho)\right),$$

with the concurrence C (2.4.1.2) and the function ε (2.4.1.1). For instance, the concurrence C of a maximal entangled state is one and the concurrence C of a separable mixed state is zero.

2.4.2 Concurrence of tripartite systems

In this section we discuss the entanglement of tripartite systems. For bipartite systems the entanglement of the system is fully described by the concurrence, but this situation is much more complicated for multipartite systems. The property of bipartite entanglement can be used to describe the entanglement of a tripartite system, if two of the qubits A and B are very entangled, then the third qubit C can only be weakly entangled with either qubit A or qubit B. For example, if we consider a singlet state, a maximally entangled state, between the pair of qubits A, B then they cannot be entangled with qubit C. This was the fundamental idea for the derivation of a quantifier for tripartite entanglement.
The tripartite entanglement of three qubits is given by the tangle τ_{ABC},introduced by Coffman, Kundu, and Wotters [4]

$$\tau_{ABC} = C_{A(BC)} - C_{AB} - C_{AC}. \tag{2.4.2.1}$$

The residual tangle is invariant under permutations of the qubits. The concurrence C_{AB} refers to a mixed state of qubit A and qubit B which is calculated with the same formula for the bipartite case (2.4.1.2) after tracing out the degrees of freedom of qubit C. The concurrence C_{AC} is defined similar for the relevant qubits. The concurrence $C_{A(BC)}$ described the entanglement of the qubit A with the pair of qubit B and C. The tangle, the degree of the entanglement $\tau \in [0,1]$, is zero if one qubit is separable from the other two, otherwise it is one if the state is maximally entangled.
The generic class of three-particle pure states can be written as

$$|\psi\rangle = \lambda_1 |000\rangle + \lambda_2 e^{i\varphi} |101\rangle + \lambda_3 |110\rangle + \lambda_4 |111\rangle,$$

where $\lambda_i \geq 0, \sum_i \lambda_i^2 = 1$ and $0 \geq \varphi \geq \pi$ [10]. This representation of pure states is defined by a five-parameter family, with equivalence up to local unitary transformation. These pure states include two classes of separable states, namely the fully separable states which can be written as a product of single-party pure states and bi-separable states which is a product of two entangled states and one single pure qubit state. All other pure states are non-separable and constitute the class of tripartite-entangled pure states. One class of this is the Greenberger-Horne-Zeilinger (GHZ) state and the remaining class is the class of Werner (W) state. The tangle τ_{ABC} can only detect GHZ-type entanglement and not W-type entanglement [13]. Thus the tangle can only detect genuine tripartite entanglement, and hence can be used as an indicator of three-party entanglement. For states which have no genuine tripartite entanglement like mixed states, we cannot make any statement about their entanglement.

For three qubit states we can only introduce a classification for the different mixed states [14]. This classification is divided in the following classes

- S, the class of separable mixed states which can be expressed as a convex roof sum of projectors onto product vectors,
- B, the class of bi-separable mixed states which can be expressed as a convex sum of projectors onto product and bipartite entanglement vectors,
- W, the class of states expressible as convex combinations of projectors onto the separable, bi-separable and pure W states,
- GHZ, the generic class of three qubits

All these classes are convex and compact and the classes are embedded by $S \subset B \subset W \subset GHZ$.

Chapter 3

Open Quantum Systems

3.1 Fully quantum-mechanical model: The Jaynes-Cummings model

Any open quantum system dynamics include environmental influences which are described by the interaction Hamiltonian. Since we are interested in the dynamics of n qubits coupled linearly to a thermal bath an introduction of the system-bath interaction is necessary.

Such an intuitive description of atom-field interaction is given by the fully quantum mechanical Rabi model, better known as the Jaynes-Cumming model [15]. This model of Edwin Jaynes and Fred Cummings studies the relationship between the quantum theory of radiation and the semi-classical theory in describing the phenomenon of spontaneous emission. To be more precise, we consider an atom which is the quantum two-level system whose Hilbert space is spanned by just two states, an excited state $|e\rangle$ and a ground state $|g\rangle$, interacting with a radiation field. We assume this field to be a single-mode free field; this has the advantage that the dynamics is well described. The single-mode cavity field in the z-direction is described by field operators, $b^\dagger$ and b which are the bosonic creation and annihilation operators

$$\hat{\vec{E}} = \vec{e}\left(\frac{\hbar\omega}{\epsilon_0 V}\right)^{\frac{1}{2}} (\hat{b} + \hat{b}^\dagger)\ \sin(kz), \tag{3.1.0.1}$$

where $\vec{e}$ is an arbitrarily oriented polarization vector, ω is the frequency of the mode and k is the wave number related to the frequency according to $k = \frac{\omega}{c}$. The interaction Hamiltonian of the atom and the field is then given by the dipole moment operator $\hat{d} = \hat{\vec{d}} \cdot \vec{e}$ and the field operator (3.1.0.1)

$$H_I = -\hat{\vec{d}} \cdot \hat{\vec{E}} = \hat{d} g(\hat{b} + \hat{b}^\dagger) \quad \text{where} \quad g = -\left(\frac{\hbar\omega}{\epsilon_0 V}\right) \sin(kz).$$

For a more optimized description we introduce the Pauli operators in the basis $|e\rangle, |g\rangle$:

$$\sigma_1 = |e\rangle\langle g| + |g\rangle\langle e|, \quad \sigma_2 = -i\,|e\rangle\langle g| + i\,|g\rangle\langle e|, \quad \sigma_3 = |e\rangle\langle e| - |g\rangle\langle g|$$

satisfy the commutation relations $[\sigma_i, \sigma_j] = 2i\epsilon_{ijk}\sigma_k$ as well as the anticommutation relations $\{\sigma_i, \sigma_j\} = 2\delta_{ij}$. It is convenient to introduce the so-called atomic transition operators

$$\hat{\sigma}_+ = |e\rangle\langle g| = \frac{1}{2}(\hat{\sigma}_1 + i\hat{\sigma}_2), \quad \hat{\sigma}_- = |g\rangle\langle e| = \frac{1}{2}(\hat{\sigma}_1 - i\hat{\sigma}_2) = \hat{\sigma}_+^\dagger.$$

The dipole operator $\hat{d}$ can be written by this definition as

$$\hat{d} = d\,|g\rangle\langle e| + d^*\,|e\rangle\langle g| = d\hat{\sigma}_- + d^*\hat{\sigma}_+ = d(\hat{\sigma}_+ + \hat{\sigma}_-),$$

where the off-diagonal elements of the dipole operator are nonzero, since by parity considerations $\langle g|\hat{d}|g\rangle = \langle e|\hat{d}|e\rangle = 0$, and we set $\langle e|\hat{d}|g\rangle = d$, and assume that d is real. Thus the interaction Hamiltonian is

$$\hat{H} = \hbar\lambda(\hat{\sigma}_+ + \hat{\sigma}_-)(\hat{b}_k + \hat{b}_k^\dagger)$$

with $\lambda = \frac{dg}{\hbar}$. We define energy to be halfway between the ground state energy level E_g and the excited state energy level E_e with $E_e = -E_g = \frac{1}{2}\hbar\omega_0$ then the atomic Hamiltonian is written as

$$\hat{H}_A = \frac{1}{2}(E_e - E_g)\hat{\sigma}_3 = \frac{1}{2}\hbar\omega_0\hat{\sigma}_3.$$

After dropping the zero-point energy $\frac{\hbar\omega}{2}$ the free-field Hamiltonian is

$$\hat{H}_F = \hbar\omega\hat{b}^\dagger\hat{b}.$$

The total Hamiltonian of this system consists of the atomic Hamiltonian H_A, the free-field Hamiltonian H_F and the interaction Hamiltonian H_I

$$\begin{aligned}\hat{H} &= \hat{H}_A + \hat{H}_F + \hat{H}_I \\ &= \frac{1}{2}\hbar\omega_0\hat{\sigma}_3 + \hbar\omega\hat{b}\hat{b}^\dagger + \hbar\lambda(\hat{\sigma}_+ + \hat{\sigma}_-)(\hat{b} + \hat{b}^\dagger).\end{aligned} \tag{3.1.0.2}$$

In the interaction picture the annihilation operator $\hat{b}$ and the creation operator $\hat{b}^\dagger$ of the bath evolve as

$$\hat{b}(t) = \hat{b}(0)e^{-i\omega t}, \quad \hat{b}^\dagger(t) = \hat{b}^\dagger(0)e^{i\omega t}$$

and similar for the atomic transition operators $\hat{\sigma}_+$ and $\hat{\sigma}_-$

$$\hat{\sigma}_\pm(t) = \sigma_\pm(0)e^{\pm i\omega_0 t}.$$

The approximate time dependence of the operator products of the interaction Hamiltonian H_I is then given by

$$\begin{aligned}H_I &= \hbar\lambda(\hat{\sigma_+}\hat{b} + \hat{\sigma_+}\hat{b}^\dagger + \hat{\sigma_-}\hat{b} + \hat{\sigma_-}\hat{b}^\dagger \\ &= \hat{\sigma_+}\hat{b}e^{i(\omega_0-\omega)t} + \hat{\sigma_+}\hat{b}^\dagger e^{i(\omega_0+\omega)t} + \hat{\sigma_-}\hat{b}e^{i(-\omega_0-\omega)t} + \hat{\sigma_-}e^{i(-\omega_0+\omega)t}.\end{aligned}$$

The two terms $e^{i(\omega_0-\omega)t}, e^{-i(\omega_0-\omega)t}$ do not conserve energy and for $\omega \approx \omega_0$ they vary much more rapidly than $e^{-i(\omega_0+\omega)t}, e^{i(\omega_0+\omega)t}$. Integrating the time-dependent Schrödinger equation will lead, for this terms, to oscillations of frequency containing $\omega_0 - \omega$ and $\omega_0 + \omega$. The energy non conserving terms are quickly oscillating terms and can be ignored for $|\omega_0 - \omega| \ll \omega_0 + \omega$ by making the rotation-wave approximation which is a averaging approximation over the fast oscillations. The total Hamiltonian in this approximation is then written as

$$\hat{H} = \frac{1}{2}\hbar\omega_0\hat{\sigma}_3 + \hbar\omega\hat{b}^\dagger\hat{b} + \hbar\lambda(\hat{\sigma}_+\hat{b} + \hat{\sigma}_-\hat{b}^\dagger). \tag{3.1.0.3}$$

The term $\hat{\sigma}_-\hat{b}_k$ corresponds to the emission of a photon while the atom goes from the excited state to the ground state. The term $\hat{\sigma}_+\hat{b}_k^\dagger$ corresponds to the absorbtion process of a photon while the atom goes from the ground state to the excited state.

3.2 The weak coupling limit

To begin with the formalism of the Markov dynamics, we use the general characterization of the dynamics of closed and open quantum systems [16],[15]. We first discuss the evolution of the dynamics of closed quantum systems and then use this knowledge to derive a time-dependent description of the reduced quantum system which is influenced by an environment.

3.2.1 Closed dynamics of an open quantum system

An open quantum system represents a subsystem of the combined total of the system S and the environment B. The Hilbert space of the total system $S+B$ is given by the tensor product space $\mathscr{H} = \mathscr{H}_S \otimes \mathscr{H}_B$ of the Hilbert space of system and environment. The total Hamiltonian H is taken in the form

$$H = H_S \otimes \mathbb{1}_B + \mathbb{1}_S \otimes H_B + H_I,$$

where H_S is the Hamiltonian of the open system S, H_B is the free Hamiltonian of the environment B, and H_I is the Hamiltonian of their interaction, the coupling of system and bath.
In most cases it is assumed that the combined system is closed following the Hamiltonian dynamics. This means, a closed quantum system that starts in a pure state evolves according to its Hamiltonian and remains in a pure state. The dynamics are governed by the time evolution operator $U(t) = e^{-iHt/\hbar}$ for the formal integration of the Schrödinger equation. The solution of the Schrödinger equation is represented in terms of the unitary time evolution $U(t)$ which transforms the state $|\psi(0)\rangle$ at some initial time $t_0 = 0$ to the state $|\psi(t)\rangle$ at time t

$$|\psi(t)\rangle = U(t)\,|\psi(0)\rangle = e^{-iHt/\hbar}\,|\psi(0)\rangle\,.$$

For a mathematically correct description of the statistical dynamics given by the density matrix we introduce the formalism of the Liouville space $\mathbb{L}$. This space is linear, and the elements are linear operators on a Hilbert space $\mathscr{H}$. The equation of motion of the density matrix can easily be derived from the Schrödinger equation. This equation can be written with the superoperator $\mathscr{L}$ which operates linearly on the density matrices $\rho(t)$ describing the state of the system at time t

$$\frac{d}{dt}\rho(t) = -i[H(t),\rho(t)] = -i\mathscr{L}\rho(t),$$

with the formal solution

$$\rho(t) = e^{-i\mathscr{L}t}\rho(0).$$

This equation is the von Neumann or Liouville-von Neumann equation. The dynamical maps $U(t) = e^{-i\mathscr{L}t}$ form a one-parameter group of linear maps on the system $U(t)\circ U(t_0) = U(t+t_0)\,\forall\, t, t_0 \in \mathbb{R}$. The Schrödinger equation therefore describes reversible dynamics, the dynamical map $U(t)$ preserves the spectrum of all state operators ρ_S, leaves the von Neumann entropy invariant and transforms pure states again to pure states.
Thus the total time evolution $U_{tot}(t)$ of the system and the environment alone can be considered temporarily by an unitary transformation

$$|\psi_{tot}\rangle = U_{tot}(t)\,|\psi(0)\rangle\,.$$

This approach breaks down for the dynamics of the reduced system if we include the interaction and as a result of this the influence of the thermal bath.

3.2.2 Reduced dynamics of an open quantum system

In realistic systems it is physically impossible to prevent outside influence. Thus we are only interested in a description of the time-dependent evolution of the reduced system influence by the environment.
A reduction of the state to the system degrees of freedom is given by tracing out the environment. The basis vectors of the system and of the environment Hilbert space are defined as $|m\rangle \in \mathscr{H}_S$ and $|\nu\rangle \in \mathscr{H}_B$. The open quantum system state is characterized as the combined state of the two subsystems $|\psi_{tot}\rangle = \sum_{m,\nu} a_{m\nu} |m\rangle |\nu\rangle$ with the corresponding density matrix $\rho_{tot} = |\psi_{tot}\rangle \langle\psi_{tot}|$. The reduced density matrix of the system is described by the partial trace over the environment's Hilbert space

$$\rho_S = \mathrm{Tr}_B\left(\rho_{tot}\right) = \mathrm{Tr}_B\left(\sum_{nm,\nu\mu} a_{m\mu} a^*_{n\nu} |m\rangle |n\rangle \langle\mu| \langle\nu|\right) = \sum_{m,n} C_{mn} |m\rangle \langle n|$$

with matrix elements $C_{mn} = \sum_\mu a_{m\mu} a^*_{n\nu}$. This description is the same for mixed states ρ_{tot}, because they are a statistical mixture of pure states to which the argument applies individually due to the linearity of the trace operation.
The effective dynamics of the system that results from the interaction with the environment is derived in the same way as the composite state of system and environment to the system alone. The effective dynamics of the system is obtained by a map Λ_t. This map is defined as the evolution of the composite system according to U_{tot}, followed by tracing over the environment of the system state

$$\rho(0) \to \rho(t) = \mathrm{Tr}_B[U_{tot}(t)\rho_{tot}(0)U^*_{tot}(t)] =: \Lambda_t[\rho(0)] = \Lambda_t\rho(0).$$

The map Λ_t described the initial state of the system transformed to a system state with $t > 0$. To obtain reduced dynamics, which provides an effective description of how the environment affects the time-evolution of the system, we introduce some assumptions in the context of the Markovian approximations. We assume that the initial state at time $t = 0$ is uncorrelated with the environment $\rho_S \otimes \rho_B$. Under this assumption the reduction of the open system dynamics can be visualized by the following diagram [15] which lead to a description on the level of the system

$$\begin{array}{ccc} \rho_{tot}(0) = \rho_S(0) \otimes \rho_B(0) & \xrightarrow{U_{tot}} & \rho_{tot}(t) = U_{tot}(t)\rho_{tot}U^\dagger_{tot}(t) \\ \mathrm{Tr}_B \downarrow & & \downarrow \mathrm{Tr}_B \\ \rho(0) & \xrightarrow[\Lambda_t]{} & \rho_t = \Lambda_t\rho(0) \end{array}$$

The time evolution of the reduced dynamics can be described by an approximation of the Schrödinger equation or more precisely the von Neumann equation under the condition of short environmental correlation times. Such times allow us to neglect memory effects and give a formulation in terms of a quantum dynamical semigroup for the reduced system dynamics. This gives an efficient description of the reduced dynamics of the system ρ_S in terms of time-evolutions consisting of the one parameter semigroups. Such semigroups define linear maps $U(t) = e^{\mathscr{L}t}$ with $t > 0$ which act on all possible initial density matrices of the system ρ_S and describe their evolution by $\rho_S(t) = U(t)\rho_S$ at time t. This defines the following abstract equation of the reduced system dynamics in the context of these maps by a generator $\mathscr{L}$

$$\frac{d\rho_S(t)}{dt} = \mathscr{L}\rho_S(t).$$

To end up in a physical correct description of the time-evolution of the system state, the generator has to fulfill several formal conditions which can be shown intuitively. A primary consequence of an environment is that the

dissipative effects transform the pure system states, projections onto the Hilbert space vectors to mixtures of projections. This means that after a certain time the pure initial state of the system evolves to a generic density matrix. These are operators with discrete spectrums consisting of positive eigenvalues summing up to one in the context of the statistical interpretation of quantum mechanics. Thus any description of a reduced system must include a map Λ_t which fulfils the following properties with the assumption that the initial state is uncorrelated [15].

- **Linearity:** $\Lambda_t(p_A\rho_A + p_B\rho_B) = p_A\Lambda_t(\rho_A) + p_B\Lambda_t(p_B)$,
- **Positivity:** $\Lambda_t(\rho) \geq 0 \, \forall \rho \geq 0$,
- **Complete positivity:** $\mathbb{1}_d \otimes \Lambda_t(\rho) \geq 0 \forall \rho \geq 0$ and any size d of the trivial extension to a higher dimension space,
- **Hermiticity-preserving:** $\Lambda_t(\rho)^\dagger = \Lambda_t(\rho)$ for a Hermitian ρ
- **Trace-preserving:** $Tr[\Lambda_t(\rho)] = Tr\rho = 1$.

The detailed mathematical proof for several conditions of the generator $\mathscr{L}$ of a quantum dynamical semigroup for the case of a finite-dimensional Hilbert space is given by Lindblad.
The reduced dynamics is a non-unitary dynamics which shows dissipative effects and thus cannot be evolved backwards in time. For example, an excited atom which is in a thermal bath will radiate a photon and decohere, but the bath will not return the atom back to its excited state. Thus if we consider a system influenced by a thermal bath, the considered reduced system dynamics converges to a unique stationary state regardless of the initial condition. The Lindblad equation describes the reduced system dynamics or more precise the long time behavior, the asymptotic dynamics and the steady-state properties of the thermal occupation of the system where we are interested in. The representation of a trace-preserving, strongly continuous, completely positive semi-group leads to the first standard form of the generator and thus to the Linblad equation [17]

$$\frac{d\rho}{dt} = -i[H_S, \rho] + \sum_{lk} a_{lk}\left(V_i\rho V_j^\dagger - \frac{1}{2}\{V_j^\dagger V_i, \rho\}\right)$$

with the coefficient matrix (a_{lk}) being hermitian and positive. The equation can be diagonalized with the help of an appropriate unitary transformation u $(ua_{kl}u^\dagger)$,

$$\frac{d\rho}{dt} = -i[H_S, \rho] + \sum_k \gamma_k\left(2A_k\rho A_k^\dagger - A_k^\dagger A_k\rho - \rho A_k^\dagger A_k\right)$$

The first term of the above representation is the unitary part of the dynamics generated by the system Hamiltonian H_S. The second term describes the influence of a perturbation, the coupling to an infinite reservoir generates the dissipative dynamics, also known as the dissipator. The operators A_k introduced above are usually referred to as Lindblad operators. Any Markovian master equation that fulfills the requirements of generating trace-preserving and completely positive dynamics has Lindblad form.

3.2.3 Derivation of the master equation

For the derivation of the master equation we use the iterative method according to Breuer and Petuccione [15]. We consider a system of n degenerate qubits linearly coupled to a thermal bath with temperature T, where we assume that the coupling is weak. The total Hamiltonian of the full system is then defined by the system H_S, its environment H_B and a system-bath interaction H_I: $H = H_S + H_B + H_I$. The von Neumann equation in the interaction picture has the form

$$\frac{d}{dt}\rho^I(t) = -i[H_I^I, \rho^I(t)] \tag{3.2.3.1}$$

with the solution

$$\rho^I(t) = \rho^I(0) - i\int_0^t [H_I^I(s), \rho^I(s)]ds.$$

The index I indicates the interaction picture representation of the Hamiltonian. We assume that $\mathrm{Tr}_B([H_I^I(t), \rho^I(0)]) = 0$, insert this expression into equation (3.2.3.1) and trace over the bath with its equilibrium distribution ρ_B^I. The first iteration of the von Neumann equation for the reduced density matrix $\rho_S^I = \mathrm{Tr}_B(\rho^I)$ is then given by

$$\frac{d}{dt}\rho_S^I = -\int_0^t \mathrm{Tr}_B([H_B^I(t), [H_I^I(s), \rho^I(s)]])ds.$$

This equation contains the Born approximation $\rho(t) \approx \rho_S(t) \otimes \rho_B$ so that the influence of the system on the reservoir can be neglected as a justification of the assumed weak coupling between the system and the bath. The Markov approximation is justified by assuming that the bath correlation time τ_B is small compared to the relaxation time of the system τ_S ($\tau_B << \tau_S$) and thus we can change the integration over s into one over $t-s$ and evolve ρ at time t only

$$\frac{d}{dt}\rho_S^I(t) = -\int_0^\infty \mathrm{Tr}_B([H_I^I(t), [H_I^I(t-s), \rho^I(t)]])ds. \tag{3.2.3.2}$$

The interaction Hamiltonian H_I for an n qubit system interacting with a thermal bath is described by the Jaynes-Cummings model (3.1.0.3). To obtain a mathematically correct formulation for such a system, we introduce a summation over the creation operator $\hat{\sigma}_+$ and annihilation operator $\hat{\sigma}_-$ of each qubit.

$$H_I = \sum_i \sum_k d_i(\hat{\sigma}_+^i \hat{b}_k) + d_i^*(\hat{\sigma}_-^i \hat{b}_k^\dagger), \tag{3.2.3.3}$$

where the d_i and d_i^* describe the coupling between the system and the bath. The system operators are eigenoperators of the system Hamiltonian H_S with a continuous spectrum of the frequency ω. The corresponding interaction picture system operators have the form

$$e^{iH_St}\hat{\sigma}_\pm e^{-iH_St} = e^{-i\omega t}\hat{\sigma}_\pm,$$
$$e^{iH_St}\hat{\sigma}_\pm^\dagger e^{-iH_St} = e^{i\omega t}\hat{\sigma}_\pm^\dagger.$$

The representation of the bath operators b_k and $b_k^\dagger$ in the interacting picture is defined similar. In our derivation we use the interaction picture representation of the interaction Hamiltonian (3.2.3.3) and insert it in the equation of motion (3.2.3.2)

$$
\begin{aligned}
\frac{d}{dt}\rho_S^I(t) &= \int_0^\infty ds \,\mathrm{Tr}_B H_I(t-s)\rho_S(t)\rho_B H_I(t) H_I(t-s)\rho_S(t)\rho_B + h.c \\
&= \int_0^\infty ds \sum_{i,j}\sum_{\omega,\omega'} e^{i\omega(t-s)}[d_j\sigma_-^{(j)} b_k(\omega,t-s)\rho_S(t)e^{-i\omega t} d_i^*\sigma_+^{(i)} b_k^\dagger(\omega,t) \\
&\qquad - e^{i\omega' t} d_j^*\sigma_+^{(i)} b_k^\dagger(\omega,t) e^{-i\omega(t-s)} d_j\sigma_-^{(j)} b_k(\omega,t-s)\rho_S(t) + h.c \\
&\qquad + d_i^*\sigma_+^{(i)} b_k^\dagger(\omega,t-s)\rho_S(t)e^{-i\omega t} d_j\sigma_-^{(j)} b_k(\omega,t) \\
&\qquad - e^{-i\omega' t} d_j\sigma_-^{(j)} b_k(\omega,t) e^{-i\omega(t-s)} d_i^*\sigma_+^{(i)} b_k^\dagger(\omega,t-s)\rho_S(t) + h.c] \\
&= \sum_{i,j}\sum_{\omega,\omega'} e^{i(\omega'-\omega)t}\int_0^\infty ds e^{i\omega s}[(d_j\sigma_-^{(j)} b_k(\omega,t-s)\rho_s(t) d_i^*\sigma_+^{(i)} b_k^\dagger(\omega',t) \\
&\qquad - d_i^*\sigma_+^{(i)} b_k^\dagger(\omega,t) d_j\sigma_-^{(j)} b_k(\omega,t-s)\rho_S(t)) + h.c. \\
&\qquad + (d_i^*\sigma_+^{(i)} b_k(\omega,t-s)\rho_S(t) d_j\sigma_-^{(j)} b_k^\dagger(\omega',t) \\
&\qquad - d_j\sigma_-^{(j)} b_k^\dagger(\omega,t) d_i^*\sigma_+^{(i)} b_k(\omega,t-s)\rho_S(t)) + h.c.] \\
&\overset{1}{=} \sum_{i,j}\sum_{\omega,\omega'} e^{i(\omega-\omega')t}\int_0^\infty ds e^{i\omega s}[\langle b_k^\dagger(\omega,t) b_k(\omega,t-s)\rangle (d_j\sigma_-^{(j)}\rho_S(t) d_i^*\sigma_+^{(i)} - d_i^*\sigma_+^{(i)} d_j\sigma_-^{(j)}\rho_S(t)) + h.c \\
&\qquad + \langle b_k(\omega,t) b_k^\dagger(\omega,t-s)\rangle (d_i^*\sigma_+^{(i)}\rho_S(t) d_j\sigma_-^{(j)} - d_j\sigma_-^{(j)} d_i^*\sigma_+^{(i)}\rho_S(t)) + h.c.] \\
&\overset{2}{=} \sum_{i,j}\sum_{\omega}\int_0^\infty ds e^{i\omega s}[\langle b_k^\dagger(\omega,t) b_k(\omega,t-s)\rangle (d_j\sigma_-^{(j)}\rho_S(t) d_j^*\sigma_+^{(j)} - d_i^*\sigma_+^{(i)} d_j\sigma_-^{(j)}\rho_S(t)) + h.c. \\
&\qquad + \langle b_k(\omega,t) b_k^\dagger(\omega,t-s)\rangle (d_i^*\sigma_+^{(i)}\rho_S(t) d_j\sigma_-^{(j)} - d_j\sigma_-^{(j)} d_i^*\sigma_+^{(i)}\rho_S(t)) + h.c.],
\end{aligned}
$$

The one-sided Fourier transform of the reservoir correlation function is calculated with the formula

$$
\int_0^\infty ds e^{-i\epsilon s} = \pi\delta(\epsilon)s - i\mathscr{P}\frac{1}{\epsilon}
$$

for both frequencies,

$$
\begin{aligned}
\text{for} \quad \omega<0 \quad \Gamma_{kk'}(\omega) &= \int_0^\infty ds e^{i\omega s}\langle b_k^\dagger b_k(\omega,t-s)\rangle \\
&= N(\omega_k)\int_0^\infty ds e^{i(\omega_k+\omega)s} \\
&= N(\omega_k) + i\mathscr{P}\int_0^\infty d\omega_k\left[\frac{N(\omega_k)}{\omega+\omega_k}\right] \\
\text{for} \quad \omega>0 \quad \Gamma_{kk'}(\omega) &= \int_0^\infty ds e^{i\omega s}\langle b_k b_k^\dagger(\omega,t-s)\rangle \\
&= (1+N(\omega_k))\int_0^\infty ds e^{-i(\omega_k-\omega)s} \\
&= (1+N(\omega_k)) + i\mathscr{P}\int_0^\infty d\omega_k\left[\frac{(1+N(\omega_k))}{\omega-\omega_k}\right]
\end{aligned}
$$

[1] $\omega' \to -\omega$

[2] Rotating wave approximation, averaging approximation over fast oscillations

where $\mathscr{P}$ denotes the Cauchy principal value. The decomposition of these two transformations in the real and the imaginary part define the contribution to the dissipative part $\gamma(\pm\omega)$ and the unitary part $S(\pm\omega)$

$$\gamma(\omega) = (1+N(\omega_k)) \quad S(\omega) = \mathscr{P}\int_0^\infty d\omega_k \left[\frac{(1+N(\omega_k))}{\omega-\omega_k}\right]$$
$$\gamma(-\omega) = N(\omega_k) \qquad S(-\omega) = \mathscr{P}\int_0^\infty d\omega_k \left[\frac{N(\omega_k)}{\omega+\omega_k}\right].$$

With these definitions we finally arrive at the interaction picture master equation

$$\frac{d}{dt}\rho_S(t) = -i[H_{LS},\rho_S(t)] + \mathscr{D}(\rho_S(t)) \tag{3.2.3.4}$$

with

$$\begin{aligned} H_{LS} &= \sum_{\pm\omega}\sum_{i,j}[S(-\omega)d_j\sigma_-^{(j)}d_i^*\sigma_+^{(i)} + S(\omega)d_i^*\sigma_+^{(i)}d_j\sigma_-^{(j)}] \\ &= \mathscr{P}\int_0^\infty d\omega_k \left[\left[\frac{(1+N(\omega_k))}{\omega-\omega_k}\right]\sum_{i,j} d_i^*\sigma_+^{(i)}\sigma_-^{(j)} + \mathscr{P}\int_0^\infty d\omega_k\left[\frac{N(\omega_k)}{\omega+\omega_k}\right]\sum_{i,j} d_j d_i^*\sigma_-^{(j)}\sigma_+^{(i)}\right]. \end{aligned} \tag{3.2.3.5}$$

This term is often called the Lamb-shift Hamiltonian since it leads to a Lamb-type renomalization of the unperturbed energy levels induced by the system-reservoir coupling. The dissipator of the master equation takes the form

$$\begin{aligned} \mathscr{D}(\rho_S) =& N(\omega_k)(\sum_{i,j} d_i^*\sigma_+\rho_S(t)d_j\sigma_-^{(j)} - \frac{1}{2}\sum_{i,j} d_j\sigma_-^{(j)}d_i^*\sigma_+^{(i)}\rho_S(t) - \frac{1}{2}\rho_S(t)\sum_{i,j} d_j\sigma_-^{(j)}d_i^*\sigma_+^{(i)}) \\ & (1+N(\omega_k))(\sum_{i,j} d_j\sigma_-\rho_S(t)d_i^*\sigma_+^{(i)} - \frac{1}{2}\sum_{i,j} d_i^*\sigma_+^{(i)}d_j\sigma_-^{(j)}\rho_S(t) - \frac{1}{2}\rho_S(t)\sum_{i,j} d_i^*\sigma_+^{(i)}d_j\sigma_-^{(j)}). \end{aligned}$$

The dissipator of the master equation describes thermally induced emission $\propto (1+N(\omega_k))$ and absorption process $\propto N(\omega_k)$. The master equation (3.2.3.4) can be considered in two different limits.

Spontaneous emission

In the limit of small temperatures $T \to 0$, the system dynamics is dominated by spontaneous emission of energy quanta into the bath modes. Therefore there is only the term of spontaneous emission

$$\gamma(\omega) = N(\omega_k)$$

so that the system evolution is described by the following master equation

$$\frac{d}{dt}\rho_S(t) = N(\omega_k)\left(\sum_{i,j} d_i^*\sigma_+\rho_S(t)d_j\sigma_-^{(j)} - \frac{1}{2}\sum_{i,j} d_j\sigma_-^{(j)}d_i^*\sigma_+^{(i)}\rho_S(t) - \frac{1}{2}\rho_S(t)\sum_{i,j} d_j\sigma_-^{(j)}d_i^*\sigma_+^{(i)}\right).$$

This decoherence process is the fundamental limit for coherent atomic dynamics.

T infinity case

In the limit of large bath temperatures $T \to \infty, N(\omega_k) \to \infty, (1+N(\omega_k)) \to N(\omega_k) < \infty$, the emission and absorption rates are almost equal

$$\frac{N(\omega_k)}{N(\omega_k)} \overset{T\to\infty}{\longrightarrow} 1$$

The T-infinity case is a process with equal probabilities for a jump from the ground to the excited state and vice versa (bit-flips). The jump operators are

$$\gamma(-\omega) = N(\omega_k) \quad \gamma(\omega) = N(\omega_k)$$

and the master equation reads

$$\begin{aligned}\frac{d}{dt}\rho = N(\omega_k)(d_i^*\sigma_+^{(i)}\rho_S(t)d_j\sigma_-^{(j)} - \frac{1}{2}d_j\sigma_-^{(j)}d_i^*\sigma_+^{(i)}\rho_S(t) - \frac{1}{2}\rho_S(t)d_j\sigma_-^{(j)}d_i^*\sigma_+^{(i)} \\ + N(\omega_k)(d_j\sigma_-^{(j)}\rho_S(t)d_i^*\sigma_+^{(i)} - \frac{1}{2}d_i^*\sigma_+^{(i)}d_j\sigma_-^{(j)}\rho_S(t) - \frac{1}{2}\rho S(t)d_i^*\sigma_+^{(i)}d_j\sigma_-^{(j)}).\end{aligned}$$

3.2.4 Calculation of the Lamb-shift integrals

The principal-value integrals need to be calculated for the numerical results of the master equation

$$\begin{aligned}\mathscr{P}_1 = \mathrm{Im}(|\omega|) = \mathscr{P}\int_0^\infty d\omega_k \left[\frac{(1+N(\omega_k))}{\omega-\omega_k}\right] \\ \mathscr{P}_2 = \mathrm{Im}(-|\omega|) = \mathscr{P}\int_0^\infty d\omega_k \left[\frac{N(\omega_k)}{\omega+\omega_k}\right].\end{aligned} \tag{3.2.4.1}$$

The integrals have the following dependence

$$\mathscr{P}_1 = \mathscr{P}\int_0^\infty d\omega_k \frac{1}{\omega-\omega_k} + \int_0^\infty \frac{N(\omega_k)}{\omega-\omega_k} = \mathscr{P}\int_0^\infty d\omega_k \frac{1}{\omega-\omega_k} - \mathscr{P}_2. \tag{3.2.4.2}$$

These integrals diverge for low and high frequencies, thus we have to introduce a correct approximation of these integrals. G.S Agrawal [18] introduced such an approximation in the context of two assumptions. The first assumption is that the frequency dependent pre-factors of the Jaynes-Cummings interaction Hamiltonian (3.2.3.3) can be ignored by introducing the dipole approximation in the derivation. The second assumption is that the spectral function $J(\omega)$ is constant. Then it is possible to introduce the following cut-off and integrate only from 2ω to ω_c

$$\int_{2\omega}^{\omega_c} d\omega_k \frac{1}{\omega-\omega_k} = -\ln\left(\frac{\omega_c}{\omega} - 1\right),$$

where ω_c is the cut-off frequency. With this property we end up with a logarithmic divergence of the principal-value integrals which has a qualitative influence of the Lamb-shift. The values of the integrals can be estimated as $\mathscr{P}_1 = -3,2$ whereby we set the integral $\mathscr{P}_2 = 1$ and use the dependency (3.2.4.2) for the calculation of the second integral.

3.3 Decoherence-free subspaces

So far, we have discussed the theory of an open system involving a single quantized mode of the field interaction with atoms, described by the Jaynes-Cummings model introduced in section 2.1. As we saw in this model, the transition dynamics between the two energy levels of the ground and the excited states are coherent and reversible. In contrast to the reduced system dynamics of an open quantum system which is not reversible and shows decoherence as a result of the interaction between the system and the environment. Decoherence can be described as a transformation over the time of an initial system state into a classical mixture as a result of

the interaction with an environment. Thus the degrees of freedom of the environment affect the state of the reduced system, and the information given by correlations of the originally state is lost. To prevent decoherence in systems of open quantum systems we introduce decoherence-free subspaces and subsystems [19]. The theory of such subsystems is based on the symmetry of the system-environment coupling. We have to consider two different constructions of the decoherence-free subspaces and subsystems, because the symmetry is different for an even or an odd number of qubits. We first discuss the decoherence-free subspace for an even number of qubits which gives a fundamental description of the theory and then the more difficult description for an odd number of qubits.

3.3.1 Decoherence-free subspaces for an even number of qubits

As remarked above, decoherence is the result of entanglement between the system and the thermal bath caused by the interaction Hamiltonian H_I [20]. Thus a reduced system will show no decoherence when the interaction Hamiltonian is zero. Then the system and the bath are decoupled and both evolve unitarily by their Hamiltonians H_S and H_B. Most physical systems cannot be described without interaction between the bath and the system, and thus $H_I \equiv 0$ is not a satisfactory condition for a decoherence-free subspace. To obtain a decoherence-free subspace of the full Hilbert space $\mathscr{H}$ without switching off the system bath interaction it must be possible to attain a unitary evolution of the reduced system. This can be achieved by a set $\{|k\rangle\}$ of eigenvectors of the system operators S_α with the characteristic

$$S_\alpha |\tilde{k}\rangle = c_\alpha |\tilde{k}\rangle \quad \forall \alpha, |\tilde{k}\rangle\,, \tag{3.3.1.1}$$

where the eigenvalue c_α depends only on the index α of the system operator, but not on the state index k. If the system Hamiltonian H_S leaves the subspace spanned by the degenerate eigenvectors $\tilde{\mathscr{H}} = \mathrm{Span}\,[|k\rangle]$ invariant, the time evolution is unitary and the interaction Hamiltonian has no influence on the system Hamiltonian [20].

To prove this definition of the decoherene free-subspace we follow the derivation in [19]. The initial density matrices of the system and the bath can be described in their basis $\rho_S(0) = \sum_{mn} a_{mn} |\tilde{m}\rangle \langle\tilde{n}|$ and $\rho_B(0) = \sum_{\nu\mu} b_{\nu\mu} |\tilde{\nu}\rangle \langle\tilde{\mu}|$. We define a combined Hamiltonian of the system and the bath as $H_C = H_S + H_B$ which clearly commutes $[H_C, H_S]$ with the system Hamiltonian H_S over the Hilbert space $\tilde{H}$. Thus the time evolution of both systems is unitary by $U_S = \exp(-i H_S t)$ and $U_C = \exp(-i H_C t)$. It can be written in the following way

$$U[|\tilde{m}\rangle \otimes |\tilde{\nu}\rangle] = U_S |\tilde{m}\rangle \otimes U_C |\tilde{\nu}\rangle\,.$$

The initially decoupled state of the density matrix evolves then as $\rho_{SB}(t) = \sum_{mn} a_{mn} U_S |\tilde{m}\rangle \langle\tilde{n}| U_S^\dagger \otimes \sum_{\nu\mu} b_{\nu\mu} U_S |\tilde{\nu}\rangle \langle\tilde{\mu}| U_S^\dagger$. The reduced density matrix of the system is obtained by tracing out the degrees of freedom of the environment $\rho_S(t) = \mathrm{Tr}_B[\rho_{SB}(t)] = U_S \rho_S(0) U_S^\dagger$. This shows that the system evolves completely unitary on $\tilde{H}$ and $\tilde{H}$ is a decoherence-free subspace. Thus we end up with the following theorem of a decoherence-free subsystem [20].

Theorem 1. Let the interaction between a system and a bath be given by the Hamiltonian $H = H_S \otimes \mathbb{1}_B + \mathbb{1}_S \otimes H_B + H_I$. If H_S leaves the Hilbert subspace $\tilde{\mathscr{H}} = Span[\{|\tilde{k}\rangle\}]$ invariant and if we start within $\tilde{\mathscr{H}}$, then $\tilde{\mathscr{H}}$ is a decoherence-free subspace if and only if it satisfies the condition $S_\alpha |\tilde{k}\rangle = c_\alpha |\tilde{k}\rangle \quad \forall \alpha, |\tilde{k}\rangle$

A decoherence-free subspaces can also be defined in the Lindblad-semigroup formulation which we introduced in section 2.3. The Lindblad master equation describes the time-dependent evolution of the reduced system by the unitary part and the perturbative part which lead to dissipative effects. It is obvious that the dissipative term defined by the Linblad operators A_α leads to decoherence of the subsystem.

$$\mathscr{D}(\rho_S) = \sum_{\alpha,\beta} \gamma_{\alpha\beta} \left(A_\alpha \rho_S A_\beta^\dagger - \frac{1}{2} A_\beta^\dagger A_\alpha \rho_S - \frac{1}{2} \rho_S A_\beta^\dagger A_\alpha \right). \tag{3.3.1.2}$$

A necessary and sufficient condition for a decoherence-free subspace in the context of the Lindblad equation is that the influence of the dissipator should not play a role. With this knowledge we can derive a mathematical formalism of decoherence-free subspaces especially for the Lindblad master equation [20]. Let $\{|\tilde{k}\rangle\}_{k=1}^N$ be the basis of an N-dimensional subspace $\tilde{\mathscr{H}} \subseteq \mathscr{H}$ and the density matrix given in this basis is

$$\tilde{\rho} = \sum_{k,j=1}^{N} \rho_{kj} |\tilde{k}\rangle \langle \tilde{j}|.$$

The Lindblad operators A_α applied to the basis lead to $A_\alpha |\tilde{k}\rangle = \sum_{j=1}^N c_{kj}^\alpha |j\rangle$. The dissipator term of the master equation 3.3.1.2 can be rewritten in terms of this basis transformation in the following way

$$\begin{aligned}
\mathscr{D}(\rho_S) &= \sum_{\alpha,\beta} \gamma_{\alpha,\beta} \sum_{k,j=1} \left(A_\alpha \rho_{kj} |\tilde{k}\rangle \langle \tilde{j}| A_\beta^\dagger - \frac{1}{2} A_\beta^\dagger A_\alpha \rho_{kj} |\tilde{k}\rangle \langle \tilde{j}| - \frac{1}{2} \rho_{kj} |\tilde{k}\rangle \langle \tilde{j}| A_\beta^\dagger A_\alpha \right) \\
&= \sum_{\alpha,\beta} \gamma_{\alpha,\beta} \sum_{k,j=1} \rho_{kj} \left(A_\alpha |\tilde{k}\rangle \langle \tilde{j}| A_\beta^\dagger - \frac{1}{2} A_\beta^\dagger A_\alpha |\tilde{k}\rangle \langle \tilde{j}| - \frac{1}{2} |\tilde{k}\rangle \langle \tilde{j}| A_\beta^\dagger A_\alpha \right) \\
&\overset{1}{=} \sum_{\alpha,\beta} \gamma_{\alpha,\beta} \sum_{k,j=1} \rho_{kj} \left(c_{jm}^{*\beta} c_{kn}^\alpha |\tilde{n}\rangle \langle \tilde{m}| - c_{km}^{*\beta} c_{kn}^\alpha |\tilde{m}\rangle \langle \tilde{j}| - c_{jm}^{*\beta} c_{kn}^\alpha |\tilde{m}\rangle \langle \tilde{j}| \right)
\end{aligned}$$

with $c_{kn}^\alpha = c_\alpha \delta_{kn}$ we get

$$\mathscr{D}(\rho_S) = \sum_{\alpha,\beta} \gamma_{\alpha,\beta} \sum_{k,j=1} \rho_{kj} |\tilde{k}\rangle \langle \tilde{j}| \left(c_j^{*\beta} c_k^\alpha - \frac{1}{2} c_k^{*\beta} c_k^\alpha - \frac{1}{2} c_j^{*\beta} c_j^\alpha \right).$$

The last two terms of this equation can be rewritten as $\frac{c_j^\alpha}{2c_k^\alpha} + \frac{c_k^\beta}{2c_j^\beta} = 1$ for $\alpha = \beta$. Thus the dissipator $\mathscr{D}(\rho_S)$ is zero and does not lead to decoherence of the reduced system when we assume that there is no dependence on ρ_{jk} and every term of the dissipator vanishes separately. This is achieved by only one projection operator $|\tilde{n}\rangle \langle \tilde{m}|$. The unitary part of the master equation is a decoherence-free subspace when the system Hamiltonian H_S commutes with the full Hamiltonian H over the N-dimensional subspace which is always fulfilled when there are no special conditions on the reduced system. Thus we end up with the following theorem of a decoherence-free subspace for the Lindblad master-equation [20]:

Theorem 2. If no special assumptions are made on the coefficient matrix $\gamma_{\alpha\beta}$ and on the initial conditions ρ_{kj} then a necessary and sufficient condition for a subspace $\tilde{\mathscr{H}} = Span[\{\tilde{k}_{k=1}^N\}]$ to be decoherence-free is that all basis states $|\tilde{k}\rangle$ are degenerate eigenstates of all the Lindblad operators $\{A_\alpha\}$

$$A_\alpha |\tilde{k}\rangle = c_\alpha |\tilde{k}\rangle \quad \forall \alpha, |\tilde{k}\rangle. \tag{3.3.1.3}$$

This theoretical description of decoherence-free subspaces for an even number of qubits can be clarified by using the example of two qubits embedded in a thermal bath. The system operators are defined by the annihilation σ_- and creation operator σ_+ of the qubits. For this system in the basis $\{|11\rangle, |10\rangle, |01\rangle, |00\rangle$ there is only one degenerate eigenvector $|k\rangle$ that fulfills the condition (3.3.1.1) which is the entangled singlet state

[1] $\sum_k F_\alpha |\tilde{k}\rangle = \sum_k c_{kn}^\alpha |\tilde{k}\rangle$ and $\sum_j F_\beta |\tilde{j}\rangle = \sum_j c_{jm}^\beta |\tilde{m}\rangle$

$|s\rangle = \frac{1}{\sqrt{2}}(|10\rangle - |01\rangle)$. That this is an eigenvector can easily be shown by applying the interaction Hamiltonian H_I to the singlet state.

$$\begin{aligned} H_I|s\rangle &= \sum_{i,j}[d_i^*(\sigma_+^{(i)}b_k) + d_j(\sigma_-^{(j)}b_k^\dagger)]\,|s\rangle \\ &= \frac{1}{\sqrt{2}}(d_1^*\sigma_+ b_k|10\rangle + d_2^*\sigma_+ b_k|10\rangle + d_1\sigma_- b_k^\dagger|10\rangle + d_2\sigma_- b_k^\dagger|10\rangle \\ &- d_1^*\sigma_+ b_k|01\rangle + d_2^*\sigma_+ b_k|01\rangle + d_1\sigma_- b_k^\dagger|01\rangle + d_2\sigma_- b_k^\dagger|01\rangle) \\ &= \frac{1}{\sqrt{2}}(d_2^* - d_1)|10\rangle + (d_1^* - d_2)|01\rangle \\ &= |s\rangle \end{aligned}$$

For equal coupling constants $|d_1| = |d_2|$ the applied Hamiltonian to the singlet gives zero. Therefore, the interaction Hamiltonian has no influence on this state, and is shown that there is a decoherence-free subspace for two qubits.

3.3.2 Decoherence-free subspaces for an odd number of qubits

For an odd number of qubits there is no set $\{|k\rangle\}$ of eigenvectors of the system operator S_α with the property (3.3.1.1). Therefore, we must introduce another formulation for decoherence-free subspaces which is based on the symmetries of the coupling between the system and the bath. Such a symmetric coupling to the thermal bath can only be obtained by transforming the originally reduced system states to an encoded subspace with higher dimensions. This definition of an encoded subspace allows a symmetric consideration of the bath's influences on the different states. To be more precise, as a result of the higher dimensions it is possible to encode the qubit in different subclasses where the bath's influences keep the state in there classes and thus this encoded space is a decoherence-free subspace. Brooke et al [21] introduced such kinds of decoherence-free subspaces by encoding a number of qubits.

To obtain an intuitive understanding of decoherence-free subspaces of an odd number of qubits we consider the case of one qubit encoded with the symmetry properties of the spin-half of three qubits. The total spin of three qubits is either $S = \left(\frac{3}{2}\right)$ or $S = \left(\frac{1}{2}\right)$ with the spin projection $m_S = \left(\frac{3}{2}, \frac{-3}{2}, \frac{1}{2}, \frac{-1}{2}\right)$. The spin states in the basis $|S, m_S\rangle$ are defined as $\{|\frac{3}{2}, \frac{-3}{2}\rangle, |\frac{3}{2}, \frac{-1}{2}\rangle, |\frac{1}{2}, \frac{-1}{2}\rangle, |\frac{1}{2}, \frac{-1}{2}\rangle, |\frac{1}{2}, \frac{1}{2}\rangle, |\frac{1}{2}, \frac{1}{2}\rangle, |\frac{3}{2}, \frac{1}{2}\rangle, |\frac{3}{2}, \frac{3}{2}\rangle\}$. The subsystem for the logical $|1\rangle_L$ and $|0\rangle_L$ is obtained by writing the spin basis states $|\frac{1}{2}, \frac{-1}{2}\rangle, |\frac{1}{2}, \frac{1}{2}\rangle$ in the Clebsch-Gordan basis.

Total spin $S = 0$ with spin projection $m_s = 0$

- $|\frac{1}{2}\frac{1}{2}\rangle \longrightarrow |0,0\rangle \otimes |\frac{1}{2}\rangle = \frac{1}{\sqrt{2}}(|101\rangle - |011\rangle)$
- $|\frac{1}{2}\frac{-1}{2}\rangle \longrightarrow |0,0\rangle \otimes |\frac{1}{2}\rangle = \frac{1}{\sqrt{2}}(|100\rangle - |010\rangle)$

Total spin $S = \frac{1}{2}$ with spin projection $m_s = \pm\frac{1}{2}$

- $|\frac{1}{2}\frac{1}{2}\rangle \longrightarrow \sqrt{\frac{3}{2}}(|1,1\rangle \otimes |\frac{1}{2}, \frac{-1}{2}\rangle) = \frac{1}{\sqrt{6}}(2|110\rangle - |101\rangle - |011\rangle)$
- $|\frac{1}{2}\frac{-1}{2}\rangle \longrightarrow \frac{1}{\sqrt{6}}(|010\rangle + |100\rangle) - \sqrt{\frac{2}{3}}|001\rangle = \frac{1}{\sqrt{6}}(-2|001\rangle + |010\rangle + |100\rangle$

The qubit is therefore encoded as

$$|1\rangle_L = \begin{cases} |c\rangle = \frac{1}{\sqrt{2}}(|010\rangle - |100\rangle) \\ |f\rangle = \frac{1}{\sqrt{2}}(|011\rangle - |101\rangle) \end{cases}$$

$$|0\rangle_L = \begin{cases} |b\rangle = \frac{1}{\sqrt{6}}(-2|001\rangle + |010\rangle + |100\rangle) \\ |e\rangle = \frac{1}{\sqrt{6}}(2|110\rangle - |101\rangle - |011\rangle) \end{cases} .$$

The results are depicted in the following picture, where the states are labeled according to $|S, m_s\rangle$ and the two isolated subspaces are circled according to the logical basis.

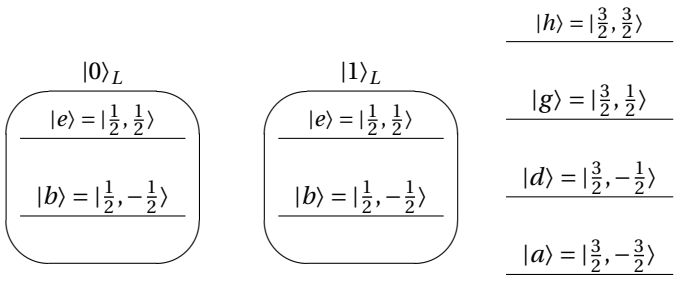

Figure 3.1: Representation of the decoherence-free subspaces for one encoded qubit by three qubits [21].

That the encoded logical $|0\rangle_L$ and $|1\rangle_L$ define a decoherence-free subspace by their symmetry properties can be proved by applying the interaction Hamiltonian to the encoded states. Thus we consider the effect of the thermal bath to these encoded subspaces by superpositions of these states $|1\rangle_L = \alpha|c\rangle + \beta|f\rangle$ and $|0\rangle_L = \alpha|b\rangle + \beta|e\rangle$ with the normalization $|\alpha|^2 + |\beta|^2 = 1$. This gives for the logical $|1\rangle_L$

$$
\begin{aligned}
H_I|1\rangle_L = H_I(\alpha|c\rangle + \beta|f\rangle) &= \sum_{i,j}^{3}[d_i^*(\sigma_+^{(i)} b_k) + d_j(\sigma_-^{(j)} b_k^\dagger)]\frac{1}{\sqrt{2}}(\alpha(|010\rangle - |100\rangle) + \beta(|011\rangle - |101\rangle)) \\
&= \frac{1}{\sqrt{2}}(d_1^*\sigma_+ b_k(-\alpha|100\rangle - \beta|101\rangle) + d_2^*\sigma_+ b_k(\alpha|010\rangle + \beta|011\rangle) + d_3^*\sigma_+ b_k(\beta|011\rangle - \alpha|101\rangle) \\
&+ d_1\sigma_- b_k^\dagger(\alpha|010\rangle + \beta|011\rangle) + d_2\sigma_- b_k^\dagger(-\alpha|100\rangle - \beta|100\rangle) + d_3\sigma_- b_k^\dagger(\alpha|010\rangle - \beta|100\rangle)) \\
&= \frac{1}{\sqrt{2}}(\alpha((d_1 + d_2^* + d_3)|010\rangle - (d_1^* + d_2 + d_3)|100\rangle) + \beta((d_1 + d_2^* + d3^*)|011\rangle - (d_1^* + d_2 + d3^*)|101\rangle) \\
&= |1\rangle_L
\end{aligned}
$$

and the calculation for the logical $|0\rangle_L$ is similar

$$H_I|0\rangle_L = |0\rangle_L$$

Thus the interaction Hamiltonian has no influence when the qubits are coupled equally to the thermal bath $|d_1| = |d_2| = |d_3|$. The interaction Hamiltonian does not lead to transitions between states which have different symmetry. This means the bath operators $\hat{b}_k, \hat{b}_k^\dagger$ do not cause quantum information to decay from $|1\rangle_L$ to $|0\rangle_L$ or vice versa. Thus these defined encoded subspaces are really decoherence-free subsystems.

But this definition of the decoherence-free subspaces has the disadvantage that the transformation to the encoded subspace with higher dimensions is necessary and thus this mathematical formalism cannot be used for real physical systems.

Chapter 4

Entanglement dynamics for two qubits interacting with an environment

4.1 Theory of the entanglement dynamics for two qubits

The consideration of two qubits is the simplest model for entanglement; there is a fundamental description of the full entanglement of these quantum systems. We consider a bipartite quantum system embedded in a thermal bath, the interaction between the qubit system and the entanglement dynamics leads to an exchange in energy and entropy and thus to entanglement effects. Such effects are related to the coupling constants d_1 and d_2, which define the coupling between system and environment. The dynamics of this open quantum system is described by the master equation which leads to the long-time behavior, the stationary solution of this reduced qubit system. The stationary solution for two qubits depends on the pseudo-spin representation

$$\vec{S} := \hat{\sigma} \otimes \mathbb{1} + \mathbb{1} \otimes \hat{\sigma},$$

where $\hat{\sigma}$ represents the spin state by the corresponding Pauli matrices (2.1.0.1). In the z-component the pseudo-spin $\vec{S}$ decomposes into a three-dimensional triplet and a one-dimensional singlet representation of $SU(2)$. These two representations of the pseudo-spin $\vec{S}$ define two different stationary solutions and thus two different entanglement behaviors which can easily be shown.
For equal coupling-constants $d_1 = d_2$, the dimensionality of the spin representation of two qubits in a singlet state $|s\rangle = \frac{1}{\sqrt{2}}(|10\rangle - |01\rangle)$ is conserved even by the dissipative dynamics of the master equation $[H, \vec{S}^2] = 0$. Such states do not radiate into the environment and are also known as dark states. We have introduced the singlet state $|s\rangle$ as a decoherence-free subspace in the previous section and shown that if cause a dependence of the stationary dynamics on the initial states. The entanglement as a function of time remains constant for a singlet state.
In general the thermal bath influences the evolution of an initially pure system state to a mixed state. To be more precise, the initial occupation changes through this influence based on the energy and the rotating-wave approximation. The rotating-wave approximation guarantees that no stationary coherence is possible between states with different energies. Thus the non-degenerate coherences are decoupled from the rest of the density matrix, particularly from the diagonal elements of the density matrix and decay. The initial populations of the excited and the ground state are distributed into the degenerate diagonal elements due to the influence of the bath. This process depends on the bath temperature. If the bath temperature is higher the qubit can receive energy in form of photons which leads to a higher thermal occupation of the excited state. All degenerate single excited states have the same energy which leads to an exchange of the thermal occupation between these states. Thus every stationary solution of the master equation has the form

$$\rho = \begin{pmatrix} a & 0 & 0 & 0 \\ 0 & b & z & 0 \\ 0 & z^* & c & 0 \\ 0 & 0 & 0 & d \end{pmatrix}. \tag{4.1.0.1}$$

In review, the concurrence is given by the eigenvalues λ_i of $\rho(\sigma_y \otimes \sigma_y)\rho^*(\sigma_y \otimes \sigma_y)$ with $C(\rho) = \max\{0, \sqrt{\lambda_i} - \sum_{i>1}\sqrt{\lambda_i}\} = \max\{0, \tilde{C}(\rho)\}$. The concurrence modified $\tilde{C}(\rho)$ of every general stationary solution is given by

$$\tilde{C}(\rho) = 2(|z| - \sqrt{ad}).$$

Every time dependent solution of the master equation where the concurrence is $\tilde{C}(\rho) < 0$ for $|z| < \sqrt{ad}$ ends up in a disentangled state. In summary, any state which is not an entangled state, shows a decay of the entanglement.

For example, we consider a mixed state which is defined by a superposition of a singlet state $|s\rangle$ and a triplet state $|t\rangle$. The initial density matrix in the basis $\{|11\rangle, |10\rangle, |01\rangle, |00\rangle\}$ is then

$$\rho = \rho_s + \rho_t = \begin{pmatrix} 0 & 0 & 0 & 0 \\ 0 & \frac{1}{2} & 0 & 0 \\ 0 & 0 & \frac{1}{2} & 0 \\ 0 & 0 & 0 & 0 \end{pmatrix}.$$

The coupling leads to a separated distribution of this initial occupation, namely for the singlet part it remains constant. On the contrary to the triplet part where the occupation is distributed into the form of the stationary solution. Thus a superposition of a singlet and a triplet state generates entanglement which remains constant for the singlet part.

4.1.1 Entanglement sudden death

Quantum entanglement can be described in the context of nonlocal correlations which are stronger than all other types of correlations. Such correlations always decay as a result of noisy backgrounds which cannot be avoided. For example, if we consider the process of spontaneous emission of an atom into the vacuum, the noisy degrading effects through its quantum fluctuations cannot be prevented and lead to spontaneous emission of the atom. It loses its excitation and comes to its ground state after the time τ. For two qubits this effect leads to a degraded correlation and thus to a completely disentangled state.

Many experiments of two-atom spontaneous emission with an environment show that quantum entanglement does not always obey the half-life law. Even a very weakly dissipative environment can degrade the correlations between the atoms and thus the entanglement decreases to zero in finite time, rather than by successive halves. This effect is known as entanglement sudden death (ESD) [22], also called early-stage disentanglement. In our case, the ESD is provided by the weakly dissipative processes of spontaneous emissions through the coupling of the thermal bath which has extremely short internal correlation times. Thus the time evolution of the entanglement depends on the dissipative dynamics, if the perturbation of the reduced system caused by the thermal environment is stronger, the entanglement decays faster. This means, the dissipative effects lead to a mixed state described by the stationary solution (5.1.0.1) and as result of this the concurrence of this states shows ESD.
The effect of ESD can be prevented by isolating the information of the qubits from interacting with the environment. This is possible by introducing decoherence-free subspaces or by different symmetry properties as we have shown in section 2.3.

4.2 Numerical results of the occupation

We first consider the time-dependent occupation of a mixture of the states with zero excitation $p_0 = 0.5$ and with two excitations $p_2 = 0.5$, where the index of the occupation describes the excitation of the corresponding state. We assume a temperature so that the expected value of the Planck distribution of the thermal bath is given by $N = 1$. As we expected this initial occupation is balanced out in the diagonal elements. The occupation of the excited state decreases as a result of the dissipative effects through the coupling to the thermal bath. As a consequence of this the thermal occupation of the ground state increases. This effect depends on the bath temperature. If the bath temperature is higher the qubits can receive more energy as photons from the thermal bath and thus the thermal occupation of the excited state will be higher. The detailed temperature dependence of the thermal occupation is discussed for one qubit embedded in a thermal bath in the appendix.

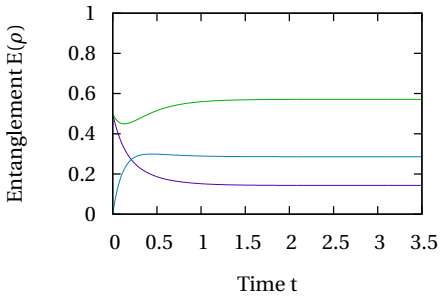

Figure 4.1: Time-evolution of the occupation with the initial occupation of the state with two excitations $p_2 = 0.5$ (violet) and the state with no excitation $p_0 = 0.5$ (green) and the diagonal elements with one excitation p_1 (blue).

By comparing the distribution of occupation of the initial occupation of this state and the triplet state Figure 4.2, we see that they reach the same occupation within time.

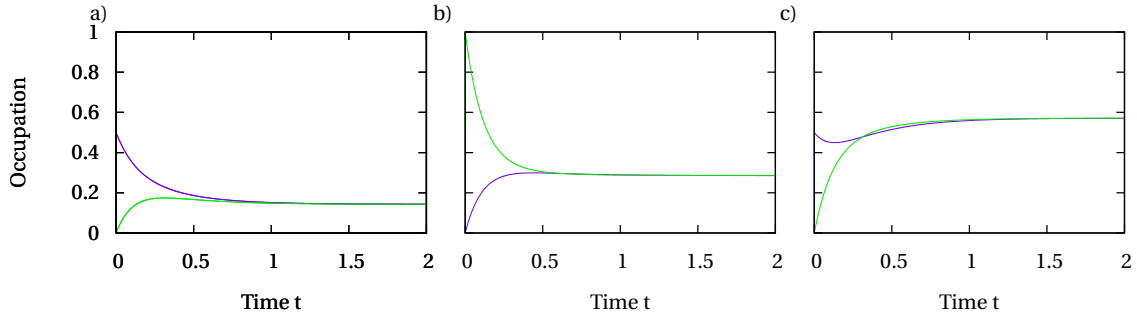

Figure 4.2: Time-evolution of the occupation for two different initial states, the triplet-state (violet) and for an initial occupation of a the state with no excitations $p_0 = 0.5$ and the state with two excitations $p_2 = 0.5$ (green) for (a) the state with two excitations, (b) the diagonal elements with one excitation and (c) the state with no excitation.

Thus the numerical result coincides with our theory and shows that this occupation corresponds to the general stationary solution of two qubits. This means, if the steady state between the qubit system and the thermal bath is reached, the distribution of occupation remains constant. The numerical result of the time-dependent occupation shows that the interaction of the qubits and the environment does not only lead to a loss of the energy of the qubit system, it can also receive energy from the thermal bath which is shown by the degenerate non-diagonal elements which increase.

4.3 Numerical results of the concurrences

We first consider the singlet state $|s\rangle = \frac{1}{\sqrt{2}}(|10\rangle + |01\rangle)$ as an initial state and different couplings d_1, d_2 of the qubits to the bath.

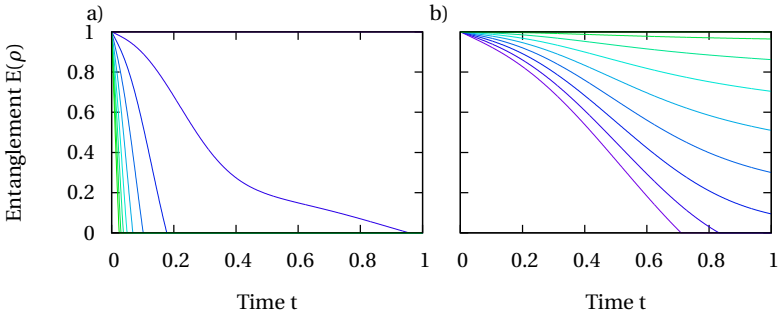

Figure 4.3: The time-dependent concurrences, when the singlet $|s\rangle$ is used as the initial state and different couplings for (a) constant $d_1 = 1$ and d_2 ranging from $d_2 = 1.5$ (violet) to $d_2 = 4$ (green) in steps of 0.5 and (b) constant $d_1 = 1$ and d_2 ranging from $d_2 = 1$ (violet) to $d_2 = 0$ (green) in steps of 0.2.

For equal couplings $d_1 = d_2$ the singlet-state is a decoherence-free subspace. The numerical results show that the thermal bath has no influence and the entanglement of this state remains. For different couplings $d_1 \neq d_2$ the concurrence as a function of time decays, the initial singlet state becomes a mixed state through the influence of the dissipative effects given by the thermal bath. This dissipative effects increase when the coupling between one qubit to the thermal bath is stronger and thus the ESD effect of concurrences is stronger.

The entangled GHZ-state $|GHZ\rangle = \frac{1}{\sqrt{2}}\left(|00\rangle + e^{i\varphi}|11\rangle\right)$ is difficult to generate experimentally [23], because it consists of a superposition of the state with no excitation $|00\rangle$ and the state with two excitations $|11\rangle$. The local phase factor $e^{i\varphi}$ of this state decays exponentially as a result of the rotating wave approximation. As a consequence of this the concurrence decays exponentially, because the thermal occupation of the ground and the excited state are balanced on the diagonal elements and have no effect of the behavior of the entanglement dynamics.

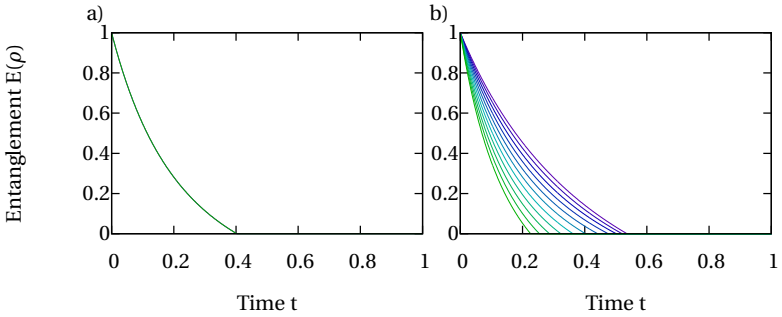

Figure 4.4: The time-dependent concurrences of the initial GHZ-state for (a) different phase factors and (b) a constant coupling $d_1 = 1$ and d_2 varying form $d_2 = 0.5$ (violet) to $d_2 = 1.5$ (green) in steps of 0.1.

The numerical results of Figure 4.2(b) show that the concurrences of the initial GHZ-state decay exponentially with the following dependence of the couplings $e^{2\Gamma t}$ where $\Gamma = |d_1|^2 + |d_2|^2$. Thus for different coupling constants $d_1 \neq d_2$ the time evolution of the concurrences decay with different exponents.

The Werner-state $|W\rangle = \frac{1}{\sqrt{2}}\left(|10\rangle + e^{i\varphi}|01\rangle\right)$ is another entangled state. The time-dependent concurrences of this state depend on the thermal occupation of the non-diagonal elements of ρ given by the local phase factor $|z| = \frac{1}{2}e^{i\varphi}$, $C(\rho) = 2|z| = 1$. Thus the initial state is determined by the angle φ which describes the amount of singlet admixture of the initial state. The time-dependent dynamics of the master equation splits into two parts, for singlet $|s\rangle$ and for triplet states $|t\rangle$.

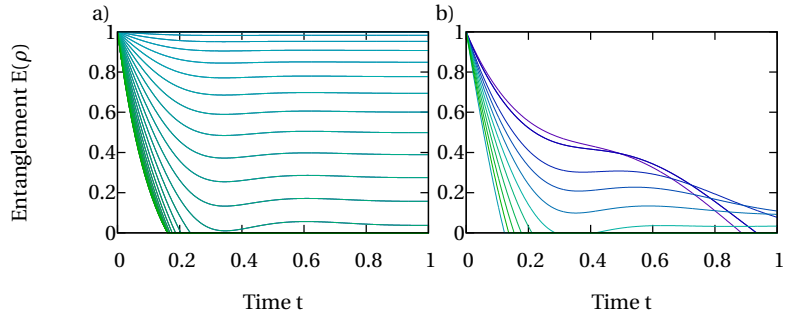

Figure 4.5: The time evolution of the initial Werner-state for (a) different local phase factors φ ranging from $\varphi = 0$ (violet) to $\varphi = 2\pi$ (blue) in steps of 0.2 and (b) couplings for a constant $d_1 = 1$ and d_2 ranging from $d_2 = 0.8$ (violet) to $d_2 = 2$ (green) in steps of 0.16.

For the situation with equal coupling constants $d_1 = d_2 = 1$, we find dark states which are singlet states and thus are conserved by the dissipative dynamics. All other states are triplet states with a stationary solution (5.1.0.1) where $|z| > \sqrt{ad}$ and thus the concurrence shows entanglement sudden death. A slight perturbation of the couplings $d_1 \neq d_2$ Figure 4.4(b) destroys the presence of the dark states and the concurrence decays.

In addition to entangled states which show dark states or entanglement sudden death another possibility is to consider a mixed state of a singlet $|s\rangle$ and a triplet $|t\rangle$, a decoherence-free subspace and a non-decoherence-free subspace. The theory of the thermal occupation of this state was already described in the theory section. The numerical result of this initial superposition shows what we expected; it generates entanglement.

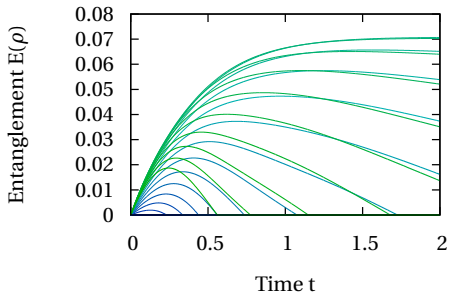

Figure 4.6: Time evolution of the concurrences of the initial superposition of the singlet state $|s\rangle$ and the triplet state $|t\rangle$ for a constant coupling $d_1 = 1$ and d_2 varying from $d_2 = 1$ (violet) to $d_2 = 0.2$ (green) in steps of 0.1.

Different coupling constants $d_2 \neq d_1$ destroy the presence of the decoherence-free subspace. The numerical results show that the deviations of the coupling constants d_2 do not have the same influence for $d_2 = 0$ and $d_2 = 2$ and thus we see two lines (the blue line for a weaker coupling and the green line for a stronger coupling) for the decay of the concurrences. Slight perturbations in the couplings have less influence and the concurrence decays linearly in contrast to strong perturbations which show that the concurrences decay faster.

4.4 Lamb-Shift contribution of the master equation

The general master equation of two qubits with the basis $\{|\uparrow\uparrow\rangle, |\uparrow\downarrow\rangle, |\downarrow\uparrow\rangle, |\downarrow\downarrow\rangle\}$ lives in a product Hilbert space $\mathbb{C}^2 \otimes \mathbb{C}^2$ and the density matrix is given in this basis by

$$\rho_S = \begin{pmatrix} |\uparrow\uparrow\rangle\langle\uparrow\uparrow| & |\uparrow\uparrow\rangle\langle\uparrow\downarrow| & |\uparrow\uparrow\rangle\langle\downarrow\uparrow| & |\uparrow\uparrow\rangle\langle\downarrow\downarrow| \\ |\uparrow\downarrow\rangle\langle\uparrow\uparrow| & |\uparrow\downarrow\rangle\langle\uparrow\downarrow| & |\uparrow\downarrow\rangle\langle\downarrow\uparrow| & |\uparrow\downarrow\rangle\langle\downarrow\downarrow| \\ |\downarrow\uparrow\rangle\langle\uparrow\uparrow| & |\downarrow\uparrow\rangle\langle\uparrow\downarrow| & |\downarrow\uparrow\rangle\langle\downarrow\uparrow| & |\downarrow\uparrow\rangle\langle\downarrow\downarrow| \\ |\downarrow\downarrow\rangle\langle\uparrow\uparrow| & |\downarrow\downarrow\rangle\langle\uparrow\downarrow| & |\downarrow\downarrow\rangle\langle\downarrow\uparrow| & |\downarrow\downarrow\rangle\langle\downarrow\downarrow| \end{pmatrix}. \tag{4.4.0.1}$$

The Lamb-Shift contribution of the master equation is calculated by the standard derivation introduced in section 2.3 with the creation operator σ_+ and the annihilation operator σ_- which are matrix representations of tensor products with the 2×2 identity matrix

$$\sum_{i,j} d_i^* \sigma_+^{(i)} d_j \sigma_-^{(j)} = d_1^* d_1 (\sigma_+ \sigma_- \otimes \mathbb{1}) + d_1^* d_2 (\sigma_+ \otimes \sigma_-) + d_2^* d_1 (\sigma_- \otimes \sigma_+) + d_2^* d_2 (\mathbb{1} \otimes \sigma_+ \sigma_-)$$

$$= \begin{pmatrix} \Gamma & 0 & 0 & 0 \\ 0 & \Gamma_1 & \gamma_{12} & 0 \\ 0 & \gamma_{12}^* & \Gamma_2 & 0 \\ 0 & 0 & 0 & 0 \end{pmatrix}$$

$$\sum_{i,j} d_j \sigma_-^{(j)} d_i^* \sigma_+^{(i)} = d_1 d_1^* (\sigma_- \sigma_+ \otimes \mathbb{1}) + d_1 d_2^* (\sigma_- \otimes \sigma_+) + d_2 d_1^* (\sigma_+ \otimes \sigma_-) + d_2 d_2^* (\mathbb{1} \otimes \sigma_- \sigma_+)$$

$$= \begin{pmatrix} 0 & 0 & 0 & 0 \\ 0 & \Gamma_2 & \gamma_{12} & 0 \\ 0 & \gamma_{12}^* & \Gamma_1 & 0 \\ 0 & 0 & 0 & \Gamma \end{pmatrix}$$

where we introduced the following definitions for the coupling constants $\Gamma = |d_1|^2 + |d_2|^2$ and $\gamma_{12} = d_1^* d_2$. The full expression for the Lamb-Shift Hamiltonian is

$$H_{LS} = \underbrace{\mathscr{P}_1 \int_0^\infty d\omega \left[\frac{(1 + N(\omega_k))}{\omega - \omega_k} \right]}_{\approx -3.2} \begin{pmatrix} \Gamma & 0 & 0 & 0 \\ 0 & \Gamma_1 & \gamma_{12} & 0 \\ 0 & \gamma_{12}^* & \Gamma_2 & 0 \\ 0 & 0 & 0 & 0 \end{pmatrix} + \underbrace{\mathscr{P}_2 \int_0^\infty d\omega \left[\frac{N(\omega_k)}{\omega + \omega_k} \right]}_{\approx 1} \begin{pmatrix} 0 & 0 & 0 & 0 \\ 0 & \Gamma_2 & \gamma_{12} & 0 \\ 0 & \gamma_{12}^* & \Gamma_1 & 0 \\ 0 & 0 & 0 & \Gamma \end{pmatrix}, \tag{4.4.0.2}$$

with the calculated values of the principal-value integrals from section 3.2.4.

4.5 Numerical results of the pseudo-Spin representation of the Lamb-shift

The Lamb-shift contribution (4.4.0.2) of the master equation can be interpreted as a magnetic field in the pseudo-spin representation

$$\vec{B} \times \vec{S} = \begin{pmatrix} \gamma_{12} \\ \gamma_{12}^* \\ \Gamma \end{pmatrix} \times \begin{pmatrix} \sigma_1 \\ \sigma_2 \\ \sigma_3 \end{pmatrix} = \begin{pmatrix} \gamma_{12}^* \sigma_3 - \sigma_3 \gamma_{12}^* \\ \Gamma \sigma_1 - \sigma_1 \Gamma \\ \gamma_{12} \sigma_2 - \sigma_2 \gamma_{12} \end{pmatrix},$$

where $\sigma_{1,2,3}$ are the coefficients of the Pauli matrices in the pseudo-spin picture. This pseudo-spin representation provides a geometric explanation on a special kind of the Bloch sphere for two qubits. The Bloch sphere representation is limited to a two-level system, in general it describes the dynamics of one qubit. If we consider a four dimensional qubit system where the dynamics can be represented in a two-dimensional Hilbert space under the assumption that all other qubit states can be ignored, we can use the Bloch sphere representation to represent this reduced dynamics. Such kind of Bloch spheres give a basic understanding of the unitary part of the master equation by the representation of the pseudo-spin $\vec{S}$.

The relation between the unitary dynamics and the pseudo-spin representation is illustrated by the following initial state

$$|\psi\rangle = \cos(\varphi) |10\rangle + \sin(\varphi) |01\rangle . \tag{4.5.0.3}$$

This state is a mixture of a singlet or a triplet determined by the angle φ. The numerical results of the concurrence of the full master equation show what we expected. The concurrence as a function of time is constant for singlet states, decays for triplet states and generates entanglement for superpositions of singlet and triplet states. When comparing the whole master equation to the unitary part it is obvious that the dissipative part dominates the dynamics.

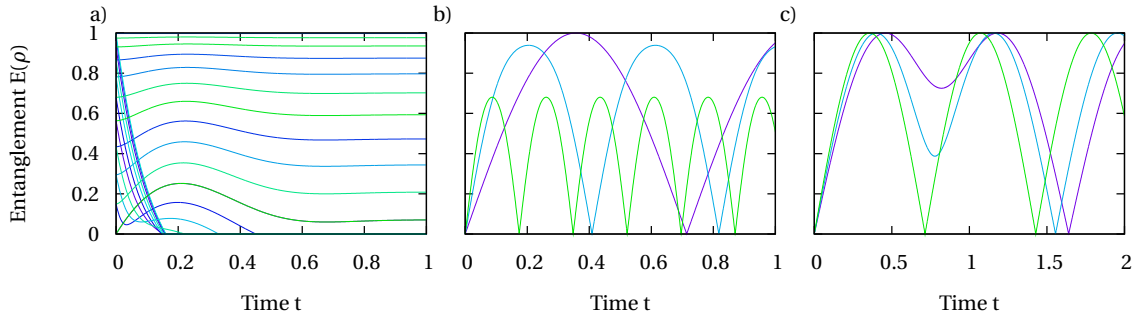

Figure 4.7: The time-dependent concurrences of the initial state $|\psi\rangle = \cos(\varphi)|10\rangle + \sin(\varphi)|01\rangle$ for (a) different angles φ varying from $\varphi = 0$ (violet) to $\varphi = 2\pi$ (green) in steps of 0.3. Concurrences as a function of time of only the Lamb-Shift contribution and different couplings for (b) a constant d_1 and a varying d_2 from $d_2 = 1$ (violet) to $d_2 = 3$ (green) in steps of 1 and (c) a constant d_1 and a varying d_2 from $d_2 = 0.8$ (violet) to $d_2 = 1$ (green) in steps of 1.

The pseudo magnetic field defined by the Lamb-shift depends on the different coupling-constants and on the pre-factors of the principal-value integrals. For equal coupling constants $d_1 = d_2$ the pseudo magnetic field lies in the y-direction and leads to a rotation of the pseudo-spin $\vec{S}_y = \sin(2.2\omega t)$ which depends on the frequency of the magnetic-field hence on the following coupling constants $\omega = 2\Gamma = 2\left(|d_1|^2 + |d_2|^2\right)$. For different coupling constants $d_1 \neq d_2$ the pseudo-magnetic field in the y-direction remains, but the difference in the coupling leads to an additional pseudo magnetic-field in the x-direction. As a consequence of this additional pseudo magnetic field the rotation of the pseudo-spin is defined by an overlap of both fields $\vec{S} = \vec{S}_y + \vec{S}_x$, where $\vec{S}_x = \sin(1.2\Omega t)$ depends on the frequency Ω of the magnetic-field in x-direction and thus on the coupling-constants $\Omega = \gamma_{12}^* = \gamma_{12}$. The dynamics of the pseudo spin $\vec{S}$ can easily be shown on the Bloch sphere representation by the two qubit states $|10\rangle$ and $|01\rangle$.

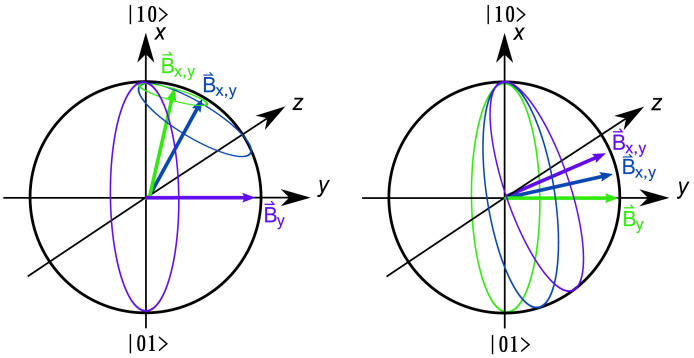

Figure 4.8: Reduced Bloch sphere representation of two qubits for the states $|01\rangle$ and $|10\rangle$ of the pseudo spin $\vec{S}$ with the influence of the pseudo-magnetic field defined by the Lamb-shift. For the left Figure a constant d_1 and a varying d_2 from $d_2 = 1$ (violet) to $d_2 = 3$ (green) in steps of 1 and in the right a constant d_1 and a varying d_2 from $d_2 = 0.8$ (violet) to $d_2 = 1$ (green) in steps of 1.

The concurrence of the pseudo-spin $\vec{S}$ is defined by its rotation $C(\tilde{\rho}) = |\vec{S}_x| + |\vec{S}_y|$. This dependency of the concurrences and the rotation of the pseudo-spin $\vec{S}$ can easily be shown by the example of the initial state (4.5.0.3). We assume that the angle φ is zero which means that the initial state is given by $|10\rangle$. The concurrence of this

state is zero and the pseudo-spin $\vec{S}$ points along the x-axis. In the following, we consider the case with equal couplings $d_1 = d_2$. The concurrence is then defined by the rotation of the pseudo-spin around the y-axis $C(\tilde{\rho}) = |\vec{S}_y|$, to be more precise in the y-z plane. Because of the pseudo-magnetic field the pseudo-spin $\vec{S}$ passes through the superposition $|\psi\rangle = \frac{1}{\sqrt{2}}(|10\rangle + |01\rangle)$ where the concurrence reach the maximum possible value one and to the state $|01\rangle$ with zero concurrence and finally returns to the initial state $|10\rangle$ while once again traversing through superposition. It is obvious that for different couplings $d_1 \neq d_2$ the pseudo-spin dynamics changes as result of the additional pseudo-magnetic field in x-direction. For all coupling constants $d_2 > 1$ the pseudo-magnetic field in x-direction increases dramatically which means that the pseudo-spin rotation path is limited to the upper hemisphere and thus does not reach the superposition. As seen in Figure 4.7(b) the amplitude of the concurrence decreases due to the higher coupling constant. When the coupling constant $d_2 < 1$ the pseudo-spin path tilts slightly towards the y-axis and thus it is unable to reach the $|01\rangle$ state. In the numerical results, Figure 4.7(c), we can see that the concurrence is only once zero for a full rotation and thus the concurrence reaches a local minima half way through the rotation.

Another intuitive description of the dynamics of the Lamb-shift provides the following separable product state $|\psi\rangle = |\psi_i\rangle|\psi_i\rangle = \cos(\varphi)^2|00\rangle + \cos(\varphi)\sin(\varphi)|01\rangle + \sin(\varphi)\cos(\varphi)|10\rangle + \sin(\varphi)^2|11\rangle$ which is a product of two equal states $|\psi_i\rangle = \cos(\varphi)|0\rangle + \sin(\varphi)|1\rangle$. To obtain a fundamental description of this initial state defined by the angle φ, the degenerate diagonal elements with one excitation can be rewritten in terms of the triplet state $|t\rangle$

$$|t\rangle = \cos(\varphi)\sin(\varphi)(|10\rangle + |01\rangle),$$

Thus the angle φ define a triplet state for $\cos(\varphi)\sin(\varphi) \neq 0$ which is the case for $\varphi \neq \{\frac{\pi n}{2} - \frac{\pi}{4}\}$ with $n \in \mathbb{Z}$. The numerical result shows that these states generate entanglement. This generated entanglement given by the triplet state decays after a certain time as a consequence of the dissipative effects which lead to a mixed state and thus to a concurrence decay. Thus we see that a separable state which consists of a triplet part create transiently entanglement. For all other states the concurrence as a function of time shows no entanglement and is constantly zero.

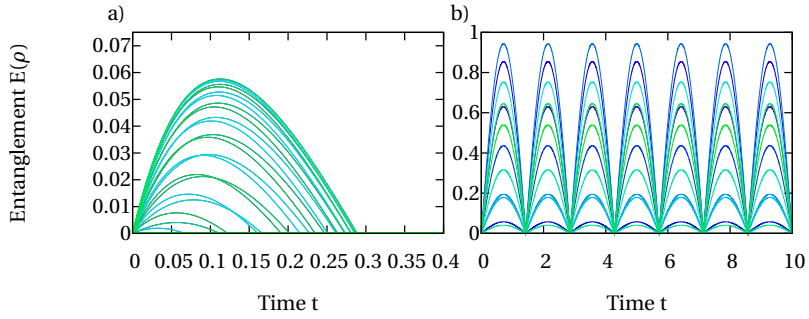

Figure 4.9: (a) The time-dependent concurrences of the initial separable state $|\psi\rangle = |\psi_i\rangle \otimes |\psi_i\rangle$ and different angles φ varying from $\varphi = 1.5\pi$ (violet) to $\varphi = 2\pi$ (green) in steps of 0.1. (b) The concurrences of only the Lamb-shift contribution of the master equation and different angles φ varying form $\varphi = 0$ (violet) to $\varphi = 2\pi$ (green) in steps of 0.2.

The concurrence due to the Lamb-shift shows again the typical oscillations which depend on different angles φ. But these oscillations cannot be represented on the Bloch sphere since it is impossible to reduce the four-dimensional Hilbert space to a two-dimensional Hilbert space because we cannot ignore any qubit states.

In addition to a separable state which is a product of two equal states we consider the separable state $|\psi\rangle = |\psi_i\rangle \otimes |\psi_j\rangle = \cos(\varphi)\sin(\varphi)|00\rangle + \cos(\varphi)^2|01\rangle + \sin(\varphi)^2|10\rangle + \sin(\varphi)\cos(\varphi)|11\rangle$ which is a product of the state $|\psi_i\rangle = \cos(\varphi)|0\rangle + \sin(\varphi)|1\rangle$ and $|\psi_j\rangle = \sin(\varphi)|0\rangle + \cos(\varphi)|1\rangle$. For this state the non diagonal elements with one excitation depend on different pre-factors

$$|01\rangle \approx \cos(\varphi)^2 \left(|t\rangle + |s\rangle\right),$$
$$|10\rangle \approx \sin(\varphi)^2 \left(|t\rangle - |s\rangle\right).$$

The numerical result of the time-dependent concurrence shows what we expected: any angle φ defines a superposition of the singlet and triplet state and thus any initial state generates entanglement. If the angle φ has one of the following values $\varphi = 0, \frac{\pi}{2}, \frac{3\pi}{2}, 2\pi$, the initial state is defined by only one superposition of a singlet and a triplet state. This has the consequence that in this case the occupation of the singlet part remains constant. Thus the constant concurrence in the numerical result represents only the concurrence of the singlet part because the triplet part decays. If we compare this result with the previous one, we notice that a superposition of a singlet and a triplet generates more entanglement as a single triplet state.

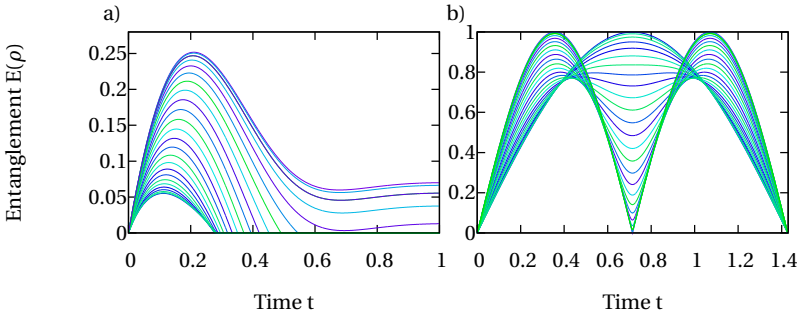

Figure 4.10: Concurrences of the initial separable state $|\psi\rangle = |\psi_i\rangle \otimes |\psi_j\rangle$ and different angles φ (a) ranging from $\varphi = 0$ (violet) to $\varphi = \pi$ (green) in steps of 0.12 and (b) is only the concurrences of the Lamb-shift contribution of the master equation with the same angles φ as in (a).

The numerical result of the time-dependent concurrences show again oscillations which cannot be described in the pseudo-spin representation as in the previous example. But we can see that there is only one angle φ which defines an initial state where the concurrence reaches the maximal value one once and for another angle φ twice.

Chapter 5

Entanglement dynamics for three qubits interacting with an environment

5.1 Theory of the entanglement dynamics for three qubits

In the previous chapter we have seen that the entanglement dynamics for a bipartite qubit system embedded in a thermal environment is fully understood. In the following we extend this bipartite system to a tripartite system and study the entanglement effect induced by the dissipative dynamics. This gives us the distinction between the entanglement behavior of a bipartite and a tripartite qubit system which we are interested in.

Any entanglement dynamics are based on the behavior of the system dynamics. Thus we begin with a discussion of the dynamics of the tripartite system described by the Markovian master equation. As a consequence of the non-existing decoherence-free subspace any initial pure system state of a tripartite system are always mapped into separable mixtures. This means, on the one hand that it is impossible to prevent the entanglement from decaying and on the other hand that the master equation has only one stationary solution. Any initial occupation is distributed under the same conditions as in the bipartite case. The rotating-wave approximation guarantees again that the non degenerate concurrences are decoupled from the rest of the density matrix. This means that all non-degenerate coherences decay and become zero with time. The occupation of states with maximal excitation of three and no excitations is distributed in the diagonal elements as a result of the thermal environment. This occupation of the diagonal elements shows the average excitation of the qubit system depending on the temperature. The thermal occupation of the degenerated states with one or two excitation is equal for $t \to \infty$. With this conditions every stationary solution of the master equation for three qubits has the following form

$$\rho = \begin{pmatrix} a & 0 & 0 & 0 & 0 & 0 & 0 & 0 \\ 0 & b & z_1 & 0 & z_2 & 0 & 0 & 0 \\ 0 & z_1^* & c & 0 & z_3 & 0 & 0 & 0 \\ 0 & 0 & 0 & d & 0 & z_4 & z_5 & 0 \\ 0 & z_2^* & z_3^* & 0 & e & 0 & 0 & 0 \\ 0 & 0 & 0 & z_4^* & 0 & f & z_6 & 0 \\ 0 & 0 & 0 & z_5^* & 0 & z_6^* & g & 0 \\ 0 & 0 & 0 & 0 & 0 & 0 & 0 & h \end{pmatrix} \tag{5.1.0.1}$$

in the basis $\{|111\rangle, |110\rangle, |101\rangle, |100\rangle, |011\rangle, |010\rangle, |001\rangle, |000\rangle\}$.

In contrast to the bipartite system a tripartite system provides a physical system where the entanglement dynamics is not fully understood yet. The main problem of such a system is that the influence of the thermal bath leads to mixed states for which no description of the degree of entanglement exists [4]. But we can use the

concurrence which gives a full description of the entanglement between each pair of qubits and consider the bipartite entanglement of the tripartite system. This leads to a differentiation of the entanglement dynamics, namely in pure tripartite entanglement and bipartite entanglement. The long-time behavior of the entanglement dynamics between each pair of qubit is then given by tracing out the degree of freedom of the third qubit of the stationary solution of the master equation and calculating the concurrences between the remaining two qubits. Thus the three different concurrences C_{BC}, C_{AC} and C_{AB}, where the indices denote the different qubits, are given by

Concurrence C_{BC} between qubits B and C

$$\mathrm{Tr}_A \rho_{ABC} = \rho_{BC} = \begin{pmatrix} a+e & 0 & 0 & 0 \\ 0 & b+f & z_1+z_6 & 0 \\ 0 & z_1^*+z_6^* & c+g & 0 \\ 0 & 0 & 0 & d+h \end{pmatrix}$$

$$\tilde{C}(\rho) = 2(|z_1+z_6| - \sqrt{(a+e)(d+h)})$$

Concurrence C_{AC} between qubits A and C

$$\mathrm{Tr}_B \rho_{ABC} = \rho_{AC} = \begin{pmatrix} a+c & 0 & 0 & 0 \\ 0 & b+d & z_2+z_5 & 0 \\ 0 & z_2^*+z_5^* & e+g & 0 \\ 0 & 0 & 0 & f+h \end{pmatrix}$$

$$\tilde{C}(\rho) = 2(|z_2-z_5| - \sqrt{(a+c)(f+h)})$$

Concurrence C_{AB} between the qubits A and B

$$\mathrm{Tr}_C \rho_{ABC} = \rho_{AB} = \begin{pmatrix} a+b & 0 & 0 & 0 \\ 0 & c+d & z_3+z_4 & 0 \\ 0 & z_3^*+z_4^* & e+f & 0 \\ 0 & 0 & 0 & g+h \end{pmatrix}$$

$$\tilde{C}(\rho) = 2(|z_3+z_4| - \sqrt{(a+b)(g+h)})$$

and $C(\rho) = \max\{0, \tilde{C}(\rho)\}$. The reduced density matrices ρ_A, ρ_B and ρ_C of the stationary solution have the same form like the stationary solution for two qubits and thus we can easily calculate the corresponding concurrences. In contrast to the behavior of two qubits, the consideration of three qubits shows another dynamics and thus other bipartite entanglement effects as a result of the coupling to the thermal bath.

5.1.1 Lamb-shift contribution of the master equation

The dynamics of three qubits embedded in a thermal bath described by the master equation is not trivial which can be shown by considering the coherent physics alone. The Lamb-Shift contribution of the master equation has in general the following form

$$\frac{d}{dt}\rho = -i[H_{LS}, \rho].$$

The full calculation of this Lamb-Shift operator H_{LS} for three qubits is shown in the appendix 7.2.3. A fundamental description of this Lamb-Shift dynamics is given by the pseudo-spin representation as we showed for the bipartite case. For the derivation of such a representation of the tripartite system we consider the degenerate matrices of the Lamb-Shift contribution with one or two excitations

$$H^1_{LS} = \begin{pmatrix} \Gamma_1+\Gamma_2 & \gamma_{23} & \gamma_{13} \\ \gamma^*_{23} & \Gamma_1+\Gamma_3 & \gamma_{12} \\ \gamma^*_{13} & \gamma^*_{12} & \Gamma_2+\Gamma_3 \end{pmatrix} \quad H^2_{LS} = \begin{pmatrix} \Gamma_1 & \gamma_{12} & \gamma_{13} \\ \gamma^*_{12} & \Gamma_2 & \gamma_{23} \\ \gamma^*_{13} & \gamma^*_{23} & \Gamma_3 \end{pmatrix},$$

where the index defines the excitation. These matrices of $SU(3)$ can be rewritten in the basis of the Gell-Mann matrices [1] and the (3×3) identity matrix, equally the corresponding (3×3) density matrix ρ. Thus we obtain the following representation of the Lamb-shift operator

$$\sum_i \frac{d}{dt} S_i \lambda_i = -i[H_{LS}, \rho] = -i \sum_{j,k} H_j S_k [\lambda_j, \lambda_k], \tag{5.1.1.1}$$

where the $\sum_i \frac{d}{dt} S_i \lambda_i$ is the spin-representation of $SU(3)$ and H_j defines the component of the generalized pseudo-magnetic field. Thus the dependence between the pseudo-spin $\vec{S} = \sum_i \frac{d}{dt} S_i \lambda_i$ and the unitary part of the master equation interpreted as a pseudo-magnetic field can be achieved by the commutation relation of the Gell-Mann matrices

$$[\lambda_i, \lambda_j] = i \sum_k f^{ijk} \lambda_k,$$

given by the structure constants f^{ijk} which are completely antisymmetric

$$\begin{aligned} f^{123} &= 1 \\ f^{147} = f^{165} = f^{246} = f^{257} = f^{345} = f^{376} &= \frac{1}{2} \\ f^{458} = f^{678} &= \frac{\sqrt{3}}{2}. \end{aligned}$$

For a complete description of the pseudo-spin dynamics the pseudo-spin vector $\vec{S}$ must include the full information of all possible spin interactions. Thus we define the spin interactions between each pair of qubits in the following way

$$S^{12}_{x,y,z}, \quad S^{23}_{x,y,z} \quad \text{and} \quad S^{13}_{x,y,z},$$

where the numbers of the indices define the involved qubits. These spin interaction can be expressed in the context of the Gell-Mann matrices by

$$\begin{aligned} S^{12}_x = \lambda_6 \quad S^{12}_x = \lambda_1 \quad S^{13}_x = \lambda_4 \\ S^{12}_y = \lambda_7 \quad S^{12}_y = \lambda_2 \quad S^{13}_y = \lambda_5 \\ S^{12}_z = \frac{1}{2}\left(-\lambda_3 + \sqrt{3}\lambda_8\right) \quad S^{12}_z = \lambda_3 \quad S^{13}_z = \frac{1}{2}\left(\lambda_3 + \sqrt{3}\lambda_8\right). \end{aligned}$$

[1] Gell-Mann matrices

$$\lambda_1 = \begin{pmatrix} 0 & 1 & 0 \\ 1 & 0 & 0 \\ 0 & 0 & 0 \end{pmatrix}, \quad \lambda_2 = \begin{pmatrix} 0 & -i & 0 \\ i & 0 & 0 \\ 0 & 0 & 0 \end{pmatrix}, \quad \lambda_3 = \begin{pmatrix} 1 & 0 & 0 \\ 0 & -1 & 0 \\ 0 & 0 & 0 \end{pmatrix}, \quad \lambda_4 = \begin{pmatrix} 0 & 0 & 1 \\ 0 & 0 & 0 \\ 1 & 0 & 0 \end{pmatrix}, \quad \lambda_5 = \begin{pmatrix} 0 & 0 & -i \\ 0 & 0 & 0 \\ i & 0 & 0 \end{pmatrix}, \quad \lambda_6 = \begin{pmatrix} 0 & 0 & 0 \\ 0 & 0 & 1 \\ 0 & 1 & 0 \end{pmatrix},$$

$$\lambda_7 = \begin{pmatrix} 0 & 0 & 0 \\ 0 & 0 & -i \\ 0 & i & 0 \end{pmatrix}, \quad \lambda_8 = \frac{1}{\sqrt{3}} \begin{pmatrix} 1 & 0 & 0 \\ 0 & 1 & 0 \\ 0 & 0 & -2 \end{pmatrix}$$

Then we rewrite the calculated commutation relations (5.1.1.1) in this nine-dimensional basis and obtain the desired pseudo-spin representation

$$\frac{d}{dt}\begin{pmatrix} S_x^{23} \\ S_y^{23} \\ S_z^{23} \\ S_x^{13} \\ S_y^{13} \\ S_z^{13} \\ S_x^{12} \\ S_y^{12} \\ S_z^{12} \end{pmatrix} = \begin{pmatrix} \left(\vec{B}^{23} \times \vec{S}^{23}\right) \\ \\ \\ \left(\vec{B}^{13} \times \vec{S}^{13}\right) \\ \\ \\ \left(\vec{B}^{12} \times \vec{S}^{12}\right) \\ \\ \end{pmatrix} + \begin{pmatrix} -\frac{1}{2}\left((B^{13} \times S^{12})_z + (B^{12} \times S^{13})_z\right) \\ -\frac{1}{2}\left((B_x \times S_x)^{23} + (B_y \times S_y)^{23}\right) \\ 0 \\ -\frac{1}{2}\left((B_y \times S_x)^{13} + (B_x \times S_y)^{13}\right) \\ \frac{1}{2}\left((B_x \times S_y)^{13} + (B_y \times S_y)^{13}\right) \\ 0 \\ -\frac{1}{2}\left((B^{13} \times S^{23})_z + (B^{23} \times S^{13})_z\right) \\ -\frac{1}{2}\left((B_x \times S_x)^{12} + (B_y \times S_y)^{12}\right) \\ 0 \end{pmatrix}.$$

This pseudo-spin representation shows another result as expected, we see that it gives an additional term which cannot be written as a cross product of the pseudo-spin $\vec{S}$ and the pseudo-magnetic field $\vec{B}$. Thus this dynamics of the pseudo-spin shows that the spin interaction between each qubit pair has not the same effect which lead to the assumption that the dynamics for three qubits embedded in a thermal bath is much more complicated as in the bipartite case.

In the following, we discuss the time-dependent numerical results of the occupation and the concurrence on this theoretical background.

5.2 Numerical results of the occupation

We first consider the time-dependent occupation of a mixture of the states with zero excitation $p_0 = 0.5$ and with three excitations $p_3 = 0.5$, where the index of the occupation describes the number of excitation. The numerical result shows what we expected, this initial occupation is distributed in the diagonal elements through the dissipative effects.

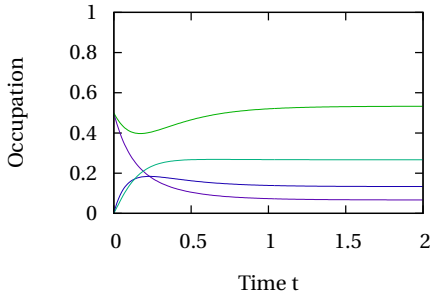

Figure 5.1: Time-evolution of the occupation with the initial occupation of the state with three excitation p_e = 0.5 (violet) and the state with no excitation $p_g = 0.5$ (green) and the degenerates diagonal elements with one excitation (blue) and two excitation (blue)

Thus the occupation of the state with three excitations decays fastest because the probability that one excited photon is emitted to a state with lower energy is greatest. These effects lead to an increase of the occupation of the other diagonal elements, especially for the state with no excitation. As a consequence of photon emissions from the excited states, the occupation of the degenerate state with one excitation is greater than the occupation for two excitations. Thus the stationary solution shows the average distribution of the occupation within time leads to a fundamental consideration of the excitations of the qubit system.

In the following, we consider the time-dependent distribution of the initial occupation of the state $|100\rangle$. The

numerical result of this initial occupation shows two effects, a part of this occupation is distributed into the diagonal elements with the same energy, namely $|010\rangle$ and $|001\rangle$ and the other part goes to the state with no excitation as a result of the photon emissions processes given by the coupling to the thermal bath. Thus the stationary solution of the occupation shows that for equal couplings $d_1 = d_2 = d_3$ the thermal occupation between the state which the the same energy is equal.

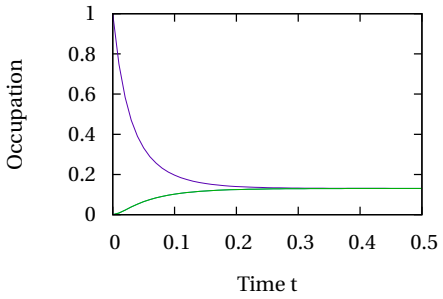

Figure 5.2: Time-evolution of the occupation with the initial occupation of an excitation of the first qubit given by the diagonal element $|100\rangle\langle 100|$ (violet), $|010\rangle\langle 010|$ and $|001\rangle\langle 001|$(green).

5.3 Numerical results of the concurrences

We first consider the GHZ-state $|GHZ\rangle = \frac{1}{\sqrt{2}}(|000\rangle + |111\rangle)$ as an initial state and different couplings d_1, d_2 and d_3 of the qubits to the bath. The GHZ-state is a genuine tripartite entangled state. The numerical result of the time-dependent concurrences shows that the bipartite entanglement of each pair of qubits remains constantly zero $C_{AB} = C_{BC} = C_{AC} = 0$. This means the coupling to the thermal bath does not change the genuine tripartite entanglement to bipartite entanglement within time. Rather surprising is the fact that different couplings $d_1 \neq d_2 \neq d_3$ have also no influence on the bipartite entanglement.

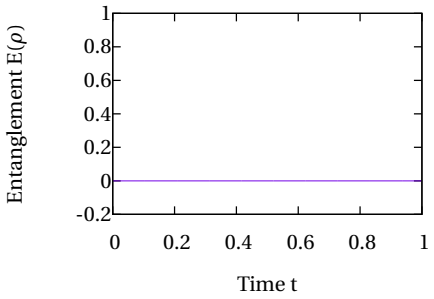

Figure 5.3: Time evolution of the concurrences of the initial GHZ-state and different couplings.

Another well-known pure maximally entangled state is the Werner-state $|W\rangle = \frac{1}{\sqrt{3}}(|100\rangle + |010\rangle + |001\rangle)$ which consists of degenerate states with one excitation. This state is symmetric under permutations of the qubits and the bipartite concurrence of this initial state for each pair of qubits is the same $C_{BC} = C_{AC} = C_{AB} = \frac{2}{3}$. In contrast to the GHZ-state this state has not only tripartite entanglement but also bipartite entanglement. The numerical result, Figure 5.4, of the time dependent concurrence show that this initial bipartite entanglement between the qubit decays. This decay is a result of the dissipative dynamics which maps the initial pure system state into a separable mixture. Therefore the reduced density matrices ρ_{BC}, ρ_{AC} and ρ_{AB} have a stationary solution for which the concurrences decay. For equal couplings $d_1 = d_2 = d_3$ the interaction between each qubit and the environment is the same hence the bipartite concurrences decay equally. If one coupling constant, in our case $d_1 > 1$, defines a stronger coupling of qubit A to the thermal bath the concurrences between this qubit and the other two qubits B, C changes the same. The numerical result, in Figure 5.4 (b), of these two concurrences C_{AB} and C_{AC} decay faster and show earlier ESD. In this case the decay is caused by the same effect as in the bipartite

qubit system. But for the time-dependent concurrence C_{BC} and $d_1 > 1$ we see a decay which is caused by the Lamb-shift. This shows that this bipartite entanglement is also affected by this varying coupling even though there is no direct connection.

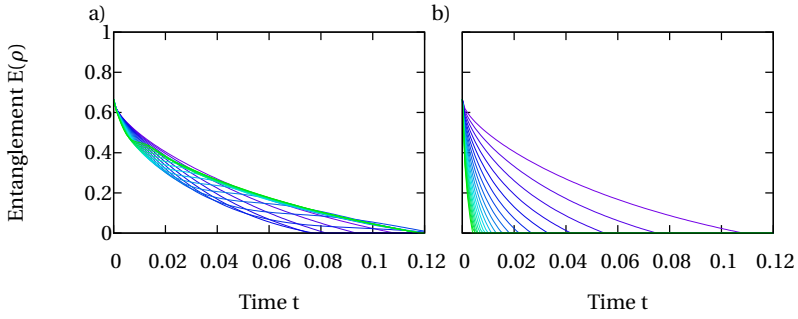

Figure 5.4: Time evolution of the concurrences of the initial GHZ-state and different couplings, $d_2 = d_3 = 1$ are constant and d_1 are varying from $d_1 = 1$ (violet) to $d_2 = 5$ (green) in steps of 0.2 for (a) C_{BC} and (b) C_{AB} and C_{AC}.

This can be shown by considering the entanglement dynamics of the Lamb-Shift contribution alone. The numerical results of the time-dependent concurrences, Figure 5.5, show a different behavior as in the bipartite case. For equal couplings constants $d_1 = d_2 = d_3 = 1$ the Lamb-shift operator has no influence on the differential equation of the unitary part of the master equation $\frac{d}{dt}\rho_W = -i[H_{LS}, \rho_W] = 0$ and thus we see that the concurrence remains constant at the initial value $\frac{2}{3}$. For differing coupling constant, $d_1 > 1$, the concurrence of the Lamb-shift starts to oscillate. As we expected the concurrences C_{AB} and C_{BC} show the same entanglement dynamics. But these oscillations show different entanglement behavior when compared to the bipartite case which is attributable to the much more complicated dynamics of this unitary contribution to the master equation which we have shown in section 5.1.1. If we consider for example the time-dependent concurrence oscillations C_{AC} and C_{AB} it is obvious that for a slight perturbation $d_1 = 2$ of the coupling the amplitude is much higher than for considerable perturbations $d_2 > 2$ but never reaches an entangled or an disentangled state. Additionally we see local minima at $\frac{2}{3}$. In contrast to the time-dependent concurrence oscillation C_{CB} which reaches a disentangled state with $d_1 = 2$ and remains below $\frac{2}{3}$. But for $d_2 > 2$ the amplitude of the oscillations decreases. These oscillations of the concurrence of the Lamb-shift appear in the numerical result for C_{BC}, Figure 5.4 (a), and explain the different decays.

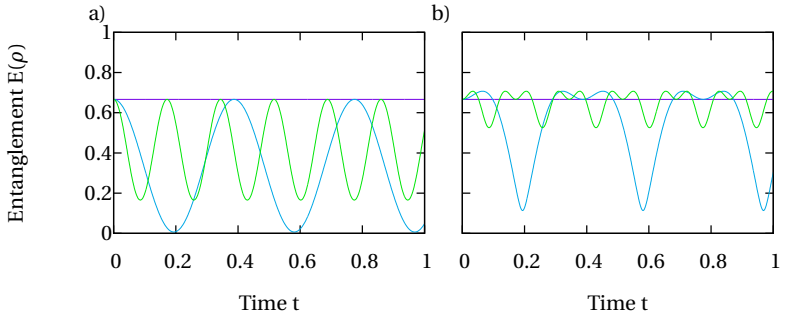

Figure 5.5: Time evolution of the concurrences of the Lamb-Shift of the initial Werner-state and different couplings, $d_2 = d_3 = 1$ are constant and d_1 varying from $d_1 = 1$ (violet) to $d_2 = 3$ (green) in steps of 1 for (a) C_{BC} and (b) C_{AB} and C_{AC}.

A similar effect can be considered when the coupling constant $d_1 < 1$ describes a weaker coupling between the qubit A and B, C, see Figure 5.6. As in the case above the concurrences C_{AB} and C_{AC} have the same entanglement dynamics due to the coupling. The numerical results show, Figure 5.6 (b), that the time-dependent concurrences C_{AB} and C_{AC} decay more slowly. This entanglement behavior is similar to the bipartite case which means that we can consider the same entanglement dynamics in the context of the different coupling constants. The concurrence C_{BC} shows again obvious influence of the concurrence of the Lamb-shift.

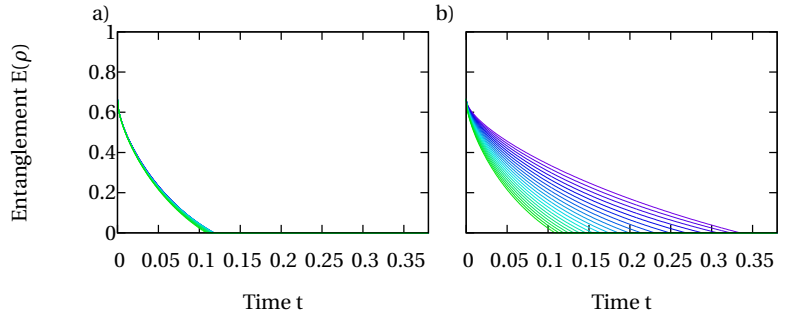

Figure 5.6: Time evolution of the concurrences due to the initial Werner-state and different couplings, $d_2 = d_3 = 1$ are constant and d_1 is varying from $d_1 = 0.8$(violet) to $d_1 = 1$ (green) in steps of 0.2 for (a) C_{BC} and (b) C_{AB} and C_{AC}.

The time-dependent concurrences of the Lamb-shift show lower frequent oscillations as a result of the weaker coupling $d_1 < 1$. For both numerical results, Figure 5.7(a) and (b), we see that the amplitude increases for a smaller coupling constant d_1. For the time-dependent concurrences C_{AB} and C_{AC}, Figure 5.7 (b), the oscillation is localized below the initial value $\frac{2}{3}$ in contrast to the time-dependent concurrence C_{BC} which is localized above the initial value. The numerical results of the Werner-state show that a bipartite entanglement of a tripartite entanglement has two additional effects compared to the bipartite system. The concurrence due to the Lamb-shift show another entanglement dynamics and influences obviously the dissipative entanglement dynamics for only one differing coupling constant.

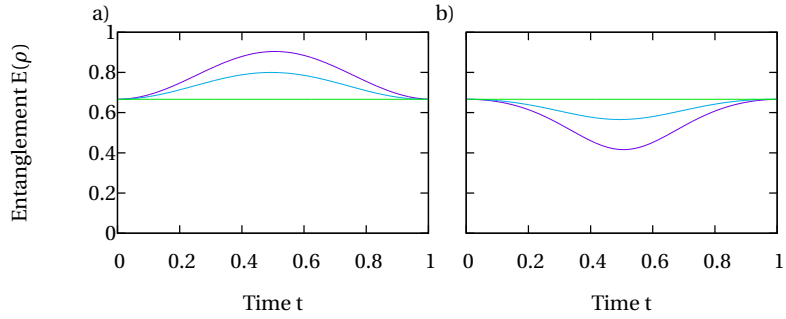

Figure 5.7: Time evolution of the concurrences due to the Lamb-Shift of the initial Werner-state and different couplings, $d_2 = d_3 = 1$ are constant and d_1 varying is from $d_1 = 0.8$ (violet) to $d_2 = 1$ (green) in steps of 1 (a) C_{BC} and (b) C_{AB} and C_{AC}.

The consideration of the singlet state between two qubits of the three qubits gives an intuitive description of the bipartite entanglement of three qubits. The qubits are invariant under permutation and thus it does not play a role between which qubit pair we use to define a singlet-state. For example, the initial state of the bipartite system is given by $|s\rangle = \frac{1}{\sqrt{2}}(|100\rangle - |010\rangle)$ which defines a singlet-state between the qubit pair A, B. The numerical result, Figure 5.8, of equal couplings $d_1 = d_2 = d_3$ shows that the concurrence C_{AB} of the singlet-state remains constant. Thus the singlet-state is once again a decoherence-free subspace for the bipartite entanglement of a tripartite system. A small perturbation of the coupling between one qubit of the singlet-state and the thermal bath shows that the presence of the decoherence-free subspace is destroyed similarly to the bipartite system. Additionally we can see that different perturbation show the same decay as in the bipartite system, see Figure 4.3(a) and (b). This means that the reduced density matrices ρ_{BC}, ρ_{AC} and ρ_{AB} have two stationary solutions as in the bipartite qubit system. Thus we can observe two different entanglement dynamics for the bipartite entanglement, namely a constant concurrence and a decay of the concurrence.

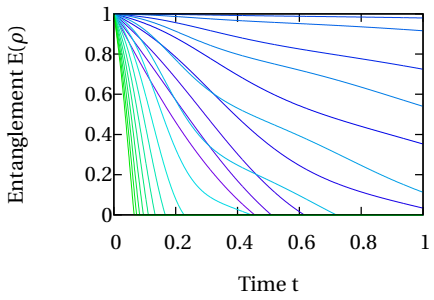

Figure 5.8: The time evolution of the concurrence C_{AB} of the initial singlet state $|s\rangle$ between the qubits A, B and different couplings, $d_2 = d_3 = 1$ and d_1 varying from $d_1 = 0$ (violet) to $d_2 = 2$ (green) in steps of 0.1.

In addition to entangled states, we can consider the time evolution of the bipartite entanglement dynamics of separable states. The simplest separable state is a product state consisting of three equal qubit states $|\psi\rangle = |\psi_i\rangle \otimes |\psi_i\rangle \otimes |\psi_i\rangle$ where $|\psi_i\rangle$ defines the superposition $|\psi_i\rangle = \sin(\varphi)|1\rangle + \cos(\varphi)|0\rangle$. The numerical results of the time-dependent concurrences C_{BC}, C_{AC} and C_{AB} show for the same coupling constants $d_1 = d_2 = d_3$ the same entanglement dynamics, see Figure 5.9. This means that the states with same excitations show identical occupations all the time. As a consequence the occupation in the reduced density matrix also act the same and thus the entanglement dynamics between the qubits equally. We see that this dynamics causes transiently entanglement between the qubits but which decays afterwards. From the numerical results of the bipartite system, in Figure 4.9(a), we can conclude due to the time-dependent dynamics of the tripartite system that the triplet states between the qubit pairs arise generating this entanglement. The fact that these states are indeed triplet states can be checked by the numerical implementation of the occupation of the reduced density matrices, ρ_{BC}, ρ_{AC} and ρ_{AB}. This result shows as well that we can generate bipartite entanglement in the tripartite case with triplet states between the qubits. But this generated entanglement is smaller as in the bipartite case because in a tripartite system every qubit has two bipartite entanglements. Although the definition of these triplet states between the qubits is not intuitive as the tripartite dynamic of the system reflects a more complicated dynamic.

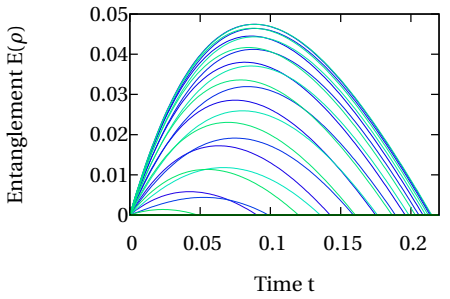

Figure 5.9: The time-dependent concurrences between all pairs of qubits C_{BC}, C_{AB} and C_{AC} of the initial separable state $|\psi\rangle = |\psi_i\rangle \otimes |\psi_i\rangle \otimes |\psi_i\rangle$ and different angles φ varying form $\varphi = 0$ (violet) to $\varphi = \pi$ (green) in steps of 0.2.

Additionally to this entanglement dynamics, we can consider the contribution of the concurrence of the Lamb-Shift alone. The numerical result, in Figure 5.10(a), shows surprisingly a similar entanglement behavior for certain angles φ and the different angles only influence the amplitude of the oscillation. But once again the complex dynamics of the tripartite system is included for different angles, Figure 5.10(b). We can see two additional minima that merge into one. In contrast to the bipartite system we see that these Lambs-shifts oscillations have a smaller amplitude. Although in this case the concurrence of the Lamb-Shift appears not obvious.

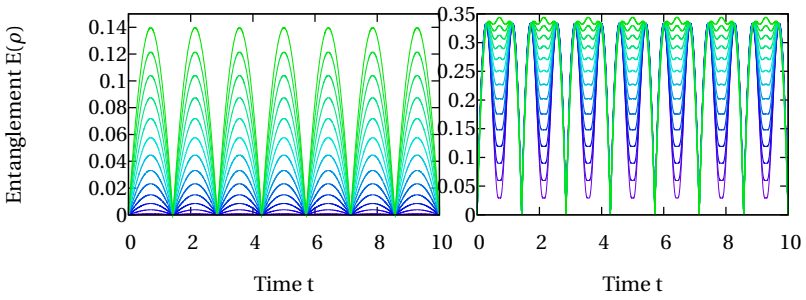

Figure 5.10: The time-dependent concurrences due to the Lamb-Shift between all pairs of qubits C_{BC}, C_{AB} and C_{AC} of the initial separable state $|\psi\rangle = |\psi_i\rangle \otimes |\psi_i\rangle \otimes |\psi_i\rangle$ and different angles φ varying for (a) from $\varphi = 0$ (violet) to $\varphi = 0.2$ (green) in steps of 0.015 and (b) form $\varphi = 0.8$ (violet) to $\varphi = 1$ (green) in steps of 0.015.

Another possibility is to consider the bipartite entanglement dynamics of an initial separable state which is a product state of only two equal qubit states $|\psi\rangle = |\psi_i\rangle \otimes |\psi_j\rangle \otimes |\psi_j\rangle$ with $|\psi_i\rangle = \sin(\varphi)|1\rangle + \cos(\varphi)|0\rangle$ and $|\psi_j\rangle = \cos(\varphi)|0\rangle + \sin(\varphi)|1\rangle$. The numerical result, Figure 5.11, shows that for the same initial states of the qubit B and C the concurrence show transiently entanglement. This can be explained with the tripartite dynamic of the system which evolves such that the reduced density matrix ρ_{BC} includes the occupation of a triplet which decays again and thus the concurrence decays as well.
For the time-dependent concurrence with different initial states of the qubits AC and AB, we can see that entanglement is generated and remains constant for several initial conditions, see Figure 5.11. This can be explained with the tripartite dynamics of the full system between the qubit pairs which generates a superposition of a singlet and a triplet state. The singlet part is preserved by the dissipative dynamics and thus the entanglement dynamics as well. By comparing the results with the same initial superposition of the qubits in the bipartite system, Figure 4.10, we can see that the entanglement dynamics show again influence by the Lamb-shift. This can be analyzed more precisely when looking at the concurrence of the Lamb-shift.

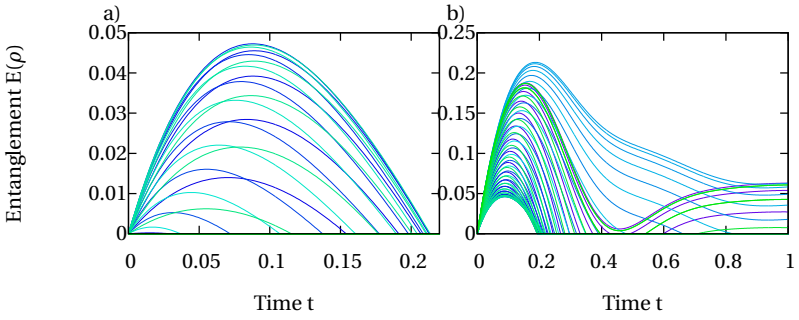

Figure 5.11: The time-dependent concurrences of the initial separable state $|\psi\rangle = |\psi_i\rangle \otimes |\psi_j\rangle \otimes |\psi_j\rangle$ and different angles φ varying form $\varphi = 0$ (violet) to $\varphi = \pi$ (green) in steps of 0.2 for (a) C_{BC} and (b) C_{AB} and C_{AC}.

The concurrence due to the Lamb-shift shows distinctly that it is being influenced by the tripartite dynamics especially if we consider the concurrence of the Lamb-shift C_{BC} which has a completely different entanglement behavior as the Lamb-shift above, despite of same initial states and angles φ. Thus we conclude that in this case the concurrence of the dissipative part overweighs because we see in Figure 5.11 (a) a similar result as in Figure 5.9. If we consider the concurrences of the Lamb-shift C_{AB} and C_{AC} we can see strong concurrence oscillations which depends on the initial state and thus on the angle φ. Exactly these different oscillation can be seen in the concurrence above, for an angle around $\frac{\pi}{2}$ the Lamb-shift oscillates with the highest amplitude. But in this case we can see the combination of the concurrence of the Lamb-shift and the dissipator very well as at the beginning the Lamb-shift part dominates and later the dissipative part.

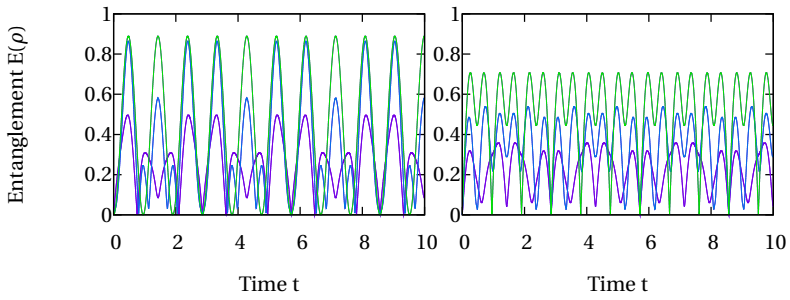

Figure 5.12: The time-dependent concurrences of the initial separable state $|\psi\rangle = |\psi_i\rangle \otimes |\psi_j\rangle \otimes |\psi_j\rangle$ and different angles φ varying from $\varphi = 0$ (violet) to $\varphi = 2\pi$) (green) in steps of 1.5 for (a) C_{BC} and (b) C_{AB} and C_{AC}.

From this point of view, the question comes up if it is possible to obtain a constant bipartite entanglement for a product state of three different qubit states $|\psi\rangle = |\psi_i\rangle \otimes |\psi_j\rangle \otimes |\psi_k\rangle$ which define superpositions of singlet and triplet states with different pre-factors given by the angle φ. Therefore, we consider such a product state consisting of the qubits state $|\psi_i\rangle = \cos(\varphi)|0\rangle + \sin(\varphi)|1\rangle$, $|\psi_j\rangle = \sin(\varphi)|0\rangle + \cos(\varphi)|1\rangle$ and $|\psi_k\rangle = \frac{1}{\sqrt{2}}(|0\rangle + |1\rangle)$, see Figure 5.13. The numerical result shows what we expected, the concurrences C_{BC}, C_{AB} and C_{AC} generate entanglement which remains constant for the singlet part. Here, we see again the influence of the entanglement dynamics due to the Lamb-shift, particularly for the time dependent concurrence C_{AB}. But the time-dependent concurrences C_{BC}, C_{AC} and C_{AB} of the bipartite entanglement dynamics do not show the same entanglement behavior. They do not remain constant for the same angles φ which is a consequence of the non existing decoherence-free subspaces for tripartite systems.

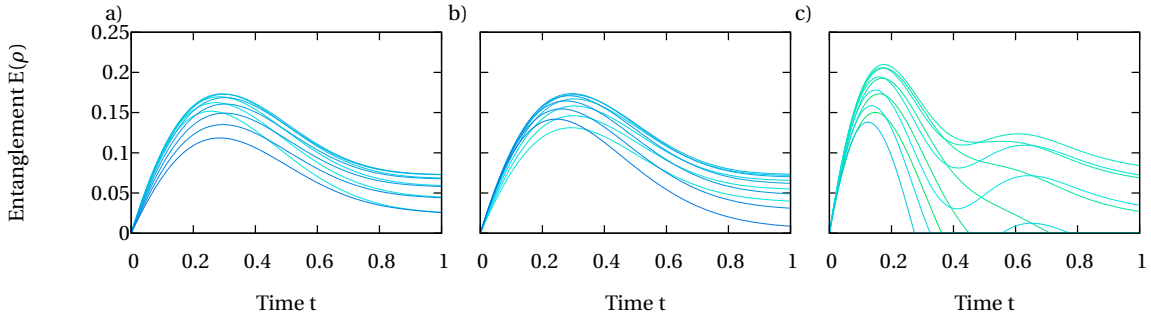

Figure 5.13: The time dependent concurrences C_{BC}, C_{AC} and C_{AB} (from left to right) of the initial separable state $|\psi\rangle = |\psi_i\rangle \otimes |\psi_j\rangle \otimes |\psi_k\rangle$ and different angles φ for (a),(b) varying from $\varphi = 2.15$(violet) to $\varphi = 2.6$ (green) in steps of 0.1 and (c) varying form $\varphi = 2.85$ (violet) to $\varphi = 3.4$ (green) in steps of 0.1.

In the context of decoherence-free subspaces we have introduced a decoherence-free subspace for one qubit consisting of three qubits by the encoded states $|\psi\rangle = \frac{1}{\sqrt{2}}(\cos(\varphi)|0\rangle_L + \sin(\varphi)|1\rangle_L)$. The numerical result for equal coupling constants $d_1 = d_2 = d_3 = 1$ shows asymptotic entanglement for differen angles φ, see Figure 5.14. This numerical result coincides with our theory of three different product states and also shows that it is impossible for a tripartite system to obtain an equal bipartite entanglement for all three qubit pairs.

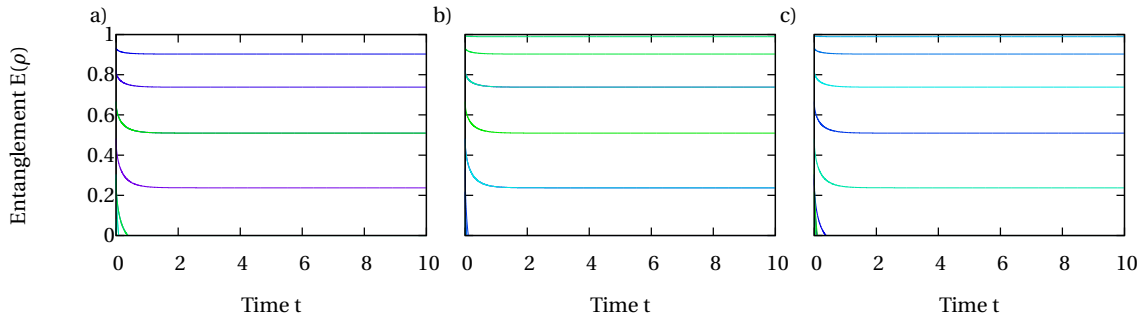

Figure 5.14: The time evolution of the concurrences C_{BC}, C_{AC} and C_{AB} (from left to right) of the initial encoded qubit state and different angles φ varying from $\varphi = 0$ (violet) to $\varphi = 2\pi$ (green) in steps of 22.

In the last example we look at the time-dependent entanglement between the qubits B and C where at the beginning qubit A has been excited. The numerical results, Figure 5.15, show that the constant concurrence C_{AB} between the qubits is preserved which allows us to conclude that a coherent transfer takes place between the excitation of the first qubit and the other qubit states such that a singlet state is generated

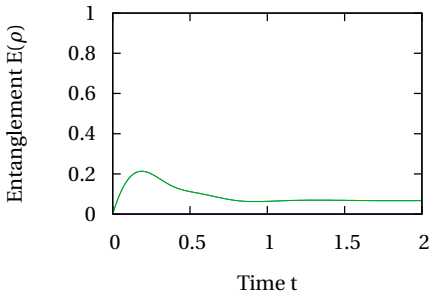

Figure 5.15: The time-dependent concurrence C_{BC} of the initial state $|\psi\rangle = |100\rangle$.

5.4 Theory of the entanglement dynamics of the three qubit chain

In the previous section we assumed that the coupling between each qubit and the thermal bath is defined by the corresponding coupling-constant which leads to a symmetric coupling of the qubit system and the thermal bath. A different approach would be to define the coupling-constants in such a way that the coupling between the system and the thermal bath is not symmetric, but a chain.
In general, all possible coupling constants of a three qubit system can be represented by the following matrix

$$D_{123} = \begin{pmatrix} \Gamma_1 & \gamma_{12} & \gamma_{13} \\ \gamma_{21} & \Gamma_2 & \gamma_{23} \\ \gamma_{31} & \gamma_{32} & \Gamma_3 \end{pmatrix},$$

where the couplings are defined by $\Gamma_i = d_i^* d_i, \gamma_{ij} = d_i^* d_j$ and the indices of this couplings denote the corresponding qubits. A qubit chain can be obtained by assuming that the coupling constants which describe a coupling of the qubits A and C to the thermal bath is zero, $\gamma_{13} = \gamma_{31} = 0$. This can only be done under the allowance that the coefficient matrix of the master equation remains positive semidefinite. The values of the coupling constants must be chosen so that the eigenvalues of the coefficient matrix remains positive. The following coupling representation is one possibility which fulfils this condition

$$\tilde{D}_{123} = \begin{pmatrix} 1 & 0.5 & 0 \\ 0.5 & 1 & 0.5 \\ 0 & 0.5 & 1 \end{pmatrix}.$$

But the decoherence-free subspace is destroyed by the different coupling constants. This means the stationary solution of the master equation has only a unique solution for which the concurrence decay. Thus all numerical results of the chain representation must show ESD. However, the arrangement of three qubit in a chain leads to another occupation distribution which we will see in the following numerical result.

5.5 Numerical result of the thermal occupation

In the following, we consider the time-dependent distribution of the initial occupation of the state again with an excitation on the first qubit $\rho = |100\rangle\langle 100|$. This allows us to compare the influence of the couplings of different qubit system representations. The numerical result of the time-dependent occupation shows a different stationary solution as for equal couplings. This result reflects the symmetry of the chain representation, the two qubits at the edge of the chain have the same coupling and hence an equal occupation within time. In contrast to the qubit in the middle which has a higher thermal occupation given by another coupling to the thermal bath. Thus this numerical result show that different couplings of the qubits to the bath influences the distribution of the occupation.

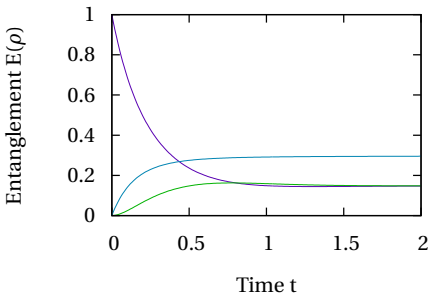

Figure 5.16: Time-evolution of the thermal occupation with the initial thermal occupation of an excitation of the first qubit given by the diagonal element $|100\rangle\langle 100|$ (violet), $|010\rangle\langle 010|$ (blue) and $|001\rangle\langle 001|$ (green).

5.6 Numerical results of the concurrences

We first consider the entangled Werner-state $|W\rangle = \frac{1}{\sqrt{3}}(|100\rangle + |010\rangle + |001\rangle)$ in the chain representation, Figure 5.17. If we compare the numerical result of the symmetric coupling to the chain coupling, the concurrences C_{BC} and C_{AB} decay faster which is a result of the stronger coupling between these pairs of qubits and the thermal environment. The time-dependent concurrence of the two qubits on the edge of the chain decays slower, because of its weaker coupling to the thermal bath. But both numerical results show ESD as we expected.

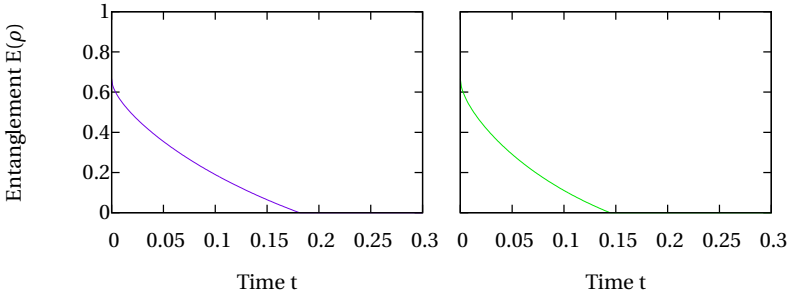

Figure 5.17: The time-dependent concurrences of the initial Werner-state in the chain representation for (a) C_{AC} and (b) C_{BC} and C_{AB}.

The numerical result of the encoded qubit Figure 5.16 contains the same effect of the chain representation, the

concurrence C_{AC} decays always weaker as the concurrences C_{BC} and C_{AC}. The decoherence-free space for one qubit is destroyed by the different coupling constants and thus the concurrences decay.

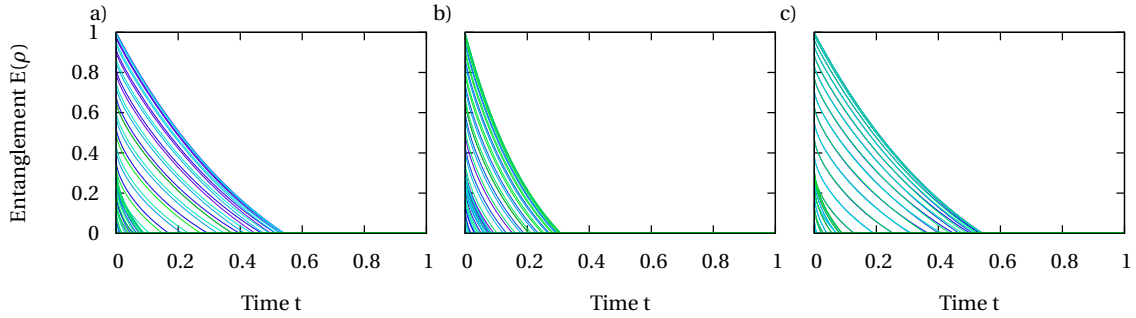

Figure 5.18: The time-dependent concurrences of the initial encoded qubit state in the chain representation and different angles φ varying form $\varphi = 0$ (violet) to $\varphi = 2\pi$ (green) in steps of 0.1 for (a) C_{BC} (b) C_{AC} and (c) C_{AB}.

Another consequence of the different couplings constants is that the concurrences of the Lamb-Shift contribution starts to oscillate. The numerical result of the time-dependent concurrence of the Lamb-Shift Figure 5.18 shows that the concurrences C_{BC} and C_{AB} oscillate above and below the initial value. In contrast, the numerical result of the time-dependent concurrence C_{AC} shows a small oscillation around the initial value. Also these result show that the tripartite dynamics is much more complicated as in the bipartite system.

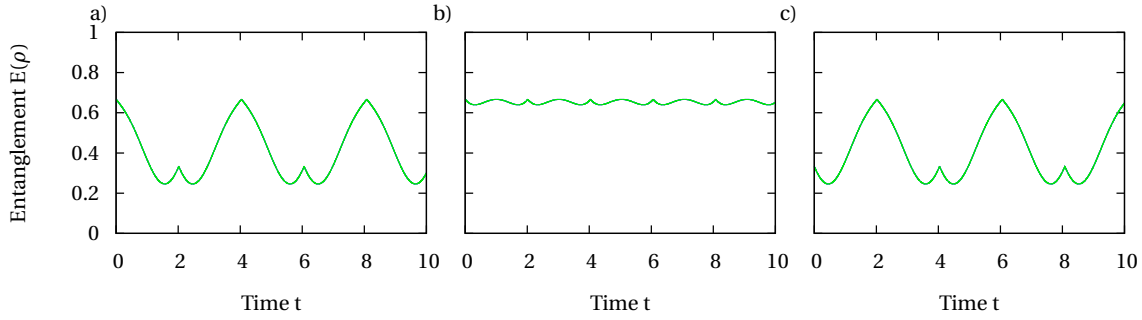

Figure 5.19: The time-dependent concurrences of the Lamb-Shift of the initial encoded qubit state in the chain representation and an angle $\varphi = 0$ for (a) C_{BC} (b) C_{AC} and (c) C_{AB}.

Chapter 6

Conclusion

In the second chapter the mathematical definitions of entanglement in the context of bipartite and multipartite systems were discussed. We found that for mixed states the Schmidt decomposition is not a sufficient criterion for separability and thus we have introduced two additional criteria, namely an operational separability, the partial transpose criterion (PPT) and a non-operational separability criterion, the criteria of positive map. The main part of this chapter was to present the theory of entanglement measure which started with the definition of entanglement. As a consequence that the entanglement is a special type of correlation, the properties of entanglement measures were studied in the context of different correlations. Then we defined the concurrence which is a correct entanglement measure for the bipartite case. For a tripartite system we saw that there is no formulation for the entanglement for mixed states.

In chapter 3 we introduced a fully quantum mechanical model: the Jaynes-Cummings model which describes the atom-field interaction. In the following the theory of open quantum systems was treated. We began with the unitary dynamics of a closed system and advanced this theory in the context of the semi-group formulation and under the Markovian assumptions to the dynamics of an open quantum system. This derivation of the Markovian master equation showed that the influence of the environment lead to an perturbation of first ordering. In the next section we used this general description of the open quantum system and derived the master equation in the Lindblad form for our qubit systems under the assumption that the coupling between the system and the bath is weak so that the Markovian assumptions were valid. After we noticed that the dynamics of an open quantum system consists not only of a unitary part but also of a dissipative part, we dealt with how it is possible to prevent the information given by the entanglement from decohering. In this context the theory of decoherence-free subspaces was discussed. This theory required a distinction between qubit systems with odd and even qubits. For an even number of qubits it is easy to find a component of an initial state which remains constant under the dissipative dynamics. This effect is only possible for decoherence-free subspaces which are fully conserved. We showed that the singlet state is such a decoherence-free subspace for a two qubit system because the interaction Hamiltonian has no influence on this state. For an odd number of qubits we found that it is not possible to define such a decoherence-free subspace. Thus we described another method to define a decoherence-free subspace. This can be done by encoding the information in another dimension. We gave the example of one qubit encoded by three qubits and showed that this subspace provides really the information of decoherence.

In chapter 4 the dynamics of two qubits embedded in a thermal environment described by the master equation was considered. We started with a discussion of the long-time behavior the steady state between the qubit system and the thermal bath. This demonstrated that the distribution of any initial occupation based on the energy of the states and the rotating-wave approximation. Further the theory of the entanglement dynamics was discussed and it was shown that the concurrence remains constant for the decoherence-free subspace alone, all other states have a stationary solution for which the time-dependent function of the concurrences de-

cays. In the following we described a typical effect which comes up in the context of dissipative dynamics; the entanglement-sudden death. Afterwards we studied the numerical results with this theoretical background and we saw that these results coincide with the theory. It proved that the entanglement dynamics is always influenced by different couplings of the qubits to the thermal bath. For a stronger coupling to the thermal bath the concurrence decays and shows entanglement-sudden-death as a result of the increasing dissipative dynamics. For a weaker coupling the concurrence decays slower. Additionally, a different coupling destroys the presence of the decoherence-free singlet state. In the context of entanglement dynamics we determined that the environment cannot only destroy the entanglement but also create it. For instance, a separable state which has a triplet part transiently generates entanglement. A superposition of a singlet and a triplet part generates entanglement which remains even constant as a consequence of the singlet part. Thus, the singlet state is the one and only state for which the concurrence and the thermal occupation remains constant. In the last part of this chapter we discussed the coherent physics, to be more precise the unitary part of the master equation. To obtain an intuitive description of this part we made use of the pseudo-spin representation which interprets the Lamb-Shift as a magnetic field. This allowed a geometrical illustration of the pseudo-spin on the Bloch sphere. We showed that the concurrence due to the Lamb-shift is given by the oscillation of the pseudo-spin caused by the pseudo-magnetic field.

In chapter 5 we extended the bipartite system in a tripartite system. We started with a discussion of the stationary solution of this master equation which showed that the initial occupation distributes under the same condition as in the bipartite case, the energy difference of the states and the rotating-wave approximation. Three qubits have a unique stationary solution as a consequence of the non existing decoherence-free subspace. To obtain an intuitive description of the dynamics of this system, the pseudo-spin representation of the Lamb-shift contribution of the master equation was derived. It turned out that the dynamics are much more complicated as in the bipartite system, because the spin interactions between the different qubits behave not equally. In the following we considered the bipartite entanglement between each qubit pair which allowed a differentiation of the entanglement dynamics, namely in tripartite entanglement and bipartite entanglement. The numerical results of the bipartite entanglement revealed some unexpected facts. The tripartite entanglement of the GHZ-state does not change into a bipartite entanglement through the influence of the thermal bath. Another unexpected entanglement dynamics shows the concurrences due to the Lamb-shift contribution of the master equation. Because of the numerical result of the Werner-state we recognized for different couplings that the much more complicated tripartite dynamics affected the entanglement dynamics of the coherent physics as a consequence of the non-trivial concurrence oscillations due to the Lamb-shift. In contrast, the concurrence of the Lamb-shift remains constant for equal couplings. The singlet state between two qubits of the tripartite system led to another interesting fact. The time-dependent concurrences of such a singlet state have the same entanglement behavior as in the bipartite system even for different couplings. Therefore this state is again a decoherence-free subspace for the bipartite entanglement of the tripartite system. The numerical results of different separable product states reflected the theory of the bipartite entanglement: we found that a triplet state between two qubits transiently generates entanglement and a superposition of a singlet and a triplet between two qubits generates entanglement which remains constant for the singlet part. Furthermore, we noticed the influence of the Lamb-shift part in the numerical result of the separable states with two different qubit states which is also a typical sign of the tripartite dynamics. The numerical results of the logical state and the product state of different initial states supported the fact that there are no decoherence-free subspaces of tripartite systems because it is impossible to obtain an equal concurrence between all qubit pairs. In the last part of this thesis we considered a chain representation of the qubits defined by different couplings. This allowed us to compare the dependency between the couplings and the occupation and the concurrence. The numerical result showed that any initial concurrence decays as a result of the unique stationary solution. Moreover, we saw that the thermal occupation changes for different couplings.

Chapter 7

Appendices

7.1 General separable state

We consider a general density matrix ρ which is defined as

$$\rho = \begin{pmatrix} a & 0 & 0 & 0 \\ 0 & b & z & 0 \\ 0 & z^* & c & 0 \\ 0 & 0 & 0 & d \end{pmatrix}, \tag{7.1.0.1}$$

with two different solutions for the concurrence

$$C(\rho) = \begin{cases} 2|z - \sqrt{ad}|, & \text{for} \quad ad < bc + z \\ -2\sqrt{bc} < 0, & \text{for} \quad bc + z < ad \end{cases}.$$

Hence, the mixed state is separable for $bc + z < ad$ and can be written as a product state of all pure-state decomposition, $\rho = \sum_k p_k |\psi_k\rangle \langle\psi_k|$. To show that we consider a general state

$$\begin{aligned} |\psi_{\alpha\beta\gamma\delta}\rangle :&= (\alpha|0\rangle + \beta|1\rangle) \otimes (\gamma|0\rangle + \delta|1\rangle) \\ &= \alpha\gamma|00\rangle + \alpha|01\rangle + \beta\gamma|10\rangle + \beta\delta|11\rangle, \end{aligned}$$

with the corresponding density matrix $\rho = |\psi\rangle\langle\psi|$

$$\rho = \begin{pmatrix} |\alpha\gamma|^2 & |\alpha|^2\gamma\delta^* & |\gamma|^2\alpha\beta^* & \alpha\gamma(\beta\delta)^* \\ |\alpha|^2\delta\gamma^* & |\alpha\delta|^2 & \alpha\delta(\beta\gamma)^* & |\delta|^2\alpha\beta^2 \\ |\gamma|^2\beta\alpha^* & \beta\gamma(\alpha\delta)^* & |\beta\gamma|^2 & |\beta|^2\gamma\delta^* \\ \beta\delta(\alpha\gamma)^* & |\delta|^2\gamma\alpha^* & |\beta|^2\delta\gamma^* & |\beta\gamma|^2 \end{pmatrix}.$$

The important observation is the following

$$\begin{aligned} |11\rangle\rho\langle 00| = \beta\delta(\alpha\gamma)^* \text{ and } |10\rangle\rho\langle 01| = \beta\gamma(\alpha\delta)^* \\ |00\rangle\rho\langle 11| = \alpha\gamma(\beta\delta)^* \text{ and } |01\rangle\rho\langle 10| = \alpha\delta(\beta\gamma)^* \end{aligned}$$

Hence, if we set either value $\alpha\beta\gamma\delta = 0$ other entries vanish. The other off-diagonal terms are not affected, because they are all in an absolute square. This will be used to set the respecting entries to zero.

We are looking for two separable states whose convex combination (with $p_i = 1$ yields to $|11\rangle\rho\langle 00| = 0, |10\rangle\rho\langle 01| = z$ and $|00\rangle\rho\langle 11| = 0, |01\rangle\rho\langle 10| = z^*$. The starting point are two states which are defined as $|\psi_{\alpha\beta\gamma\delta}\rangle$ and $|abcd\rangle$. Then the following relations are fulfilled

$$(1)\,\beta\gamma(\alpha\delta)^* + bc(ad)^* = z$$
$$(2)\,\beta\delta(\alpha\gamma)^* + bd(ac)^* = 0.$$

Now, to be more precise, assume $z \in \mathbb{R}$ and let

$$\gamma = \delta = \frac{1}{\sqrt{2}}$$
$$a = \frac{1}{\sqrt{2}}, b = \frac{i}{\sqrt{2}}$$

then the equations (1) and (2) read

$$(1)\,\frac{1}{2}\beta\alpha^* + \frac{i}{2}cd^* = z \;(1)^*\,\frac{1}{2}\alpha\beta^* - \frac{i}{2}dc^* = z^*,$$
$$(2)\,\frac{1}{2}\beta\alpha^* + \frac{i}{2}dc^* = 0 \;(2)^*\,\frac{1}{2}\alpha\beta^* - \frac{i}{2}cd^* = 0.$$

The real part is given by $(1) + (2)^* \Leftrightarrow Re(\alpha\beta^*) = z$. Thus let $\alpha = \frac{1}{\sqrt{2}}e^{i\varphi}, \beta = \alpha^*$ then the real part can be written as $Re(\alpha\beta^*) = \frac{1}{2}\cos(2\varphi) = z$ with

$$\varphi = \frac{1}{2} = \arccos(2z).$$

The imaginary part is given by $(1) - (2)^* \Leftrightarrow Im(cd^*) = -z$. Again let $c = \frac{1}{\sqrt{2}}e^{i\psi}, d = c^*$ then the imaginary part can be written as $Im(cd)^* = \frac{1}{2}\sin(2\psi)$ with

$$\psi = -\frac{1}{2}\arcsin(2z).$$

Therefore we fix the following values to the corresponding states

$$|\psi_{\alpha\beta\gamma\delta}\rangle \Rightarrow \alpha = \frac{1}{\sqrt{2}}e^{i\varphi}, \beta = \alpha^*, \gamma = \delta = \frac{1}{\sqrt{2}}$$
$$|\psi_{abcd}\rangle \Rightarrow a = \frac{1}{\sqrt{2}}, b = ia, c = \frac{1}{\sqrt{2}}e^{-i\psi}, d = c^*.$$

The convex decomposition of this two states is given by

$$\begin{aligned}\tilde{\rho} &= \frac{p}{4}[|\psi_{\alpha\beta\gamma\delta}\rangle\langle\psi_{\alpha\beta\gamma\delta}| + |\psi_{abcd}\rangle\langle\psi_{abcd}|] \\ &= \frac{p}{16}\left(\begin{pmatrix} 1 & 1 & e^{2i\varphi} & e^{2i\varphi} \\ 1 & 1 & e^{2i\varphi} & e^{2i\varphi} \\ e^{-2i\varphi} & e^{-2i\varphi} & 1 & 1 \\ e^{-2i\varphi} & e^{-2i\varphi} & 1 & 1 \end{pmatrix} + \begin{pmatrix} 1 & e^{-2i\psi} & -i & -ie{-}2i\psi \\ e^{2i\psi} & 1 & -ie^{2i\psi} & -i \\ i & ie^{-2i\psi} & 1 & e^{-2i\psi} \\ ie^{2i\psi} & i & e^{2i\psi} & 1 \end{pmatrix}\right) \\ &= \frac{p}{16}\begin{pmatrix} 2 & 1+e^{-2i\psi} & e^{2i\varphi}-i & e^{2i\varphi}-ie^{-2i\psi} \\ 1+e^{2i\psi} & 2 & e^{2i\varphi}-ie^{2i\psi} & e^{2i\varphi}-i \\ e^{-2i\varphi}+i & e^{-2i\varphi}+ie^{-2i\psi} & 2 & 1+e^{-2i\psi} \\ e^{-2i\varphi}+ie^{2i\psi} & e^{-2i\varphi}+i & 1+e^{2i\psi} & 2 \end{pmatrix}\end{aligned}$$

the additional non-diagonal elements are

- $\langle 00|\,\tilde{\rho}\,|01\rangle = \frac{P}{4}[|\alpha|^2\delta\gamma^* + |a|^2 dc^*] = \frac{P}{16}(1+e^{2i\psi})$
- $\langle 00|\,\rho\,|10\rangle = \frac{P}{4}[|\gamma|^2\beta\alpha^2 + |c|^2 ba^*] = \frac{P}{16}(i+e^{-2i\psi})$
- $|01\rangle\,\rho\,\langle 01| = \frac{P}{8}[|\delta|^2\beta\alpha^* + |d|^2 ba^*] = \frac{P}{16}(1+e^{-2i\varphi})$
- $|10\rangle\,\rho\,\langle 11| = \frac{P}{4}[|\beta|^2\delta\gamma^* + |b|^2 dc^*] = \frac{P}{16}(1+e^{2i\psi})$.

This non-diagonal terms can be generated to zero by adding the following decompositions of pure states:

$$\rho_2 = \frac{P}{8}[|\psi_{A_1B_1C_1D_1}\rangle\langle\psi_{A_1B_1C_1D_1}| + |\psi_{A_2B_2C_2D_2}\rangle\langle\psi_{A_2B_2C_2D_2}|],$$

with $-C_1 = D_1 = \frac{1}{\sqrt{2}}, -C_2 = D_2^* = \frac{1}{\sqrt{2}}e^{-i\psi}$ because $B_{1,2} = 0, A_{1,2} = 1$

$$\rho_2 = \frac{P}{16}\left(\begin{pmatrix} 1 & -1 & 0 & 0 \\ -1 & 1 & 0 & 0 \\ 0 & 0 & 0 & 0 \\ 0 & 0 & 0 & 0 \end{pmatrix} + \begin{pmatrix} 1 & e^{-2i\psi} & 0 & 0 \\ e^{2i\psi} & 1 & 0 & 0 \\ 0 & 0 & 0 & 0 \\ 0 & 0 & 0 & 0 \end{pmatrix}\right)$$
$$= \frac{P}{16}\begin{pmatrix} 2 & -(1+e^{-2i\psi}) & 0 & 0 \\ -(1+e^{2i\psi}) & 2 & 0 & 0 \\ 0 & 0 & 0 & 0 \\ 0 & 0 & 0 & 0 \end{pmatrix},$$

thus ρ_2 does generate the off-diagonal elements $\langle 10|\,\rho_2\,|11\rangle = 0$ and $\langle 11|\,\rho_2\,|10\rangle = 0$. But to the diagonal elements $\langle 11|\,\rho_2\,|11\rangle, \langle 10|\,\rho_2\,|10\rangle$ the factor $P/8$ is added.

$$\rho_2 = \frac{P}{8}[|\psi_{A_3B_3C_3D_3}\rangle\langle\psi_{A_3B_3C_3D_3}| + |\psi_{A_4B_4C_4D_4}\rangle\langle\psi_{A_4B_4C_4D_4}|],$$

with $-B_3 = A_3^* = \frac{1}{\sqrt{2}}e^{-i\varphi}, iB_4 = -A_4^* = \frac{1}{\sqrt{2}}$ because $C_{3,4} = 1, D_{3,4} = 0$

$$\rho_3 = \frac{P}{16}\left(\begin{pmatrix} 1 & 0 & -e^{2i\varphi} & 0 \\ 0 & 0 & 0 & 0 \\ -e^{-2i\varphi} & 0 & 1 & 0 \\ 0 & 0 & 0 & 0 \end{pmatrix} + \begin{pmatrix} 1 & 0 & i & 0 \\ 0 & 0 & 0 & 0 \\ -i & 0 & 1 & 0 \\ 0 & 0 & 0 & 0 \end{pmatrix}\right)$$
$$= \frac{P}{16}\begin{pmatrix} 2 & 0 & -(e^{2i\varphi} - i) & 0 \\ 0 & 0 & 0 & 0 \\ -(e^{-2i\varphi} + i) & 0 & 2 & 0 \\ 0 & 0 & 0 & 0 \end{pmatrix}.$$

Thus ρ_3 does generate the off-diagonal elements $\langle 01|\,\rho_3\,|11\rangle = 0$ and $\langle 11|\,\rho_3\,|01\rangle = 0$. But to the diagonal elements $\langle 11|\,\rho_3\,|11\rangle, \langle 01|\,\rho_3\,|01\rangle$ the factor $P/8$ is added.

$$\rho_4 = \frac{P}{8}[|\psi_{A_5B_5C_5D_5}\rangle\langle\psi_{A_5B_5C_5D_5}| + |\psi_{A_6B_6C_6D_6}\rangle\langle\psi_{A_6B_6C_6D_6}|]$$

with $-A_5^* = B_5 = \frac{1}{\sqrt{2}}e^{-i\varphi}, A_6 = iB_6 = \frac{1}{\sqrt{2}}$ because $C_{5,6} = 0, D_{5,6} = 1$

$$\rho_4 = \frac{P}{16}\left(\begin{pmatrix}0&0&0&0\\0&1&0&-e^{2i\varphi}\\0&0&0&0\\0&-e^{-2i\varphi}&0&1\end{pmatrix}+\begin{pmatrix}0&0&0&0\\0&1&0&i\\0&0&0&0\\0&-i&0&1\end{pmatrix}\right)$$
$$= \frac{P}{16}\begin{pmatrix}0&0&0&0\\0&2&0&-(e^{2i\varphi}-i)\\0&0&0&0\\0&-(e^{-2i\varphi}+i)&0&2\end{pmatrix}.$$

Thus ρ_4 does generate the off-diagonal elements $\langle 00|\rho_4|10\rangle = 0$ and $\langle 10|\rho_4|00\rangle = 0$. But to the diagonal elements $\langle 00|\rho_4|00\rangle, \langle 10|\rho_4|10\rangle$ the factor $P/8$ is added.

$$\rho_5 = \frac{P}{8}[|\psi_{A_7B_7C_7D_7}\rangle\langle\psi_{A_7B_7C_7D_7}| + |\psi_{A_8B_8C_8D_8}\rangle\langle\psi_{A_8B_8C_8D_8}|],$$

with $-D_7 = C_7 = \frac{1}{\sqrt{2}}, -D_8 = C_8^* = \frac{1}{\sqrt{2}}e^{i\psi}$ because $A_{7,8} = 0, B_{7,8} = 1$

$$\rho_5 = \frac{P}{16}\left(\begin{pmatrix}0&0&0&0\\0&0&0&0\\0&0&1&-1\\0&0&-1&1\end{pmatrix}+\begin{pmatrix}0&0&0&0\\0&0&0&0\\0&0&1&-2e^{-2i\psi}\\0&0&-2e^{-2i\psi}&1\end{pmatrix}\right)$$
$$= \frac{P}{16}\begin{pmatrix}0&0&0&0\\0&0&0&0\\0&0&2&-(1+2e^{-2i\psi})\\0&0&-(1+2e^{2i\psi})&2\end{pmatrix}.$$

Thus ρ_5 does generate the off-diagonal elements $\langle 10|\rho_5|11\rangle = 0$ and $\langle 11|\rho_5|10\rangle = 0$. But to the diagonal elements $\langle 11|\rho_5|11\rangle, \langle 10|\rho_5|10\rangle$ the factor $P/8$ is added. Therefore it is shown that the given mixed state is separable and can be written as a decomposition of the pure states defined above.

$$\begin{aligned}\rho &= \rho_1+\rho_2+\rho_3+\rho_4+\rho_5\\
&= \frac{p_1}{4}[|\psi_{\alpha\beta\gamma\delta}\rangle\langle\psi_{\alpha\beta\gamma\delta}| + |\psi_{abcd}\rangle\langle\psi_{abcd}|]\\
&= \frac{p_2}{8}[|\psi_{A_1B_1C_1D_1}\rangle\langle\psi_{A_1B_1C_1D_1}| + |\psi_{A_2B_2C_2D_2}\rangle\langle\psi_{A_2B_2C_2D_2}|]\\
&= \frac{p_3}{8}[|\psi_{A_3B_3C_3D_3}\rangle\langle\psi_{A_3B_3C_3D_3}| + |\psi_{A_4B_4C_4D_4}\rangle\langle\psi_{A_4B_4C_4D_4}|]\\
&= \frac{p_4}{8}[|\psi_{A_5B_5C_5D_5}\rangle\langle\psi_{A_5B_5C_5D_5}| + |\psi_{A_6B_6C_6D_6}\rangle\langle\psi_{A_6B_6C_6D_6}|]\\
&= \frac{p_5}{8}[|\psi_{A_7B_7C_7D_7}\rangle\langle\psi_{A_7B_7C_7D_7}| + |\psi_{A_8B_8C_8D_8}\rangle\langle\psi_{A_8B_8C_8D_8}|]\\
&= \frac{p}{16}\begin{pmatrix}6&0&0&(e^{2i\varphi}+ie^{-2i\psi})\\0&6&(e^{2i\varphi}-ie^{2i\psi})&0\\0&(e^{-2i\varphi}+ie^{-2i\psi})&6&0\\(e^{-2i\varphi}+ie^{2i\psi})&0&0&6\end{pmatrix}\end{aligned}$$

with $\varphi = \frac{1}{2}\arccos(2z)$ and $\psi = \frac{1}{2}\arcsin(2z)$

$$\tilde{\rho} = \frac{p}{8}\begin{pmatrix}3&0&0&0\\0&3&z&0\\0&z&3&0\\0&0&0&3\end{pmatrix}.$$

Every mixed state in the form (7.1.0.1) which is not entangled can be represented as

$$\rho = p_1\tilde{\rho} + p_2 \langle 00||00\rangle + p_3 \langle 11||11\rangle + p_4 \langle 01||01\rangle + p_5 \langle 10||10\rangle ,$$

with the assumption $\frac{12}{8} p_1 + p_2 + p_3 + p_4 + p_5 = 1$.
For example, a separable density matrix

$$\rho = \begin{pmatrix} \frac{2}{5} & 0 & 0 & 0 \\ 0 & \frac{1}{10} & z & 0 \\ 0 & z^* & \frac{1}{10} & 0 \\ 0 & 0 & 0 & \frac{2}{5} \end{pmatrix}$$

can be decomposed in pure states by choosing the probabilities as $p_1 = \frac{1}{5}, p_{4,5} = \frac{1}{40}, p_{2,3} = \frac{13}{40}$.

7.2 Results for one qubit

7.2.1 Analytical result for the master equation for one qubit interacting with a thermal bath

The master equation for only one qubit coupled with a thermal bath is an analytically solvable problem. The Lindblad operators are defined by the annihilation and the creation of the two-level atom operators $A_k = \hat{\sigma}_-, A_k^\dagger = \hat{\sigma}_+$. We introduce the definition of super operators to simplify the representation of the differential equation of the reduced system [1]

$$H\rho \longrightarrow (H \otimes \mathbb{1})\rho$$
$$\rho H \longrightarrow (\mathbb{1} \otimes H^T)\rho.$$

This super operators define a transformation of the Hilbert space $\mathscr{H}$ to the Hilbert space $\mathscr{H}^{\otimes 2}$ which leads the dynamics of the reduced system ρ_S unaffected, because the density matrix $\rho = \begin{pmatrix} \rho_{11} & \rho_{12} \\ \rho_{21} & \rho_{22} \end{pmatrix}$ is transformed to $\rho = (\rho_{11}, \rho_{12}, \rho_{21}, \rho_{22})^T$. The unitary contribution of the master equation, the Lamb-shift is given by $[H_{LS}, \rho]$ with $H_{LS} = dd^*\hat{\sigma_+}\hat{\sigma_-} + d^*d\hat{\sigma_-}\hat{\sigma_+}$, where d defines the coupling between the qubit and the bath. In the definition of the super operator the Lamb-shift reaches

$$H_{LS} = (H_{LS} \otimes \mathbb{1})\rho = \left(\begin{pmatrix} d^*d & 0 \\ 0 & d^*d \end{pmatrix} \otimes \begin{pmatrix} 1 & 0 \\ 0 & 1 \end{pmatrix} \right) \begin{pmatrix} \rho_{11} \\ \rho_{12} \\ \rho_{21} \\ \rho_{22} \end{pmatrix} = \begin{pmatrix} d^*d & 0 & 0 & 0 \\ 0 & d^*d & 0 & 0 \\ 0 & 0 & d^*d & 0 \\ 0 & 0 & 0 & d^*d \end{pmatrix} \begin{pmatrix} \rho_{11} \\ \rho_{12} \\ \rho_{21} \\ \rho_{22} \end{pmatrix}$$

The calculation of $\rho H_{LS} = (\mathbb{1} \otimes H^T)\rho$ gives the same result and thus the Lamb-Shift for one qubit is zero

$$\Rightarrow [H_{LS}, \rho] = H_{LS}\rho - \rho H_{LS} = 0.$$

[1] Proof of the super operator representation
Assertion: The super operator of $H\rho$ has the form $H \otimes \mathbb{1}$ in every dimension.
Proof: $\rho \rightarrow \sum_i \rho_i^{column} \otimes e_i$ (Definition of the super operator)
$H\rho \rightarrow \sum_i (H\rho)_i^{column} \otimes e_i = (H \otimes \mathbb{1}) \sum_i \rho_i^{column} \otimes e_i$
Assertion: The super operator of ρH has the form $\mathbb{1} \otimes H^T$ in every dimension .
Proof: $\rho \rightarrow \sum_i e_i \otimes \rho_i^{row}$ (Definition of the super operator)
$\rho H \rightarrow \sum_i e_i \otimes \rho_i^{row} H^{row} = (\mathbb{1} \otimes H^{row}) \sum_i e_i \otimes \rho_i^{row} = (\mathbb{1} \otimes H^T) \sum_i \rho_i^{column} \otimes e_i$

Thus the reduced qubit system embedded in a thermal bath can be described by first-order perturbation theory of the thermal bath. The dissipative contribution of the master equation described these dissipative perturbation effects by spontaneous emission processes $N(\omega_k)$ and thermally induced emission and absorption processes $(1+N(\omega_k))$. In the super operator representation the dissipator is given by

$$\begin{aligned}\mathscr{D}(\rho_S) &= N(\omega_k)(d^*\hat{\sigma}_+\rho d\hat{\sigma}_- - \frac{1}{2}d\hat{\sigma}_- d^*\hat{\sigma}_+\rho - \frac{1}{2}\rho d\hat{\sigma}_- d^*\hat{\sigma}_+) \\ &\quad + (1+N(\omega_k))(d\hat{\sigma}_-\rho d^*\hat{\sigma}_+ - \frac{1}{2}d^*\hat{\sigma}_+ d\hat{\sigma}_-\rho - \frac{1}{2}\rho d^*\hat{\sigma}_+ d\hat{\sigma}_-) \\ &\overset{1}{=} \left(N(\omega_k)\begin{pmatrix} 0 & 0 & 0 & dd^* \\ 0 & -\frac{1}{2}dd^* & 0 & 0 \\ 0 & 0 & -\frac{1}{2}dd^* & 0 \\ 0 & 0 & 0 & -dd^* \end{pmatrix} + (1+N(\omega_k))\begin{pmatrix} -d^*d & 0 & 0 & 0 \\ 0 & -\frac{1}{2}d^*d & 0 & 0 \\ 0 & 0 & -\frac{1}{2}d^*d & 0 \\ dd^* & 0 & 0 & 0 \end{pmatrix}\right)\begin{pmatrix}\rho_{11}\\ \rho_{12}\\ \rho_{21}\\ \rho_{22}\end{pmatrix}.\end{aligned}$$

The full master equation is then given only by the dissipator

$$\frac{d}{dt}\begin{pmatrix}\rho_{11}(t)\\ \rho_{12}(t)\\ \rho_{21}(t)\\ \rho_{22}(t)\end{pmatrix} = \begin{pmatrix} -(1+N(\omega_k))\Gamma & 0 & 0 & N(\omega_k)\Gamma \\ 0 & -\frac{1}{2}(N(\omega_k)\Gamma + (1+N(\omega_k))\Gamma) & 0 & 0 \\ 0 & 0 & -\frac{1}{2}(N(\omega_k)\Gamma + (1+N(\omega_k))\Gamma) & 0 \\ (1+N(\omega_k))\Gamma & 0 & 0 & -N(\omega_k)\Gamma \end{pmatrix}\begin{pmatrix}\rho_{11}\\ \rho_{12}\\ \rho_{21}\\ \rho_{22}\end{pmatrix},$$

where we introduced the following relation for the coupling-constants $\Gamma = dd^*$. This differential equation of the master equation can be easily solved and is

$$\begin{pmatrix}\rho_{11}(t)\\ \rho_{12}(t)\\ \rho_{21}(t)\\ \rho_{22}(t)\end{pmatrix} = \begin{pmatrix} \frac{\left(N(\omega_k)+e^{(-1-2N(\omega_k))t}+N(\omega_k)e^{(-1-2N(\omega_k))t}\right)C_1}{1+2N(\omega_k)} - \frac{N(\omega_k)\left(-1+e^{(-1-2N(\omega_k))t}\right)C_2}{1+2N(\omega_k)} & \rho_{11}(0) \\ e^{\frac{1}{2}(-1-2N(\omega_k)t}C_3 & \rho_{12}(0) \\ e^{\frac{1}{2}(-1-2N(\omega_k)t}C_3 & \rho_{21}(0) \\ -\frac{(1+N(\omega_k)(-1+e^{(-1-2N(\omega_k)t})C_1}{1+2N(\omega_k)} + \frac{(1+N(\omega_k)+N(\omega_k)e^{(1-2N(\omega_k))t})C_2}{1+2N(\omega_k)} & \rho_{22}(0) \end{pmatrix},$$

where C_1, C_2, C_3 and C_4 are integration constants.

7.2.2 Time-dependent occupation of the ground and the excited state for one qubit embedded in a thermal bath

In this section we discuss the change of the thermal occupation caused by the dissipative effects of the thermal bath. For only one qubit the general density matrix can be expressed by the system operators, the annihilation operator $\hat{\sigma}_-$ and the creation operator $\hat{\sigma}_+$

$$\rho(t) = \begin{pmatrix} \frac{1}{2}(1+\langle\sigma_3(t)\rangle) & \langle\sigma_-(t)\rangle \\ \langle\sigma_+(t)\rangle & \frac{1}{2}(1-\langle\sigma_3(t)\rangle)\end{pmatrix}.$$

The matrix elements of this general density matrix represents the thermal occupation of the ground state $p_g(t) = \frac{1}{2}(1-\langle\sigma_3\rangle)$ and the excited state $p_e(t) = \frac{1}{2}(1+\langle\sigma_3\rangle)$. We introduced the pre-factors γ_0 to obtain a formulation of the total transition rate of the spontaneous emission processes $\gamma_0 N(\omega_k)$ and the absorbtion processes $(1+N(\omega_k))$

[1] We used for the first terms of the dissipator the following super operator representation

$d^*\hat{\sigma}_+\rho d\hat{\sigma}_- = (d^*\hat{\sigma}_+\otimes\mathbb{1})(\mathbb{1}\otimes(d\hat{\sigma}_-^T)\begin{pmatrix}\rho_{11}\\ \rho_{12}\\ \rho_{21}\\ \rho_{22}\end{pmatrix}$ and $d\hat{\sigma}_-\rho d^*\hat{\sigma}_+ = (d\hat{\sigma}_-\otimes\mathbb{1})(\mathbb{1}\otimes(d^*\hat{\sigma}_+)^T)\begin{pmatrix}\rho_{11}\\ \rho_{12}\\ \rho_{21}\\ \rho_{22}\end{pmatrix}$

$$\gamma = \gamma_0 \left(2N(\omega_k + 1)\right),$$

where $N = N(\omega_k)$ is the Planck distribution of the transition frequency ω_k. The time-evolution of the thermal occupation can be derived by inserting the general density matrix into the dissipative contribution of the master equation

$$\begin{aligned}\frac{d}{dt}\rho(t) &= \gamma_0(1+N(\omega_k))\begin{pmatrix} -\frac{1}{2}(1+\langle\sigma_3(t)\rangle) & \langle\sigma_-(t)\rangle \\ \langle\sigma_+(t)\rangle & \frac{1}{2}(1+\langle\sigma_3(t)\rangle)\end{pmatrix} + \gamma_0 N(\omega_k)\begin{pmatrix} \frac{1}{2}(1-\langle\sigma_3(t)\rangle) & \langle\sigma_-(t)\rangle \\ \langle\sigma_+(t)\rangle & -\frac{1}{2}(1-\langle\sigma_3(t)\rangle)\end{pmatrix} \\ &= \begin{pmatrix} -\gamma\langle\sigma_3(t)\rangle - \gamma_0 & -\frac{\gamma}{2}\langle\sigma_-(t)\rangle \\ -\frac{\gamma}{2}\langle\sigma_+(t)\rangle & \gamma\langle\sigma_3(t)\rangle + \gamma_0\end{pmatrix},\end{aligned}$$

which leads to the following differential equations of the different matrix elements

$$\begin{aligned}\frac{d}{dt}\hat{\sigma_1}(t) &= -\frac{\gamma}{2}\hat{\sigma_1}(t) \\ \frac{d}{dt}\hat{\sigma_2}(t) &= -\frac{\gamma}{2}\hat{\sigma_2}(t) \\ \frac{d}{dt}\hat{\sigma_3}(t) &= -\gamma\hat{\sigma_3}(t) - \gamma_0,\end{aligned}$$

The solutions of this differential equations, the stationary solutions of the master equation describes the thermal occupation of all states. The off-diagonals $\langle\sigma_+(t)\rangle, \langle\sigma_-(t)\rangle$ are coherent states which decay exponentially by the rate $\gamma/2$. Thus the stationary solution of these matrix elements is given by

$$\langle\sigma_1\rangle_s = \langle\sigma_2\rangle_s = 0.$$

The inhomogeneous solution of the differential equation of the ground and excited state is given by

$$\langle\sigma_3(t)\rangle = ce^{-\gamma t} - \frac{\gamma_0}{\gamma},$$

and thus we obtain a solution for every initial condition $\langle\sigma(0)\rangle$

$$\langle\sigma_3(t)\rangle = \left(\langle\sigma_3(0)\rangle + \frac{\gamma_0}{\gamma}\right)e^{-\gamma t} - \frac{\gamma_0}{\gamma}$$

The factor $\frac{\gamma_0}{\gamma} = -\frac{1}{2N+1}$ is the average photon occupation. The stationary thermal occupation of the ground and the excited state can be calculated by this average photon occupation and by the corresponding matrix elements of the master equation

$$\begin{aligned}p_e(0) &= \frac{1}{2}\left(1+\langle\sigma_3\rangle_s\right) = \frac{N}{(2N+1)} \\ p_g(0) &= \frac{1}{2}\left(1-\langle\sigma_3\rangle_s\right) = \frac{2N}{(2N+1)}.\end{aligned}$$

where $p_e + p_g = 1$. With these definitions any thermal occupation of the ground and the excited state has the following time-dependent evolution

$$\begin{aligned}p_g(t) &= p_g(0)\left(\langle\sigma_3(0)\rangle + \frac{\gamma_0}{\gamma}\right)e^{-\gamma t} - \frac{\gamma_0}{\gamma}, \\ p_e(t) &= p_e(0)\left(\langle\sigma_3(0)\rangle + \frac{\gamma_0}{\gamma}\right)e^{-\gamma t} - \frac{\gamma_0}{\gamma}.\end{aligned}$$

The expectation value of the mean particle count of the thermal bath is defined by the Planck distribution

$$N(\omega_k) = \frac{1}{e^{\frac{1}{k_B T} E_k} - 1}$$

where the energy of the system is defined by $E_k = \hbar\omega_k$ and k_B is the Boltzmann constant. Thus the particle count is related to the temperature

$$T = \frac{\omega_k}{k_B \ln(N+1)}.$$

If the temperature of the thermal bath is zero, all the thermal occupation is in the ground state after a certain time. This situation changes for higher bath temperatures, then the qubit can receive energy form the thermal bath which leads to a higher occupation of the excited states. The numerical results show what we accepted for the detailed temperature dependency for the different initial thermal occupations, for the ground state it decreases and for the excited state it increases for higher temperatures.

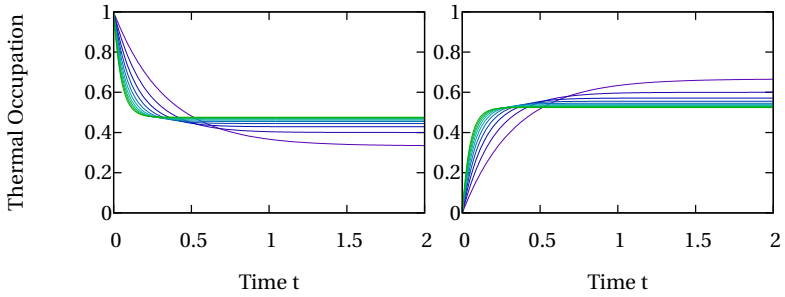

Figure 7.1: Time-dependent thermal occupation for the initial thermal occupation of the excited state $p_e = 1$ and different temperatures in the context of the Planck distribution of the thermal bath for $N = 1$ (violet) to $N = 10$ (green) in steps of 1 for (a) the excited state and (b) the ground state.

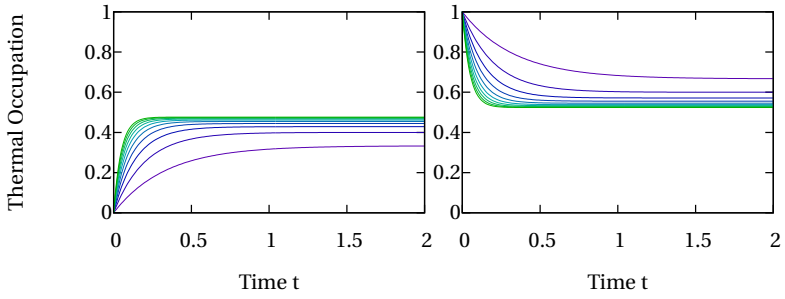

Figure 7.2: Time-dependent thermal occupation for the initial thermal occupation of the ground state $p_g = 1$ and different temperatures in the context of the Planck distribution of the thermal bath for $N = 1$ (violet) to $N = 10$ (green) in steps of 1 for (a) the excited state and (b) the ground state.

For example, we assume a temperature for which the expected value of the Planck distribution is one $N(\omega_k) = 1$, then the time-dependent thermal occupation is given by the solution of the differential equation with the corresponding initial conditions

Maximal thermal occupation of the ground state $p_g = 1$.

$$p_e(t) = p_e\left(1 + e^{-\gamma t}\right) \xrightarrow{t\to\infty} \frac{1}{3}$$
$$p_g(t) = p_g\gamma\left(1 + e^{-\gamma t}(\gamma + \gamma_0)\right) \xrightarrow{t\to\infty} \frac{2}{3}$$

Maximal thermal occupation of the excited state $p_e = 1$.

$$p_e(t) = p_e\left(1 + e^{-\gamma t}\right) \xrightarrow{t\to\infty} \frac{1}{3}$$
$$p_g(t) = p_g\left(1 + e^{-\gamma t}(\gamma - \gamma_0)\right) \xrightarrow{t\to\infty} \frac{2}{3}$$

The numerical results coincide with the analytical results, see Figure 7.2 and Figure 7.3 the violet lines and show that the thermal occupation of the ground and excited state is balanced through the influence of the thermal bath between these two states in the context of the stationary solution of the thermal occupation.

7.3 Calculation of the Lamb-Shift contribution for three qubits

The coherent physic of three qubits embedded in a thermal environment is given by the Lamb-shift contribution of the master equation. This term can be calculated by the standard derivation introduced in section 2.3.

The eigenoperators and simultaneously the Lindblad operators of the qubit system are the annihilation and creation operators

$$\begin{aligned} A_1(|\omega|) &= d_1(\hat{\sigma}_- \otimes \mathbb{1} \otimes \mathbb{1}) = d_1\sigma_-^{(1)}, \\ A_2(|\omega|) &= d_2(\mathbb{1} \otimes \hat{\sigma}_- \otimes \mathbb{1}) = d_2\sigma_-^{(2)}, \\ A_3(|\omega|) &= d_3(\mathbb{1} \otimes \mathbb{1} \otimes \hat{\sigma}_-) = d_3\sigma_-^{(3)}, \\ A_i(-|\omega|) &= A_i^\dagger(|\omega|), \end{aligned}$$

where $\mathbb{1}$ is the (2×2) identity matrix and d_i defines the coupling between the qubits and the bath. This representation in the Linblad operators splits the Lamb-Shift in two contribution -diagonal and non-diagonal terms

$$\begin{aligned} H_{LS} = \sum_{\pm\omega} S(|\omega|)[&A_1^\dagger(|\omega|)A_1(|\omega|) + A_2^\dagger(|\omega|)A_2(|\omega|) + A_3^\dagger(|\omega|)A_3(|\omega|)] \\ &+ A_1^\dagger(|\omega|)A_2(|\omega|) + A_2^\dagger(|\omega|)A_1(|\omega|) + A_1^\dagger(|\omega|)A_3(|\omega|) + A_3^\dagger(|\omega|)A_1(|\omega|) + A_2^\dagger(|\omega|)A_3(|\omega|) + A_3^\dagger(|\omega|)A_2(|\omega|)], \end{aligned}$$

where $S(|\omega|)$ is the unitary part of the reservoir correlation function. In the following we calculate the two sums of the Lamb-shift contribution in the context with these Lindblad operators.

$$\begin{aligned} \sum_{i,j} d_j^* d_i \left(A_i^*(|\omega|) \cdot A_j(|\omega|)\right) = {} & d_1^* d_1 \left(A_1^\dagger(|\omega|) A_1(|\omega|)\right) + d_1^* d_2 \left(A_1^\dagger(|\omega|) A_2(|\omega|)\right) + d_1^* d_3 \left(A_1^\dagger(|\omega|) A_3(|\omega|)\right) \\ & + d_2^* d_1 \left(A_2^\dagger(|\omega|) A_1(|\omega|)\right) + d_2^* d_2 \left(A_2^\dagger(|\omega|) A_2(|\omega|)\right) + d_2^* d_3 \left(A_2^\dagger(|\omega|) A_3(|\omega|)\right) \\ & + d_3^* d_1 \left(A_3^\dagger(|\omega|) A_1(|\omega|)\right) + d_3^* d_2 \left(A_3^\dagger(|\omega|) A_2(|\omega|)\right) + d_3^* d_3 \left(A_3^\dagger(|\omega|) A_3(|\omega|)\right) \\ = {} & \begin{pmatrix} \Gamma & 0 & 0 & 0 & 0 & 0 & 0 & 0 \\ 0 & \Gamma_1+\Gamma_2 & \gamma_{23} & 0 & \gamma_{13} & 0 & 0 & 0 \\ 0 & \gamma_{23}^* & \Gamma_1+\Gamma_3 & 0 & \gamma_{12} & 0 & 0 & 0 \\ 0 & 0 & 0 & \Gamma_1 & 0 & \gamma_{12} & \gamma_{13} & 0 \\ 0 & \gamma_{13}^* & \gamma_{12}^* & 0 & \Gamma_2+\Gamma_3 & 0 & 0 & 0 \\ 0 & 0 & 0 & \gamma_{12}^* & 0 & \Gamma_2 & \gamma_{23} & 0 \\ 0 & 0 & 0\gamma_{12}^* & 0 & \gamma_{23}^* & \Gamma_3 & 0 & \\ 0 & 0 & 0 & 0 & 0 & 0 & 0 & 0 \end{pmatrix} \end{aligned}$$

$$\sum_{i,j} d_i d_j^* \left(A_j\left(|\omega|\right) \cdot A_i^*\left(|\omega|\right)\right) = d_1 d_1^* \left(A_1\left(|\omega|\right) A_1^*\left(|\omega|\right)\right) + d_1 d_1^* \left(A_1\left(|\omega|\right) A_1^*\left(|\omega|\right)\right) + d_1 d_1^* \left(A_1\left(|\omega|\right) A_1^*\left(|\omega|\right)\right)$$
$$+ d_1 d_1^* \left(A_1\left(|\omega|\right) A_1^*\left(|\omega|\right)\right) + d_1 d_1^* \left(A_1\left(|\omega|\right) A_1^*\left(|\omega|\right)\right) + d_1 d_1^* \left(A_1\left(|\omega|\right) A_1^*\left(|\omega|\right)\right)$$
$$+ d_1 d_1^* \left(A_1\left(|\omega|\right) A_1^*\left(|\omega|\right)\right) + d_1 d_1^* \left(A_1\left(|\omega|\right) A_1^*\left(|\omega|\right)\right) + d_1 d_1^* \left(A_1\left(|\omega|\right) A_1^*\left(|\omega|\right)\right)$$
$$= \begin{pmatrix} \Gamma & 0 & 0 & 0 & 0 & 0 & 0 & 0 \\ 0 & \Gamma_1+\Gamma_2 & \gamma_{23} & 0 & \gamma_{13} & 0 & 0 & 0 \\ 0 & \gamma_{23}^* & \Gamma_1+\Gamma_3 & 0 & \gamma_{12} & 0 & 0 & 0 \\ 0 & 0 & 0 & \Gamma_1 & 0 & \gamma_{12} & \gamma_{13} & 0 \\ 0 & \gamma_{13}^* & \gamma_{12}^* & 0 & \Gamma_2+\Gamma_3 & 0 & 0 & 0 \\ 0 & 0 & 0 & \gamma_{12}^* & 0 & \Gamma_2 & \gamma_{23} & 0 \\ 0 & 0 & 0\gamma_{12}^* & 0 & \gamma_{23}^* & \Gamma_3 & 0 & \\ 0 & 0 & 0 & 0 & 0 & 0 & 0 & 0 \end{pmatrix}$$

The full expression for the Lamb-Shift Hamiltonian is then given by

$$H_{LS} = \mathscr{P}_1 \int_0^\infty d\omega \left[\frac{(1+N(\omega_k))}{\omega-\omega_k}\right] \begin{pmatrix} \Gamma & 0 & 0 & 0 & 0 & 0 & 0 & 0 \\ 0 & \Gamma_1+\Gamma_2 & \gamma_{23} & 0 & \gamma_{13} & 0 & 0 & 0 \\ 0 & \gamma_{23}^* & \Gamma_1+\Gamma_3 & 0 & \gamma_{12} & 0 & 0 & 0 \\ 0 & 0 & 0 & \Gamma_1 & 0 & \gamma_{12} & \gamma_{13} & 0 \\ 0 & \gamma_{13}^* & \gamma_{12}^* & 0 & \Gamma_2+\Gamma_3 & 0 & 0 & 0 \\ 0 & 0 & 0 & \gamma_{12}^* & 0 & \Gamma_2 & \gamma_{23} & 0 \\ 0 & 0 & 0 & \gamma_{13}^* & 0 & \gamma_{23}^* & \Gamma_3 & 0 \\ 0 & 0 & 0 & 0 & 0 & 0 & 0 & 0 \end{pmatrix}$$
$$+\mathscr{P}_2 \int_0^\infty d\omega \left[\frac{N(\omega_k)}{\omega+\omega_k}\right] \begin{pmatrix} 0 & 0 & 0 & 0 & 0 & 0 & 0 & 0 \\ 0 & \Gamma_3 & \gamma_{23} & 0 & \gamma_{13} & 0 & 0 & 0 \\ 0 & \gamma_{23}^* & \Gamma_2 & 0 & \gamma_{12} & 0 & 0 & 0 \\ 0 & 0 & 0 & \Gamma_2+\Gamma_3 & 0 & \gamma_{12} & \gamma_{13} & 0 \\ 0 & \gamma_{13}^* & \gamma_{12}^* & 0 & \Gamma_1 & 0 & 0 & 0 \\ 0 & 0 & 0 & \gamma_{12}^* & 0 & \Gamma_1+\Gamma_3 & \gamma_{23} & 0 \\ 0 & 0 & 0 & \gamma_{13}^* & 0 & \gamma_{23}^* & \Gamma_1+\Gamma_2 & 0 \\ 0 & 0 & 0 & 0 & 0 & 0 & 0 & \Gamma \end{pmatrix}.$$

Bibliography

[1] M. A. Nielsen and I. L. Chuang, *Quantum Computation and Quantum Information (Cambridge Series on Information and the Natural Sciences)*. Cambridge University Press, 2004.

[2] J. J. Slosser and G. J. Milburn, "Creating metastable schrödinger cat states," *Phys. Rev. Lett.*, vol. 75, pp. 418–421, Jul 1995.

[3] W. K. Wootters, "Entanglement of formation of an arbitrary state of two qubits," *Phys. Rev. Lett.*, vol. 80, pp. 2245–2248, Mar 1998.

[4] V. Coffman, J. Kundu, and W. K. Wootters, "Distributed entanglement," *Phys. Rev. A*, vol. 61, p. 052306, Apr 2000.

[5] D. Bohm and Y. Aharonov, "Discussion of experimental proof for the paradox of einstein, rosen, and podolsky," *Phys. Rev.*, vol. 108, pp. 1070–1076, Nov 1957.

[6] A. Einstein, B. Podolsky, and N. Rosen, "Can quantum-mechanical description of physical reality be considered complete?," *Phys. Rev.*, vol. 47, pp. 777–780, May 1935.

[7] D. Bruss, "Characterizing entanglement." J. Math. Phys. 43, 4237 (2002), 2001.

[8] A. Peres, "Separability criterion for density matrices," *Phys. Rev. Lett.*, vol. 77, pp. 1413–1415, Aug 1996.

[9] R. Horodecki, P. Horodecki, M. Horodecki, and K. Horodecki, "Quantum entanglement," *Rev. Mod. Phys.*, vol. 81, pp. 865–942, Jun 2009.

[10] M. B. Plenio and S. Virmani, "An introduction to entanglement measures." Quant. Inf. Comp. 7, 1 (2007), 2005.

[11] C. H. Bennett, D. P. DiVincenzo, J. A. Smolin, and W. K. Wootters, "Mixed-state entanglement and quantum error correction," *Phys. Rev. A*, vol. 54, pp. 3824–3851, Nov 1996.

[12] W. K. Wootters, "Entanglement of formation and concurrence," *Quantum Information and Computation*, vol. 1, pp. 27–47, 2001.

[13] L. Tamaryan, D. Park, and S. Tamaryan, "Analytic expressions for geometric measure of three-qubit states," *Phys. Rev. A*, vol. 77, p. 022325, Feb 2008.

[14] A. Acín, D. Bruß, M. Lewenstein, and A. Sanpera, "Classification of mixed three-qubit states," *Phys. Rev. Lett.*, vol. 87, p. 040401, Jul 2001.

[15] H.-P. Breuer and F. Petruccione, *The Theory of Open Quantum Systems*. Oxford University Press, USA, Mar. 2007.

[16] F. Benatti and R. Floreanini, "Open quantum dynamics: Complete positivity and entanglement." Int.J.Mod.Phys. B19 (2005) 3063, 2005.

[17] G. Lindblad, “On the generators of quantum dynamical semigroups,” *Commun. Math. Phys.*, vol. 48, no. 119, 1976.

[18] G. S. Agarwal, “Rotating-wave approximation and spontaneous emission,” *Phys. Rev. A*, vol. 7, pp. 1195–1197, Mar 1973.

[19] D. A. Lidar and K. B. Whaley, “Decoherence-free subspaces and subsystems.” in "Irreversible Quantum Dynamics", F. Benatti and R. Floreanini (Eds.), pp. 83-120 (Springer Lecture Notes in Physics vol. 622, Berlin, 2003), 2003.

[20] D. A. Lidar, I. L. Chuang, and K. B. Whaley, “Decoherence-free subspaces for quantum computation,” *Phys. Rev. Lett.*, vol. 81, pp. 2594–2597, Sep 1998.

[21] P. G. Brooke, J. D. Cresser, and M. K. Patra, “Decoherence-free quantum information in the presence of dynamical evolution,” *Phys. Rev. A*, vol. 77, p. 062313, Jun 2008.

[22] T. Yu and J. H. Eberly, “Sudden death of entanglement,” *Science*, vol. 323, pp. 598–601, Jan 2009.

[23] S. Aldana, Y.-D. Wang, and C. Bruder, “Greenberger-horne-zeilinger generation protocol for n superconducting charge qubits capacitively coupled to a quantum bus,” 2011.

Chapter 8

Acknowledgment

I am very grateful to Prof. Christoph Bruder who gave me the opportunity to work in his research group.

I would also thank Dr. Maximilian Rinck for his patience, motivation and guidance. He was always willing to listen to my question and provided great efforts in answering them.

Last but not least I owe my deep gratefulness to my uncle Karl Garni who made it possible for me to study and never stopped believing in me.